Investigating the Genomic Effects of Glucocorticoid Receptor Activation

-

an Analysis of Transcriptional Memory and Mechanisms That Direct Divergent Genomic Occupancy of Related Transcription Factors

Inaugural-Dissertation
to obtain the academic degree
Doctor rerum naturalium (Dr. rer. nat.)

submitted to the Department of Biology, Chemistry, Pharmacy
of Freie Universität Berlin

by

Anna Melissa Bothe

2021

The dissertation was prepared under the supervision of Dr. Sebastiaan H. Meijsing at the Max Planck Institute for Molecular Genetics in Berlin from October 2016 to March 2021.

1st Reviewer: Dr. Sebastiaan H. Meijsing
2nd Reviewer: Prof. Dr. Markus Wahl
Date of Defense: 02.06.2021

Selbstständigkeitserklärung

Hiermit versichere ich, dass ich die vorliegende Dissertation selbstständig und ohne unerlaubte Hilfe angefertigt habe.

Acknowledgements

First and foremost, I would like to express my gratitude to my supervisor Sebastiaan Meijsing for his invaluable support throughout my doctoral studies. Sebastiaan was always available for discussions when I needed advice on issues big and small.

I would also like to thank Martin Vingron for giving me the opportunity to be part of his research department. In addition, I would like to express my gratitude to Sarah Kinkley for letting me finish my doctoral studies in her group and for her support throughout.

Special thanks go to Edda Einfeldt for her excellent technical assistance and support in and outside of the lab. My special gratitude also goes to Marina Kulik for her contributions to this work and for being a great collaborator. I am also very grateful to Laura Glaser for all her help over the years and for always having an informative answer to any question I asked.

I would like to express my gratitude to René Buschow for his immense support with the analysis of microscopy images and to Beatrix Fauler for her help and advice on working with a fluorescent microscope.

Additionally, I would like to thank Verena Thormann, Stefanie Schöne, Anna Katharina Lübke and all members of the Vingron Department for creating a friendly and fun working environment.

I also want to thank Markus Wahl for his time in reviewing this thesis.

I am very grateful to my family for their continuous support along the way and, finally, to my husband Calum Tollick for being my rock.

List of Publications

- **Bothe, M.**, Buschow, R. and Meijsing, S. H. Glucocorticoid receptor activation induces gene-specific transcriptional memory and universally reversible changes in chromatin accessibility. *bioRxiv* (2021). doi: `https://doi.org/10.1101/2021.01.05.425406`. Peer-reviewed Preprint.

- Kulik, M., **Bothe, M.**, Kibar, G., Fuchs, A., Schöne, S., Prekovic, S., Mayayo-Peralta, I. Chung, H.-R., Zwart, W., Helsen, C., Claessens, F. and Meijsing, S. H. Androgen and glucocorticoid receptor direct distinct transcriptional programs by receptor-specific and shared DNA binding sites. *Nucleic Acids Research* (2021). doi: `https://doi.org/10.1093/nar/gkab185`. Online ahead of print.

Abstract

The glucocorticoid receptor (GR) is a transcription factor which becomes activated upon binding to glucocorticoids, a class of steroid hormones. Upon activation, GR binds to various genomic locations and induces large-scale changes in transcription and chromatin structure. Clinically, GR is an important therapeutic target, since glucocorticoids are widely applied to treat autoimmune and inflammatory conditions. However, long-term treatment with glucocorticoids is associated with glucocorticoid-resistance and severe side-effects. At the molecular level, the effects of prolonged GR activation on a cell's transcriptional responses are not fully understood. Here, I investigated if exposure to glucocorticoids results in long-term changes in chromatin and transcription. In addition, I studied GR's genomic binding preferences by investigating mechanisms that shape DNA binding specificities between GR and its paralog, the androgen receptor (AR).

In the first part of the thesis, I investigated the immediate and the long-term effects of GR activation on chromatin and transcription. By examining GR binding as well as glucocorticoid-induced changes in chromatin accessibility and transcription, I found that genomic regions that lose chromatin accessibility were enriched near downregulated genes. Interestingly, these 'closing' regions were largely not bound by GR, indicating that repression, in part, does not depend on nearby GR binding and might occur through indirect effects of GR activation. To study the long-term effects of GR activation, I investigated changes in chromatin accessibility and transcription after washout of glucocorticoids. GR-induced changes in chromatin accessibility were found to be reversible following a 24-hour washout period. Similarly, transcriptional activity reverted to basal levels after washout. Moreover, I tested if a prior exposure to hormone changes the response to a subsequent treatment. Most genes showed similar transcriptional responses upon hormone re-stimulation compared to the first stimulation. However, the GR-target gene *ZBTB16* showed enhanced upregulation upon reinduction, suggesting that prior glucocorticoid exposure results in priming of this gene. Single-cell analysis showed that enhanced expression of *ZBTB16* upon reinduction was a consequence of an increased probability of cells transcribing the gene as well as individual cells showing increased *ZBTB16* transcription.

In the second part of the thesis, I assayed the role of chromatin and DNA sequence in generating divergent genomic binding patterns of transcription factors with nearly identical DNA-binding preferences, specifically, GR and its paralog AR. Investigating binding of GR and AR in the same cell type revealed that both transcription factors occupy overlapping as well as unique sites. Examining the chromatin landscape at receptor binding regions showed that many GR-specific sites were situated within relatively inaccessible chromatin, suggesting that binding specificity is, in part, achieved through GR's ability to

bind to inaccessible chromatin. Furthermore, motif enrichment analysis at GR- and AR-specific regions provided further evidence that the receptors exhibit subtle differences in the recognition sequences they preferentially bind to. Lastly, analysis of GC-content revealed that receptor-specific binding is also driven by GC-content at the binding sites and the larger surrounding area, as mean GC-content was found to to be higher at GR- compared to AR-specific sites.

In summary, these results provide evidence that GR is capable of inducing gene-specific transcriptional memory, even though GR-induced chromatin structural and transcriptional changes are largely reversible. Given GR's biological role as an effector to fluctuating levels of glucocorticoids, the reversibility of GR-induced chromatin and transcriptional changes is to be expected. However, future experiments involving longer, or more frequently repeated, hormone exposures might yield insights into the underlying mechanisms of glucocorticoid resistance and side-effects associated with long-term glucocorticoid treatment. Furthermore, the chromatin landscape as well as DNA sequence composition contribute to driving receptor-specific genomic occupancy of GR and AR. These findings might represent a general mechanism that shapes differential binding among paralogous transcription factors and could contribute to our understanding of how genomic binding specificities are established for other related transcription factors.

Zusammenfassung

Der Glukokortikoidrezeptor (GR) ist ein Transkriptionsfaktor (TF), der durch Bindung an Glukokortikoide, die zu den Steroidhormonen gehören, aktiviert wird. Aktivierter GR bindet zahlreiche genomische Regionen und induziert weitreichende Veränderungen der Transkription und Chromatin-Struktur. Aus klinischer Sicht stellt GR ein wichtiges Medikamentenziel dar, da Glukokortikoide oft zur Behandlung von Autoimmunkrankheiten und Entzündungszuständen eingesetzt werden. Jedoch kann eine Langzeitbehandlung mit Glukokortikoiden zu schwerwiegenden Nebenwirkungen und Glukokortikoid-Resistenzen führen. Inwiefern sich eine Langzeitaktivierung von GR auf molekularer Ebene auswirkt, ist noch nicht klar. In meiner Doktorarbeit habe ich mich mit den Langzeitfolgen nach GR-Aktivierung befasst, die sich auf Chromatin-Struktur und Transkription auswirken. Zusätzlich habe ich die genomischen Bindungspräferenzen von GR untersucht und diese mit den Präferenzen des verwandten Androgenrezeptors (AR) verglichen.

Im ersten Teil meiner Doktorarbeit befasste ich mich mit den kurz- und längerfristigen Auswirkungen auf Transkription und Chromatin nach einer GR-Aktivierung. Zu diesem Zweck untersuchte ich genomweite GR-Bindestellen, Veränderungen in der Chromatin-Zugänglichkeit genomischer Regionen und transkriptionelle Veränderungen. Ich konnte zeigen, dass genomische Regionen, die an Chromatin-Zugänglichkeit verlieren und nicht von GR gebunden sind, in der Nähe von reprimierten Genen angereichert waren. Diese Erkenntnisse legen nahe, dass Glukokortikoid-induzierte transkriptionelle Repression mancher Gene ohne lokaler Binding von GR stattfinden kann. Darüber hinaus untersuchte ich, ob Glukokortikoid-induzierte Veränderungen der Chromatin-Zugänglichkeit, über einen längeren Zeitraum bestehen bleiben können oder ob sie reversibel sind. Ich fand, dass die erhöhte oder verringerte Chromatin-Zugänglichkeit infolge einer einmaligen GR-Aktivierung 24 Stunden nach dem Auswaschen der Glukokortikoide reversibel war. Ähnlich verhielt sich die transkriptionelle Aktivität, welche nach dem Auswaschen von Glukokortikoiden wieder auf Basallevel zurückfiel. Außerdem untersuchte ich den Einfluss einer vorherigen Hormon-Exposition auf Transkription nach einer zweiten Stimulation. Die meisten Gene zeigten eine ähnliche transkriptionelle Antwort nach einer solchen Re-stimulation im Vergleich zur ersten Hormonexposition. Jedoch zeigte das GR-Zielgen *ZBTB16* eine gesteigerte Hochregulierung nach Re-induktion, was eine Sensibilisierung dieses Gens durch eine vorherige Exposition nahelegt. Einzelzellanalyse nach Re-induktion konnte zeigen, dass die gesteigerte Expression von *ZBTB16* eine Konsequenz der erhöhten Wahrscheinlichkeit von Genexpression sowie höherer Expressionsraten einzelner Zellen ist.

Im zweiten Teil der Arbeit fokussierte ich mich auf die Rolle von Chromatin und DNA-Sequenz in der Etablierung von spezifischen Bindeverhalten von TF mit fast identischen DNA-Bindepräferenzen am Beispiel von GR und AR. Die Analyse von GR- und

AR-Bindepräferenzen im gleichen zellulären Hintergrund konnte zeigen, dass beide TF überlappende sowie spezifische Bindestellen targetieren. Die Untersuchung der Chromatinlandschaft von Rezeptorbindestellen zeigte, dass viele GR spezifische Bindestellen in relativ unzugänglichem Chromatin liegen, was suggeriert, dass GR Spezifität über die Fähigkeit geschlossenes Chromatin zu binden vermittelt wird. Außerdem konnten Sequenzmotifanalysen von GR- und AR-spezifischer Binderegionen weiter auf subtile Differenzen in Erkennungssequenzen hinweisen. Abschließend zeigte eine GC-Gehaltsanalyse, dass rezeptorspezifisches Binden auch vom GC-Gehalt der Bindestellen sowie der weiteren Umgebung abhängt, da der durchschnittliche GC-Gehalt höher an GR- gegenüber AR-spezifischen Bindestellen war.

Zusammenfassend konnten diese Ergebnisse zeigen, dass GR genspezifische transkriptionelle Erinnerung induzieren kann, obwohl GR-induzierte Änderungen in Chromatin-Struktur und Transkription größtenteils reversibel sind. Da GR als Effektor fluktuierender Glukokortikoid-Spiegel, aufgrund natürlicher Tagesschwankungen, fungiert, ist eine Reversibilität der GR-induzierten Änderungen teilweise zu erwarten. Zukünftige Experimente könnten längere oder häufiger wiederholte Hormon-Behandlungen beinhalten, um die molekularen Mechanismen, welche den Nebenwirkungen und Glukokortikoid-Resistenzen einer Langzeitbehandlung mit Glukokortikoiden zugrunde liegen, vollständig zu ergründen. Zusätzlich tragen Chromatin-Landschaft sowie DNA-Sequenz zum rezeptorspezifischen genomischen Bindeverhaltens von GR und AR bei. Diese Erkenntnisse könnten möglicherweise generelle Mechanismen spezifischen Verhaltens paraloger TF darstellen und deshalb zu unserem Verständnis der genomischen Bindepräferenzen anderer verwandter TF beitragen.

Contents

1 Introduction

1.1 Transcriptional Regulation

The genetic information encoded in genes provides the instructions to synthesize molecules, which are essential in maintaining cellular function and identity. The process by which genes are 'switched on' to generate these gene products, namely proteins or functional RNAs, is known as gene expression. In order to ensure precise and correct expression of genes, this complex, multi-step process is precisely regulated.

Gene expression starts with the process of transcription, during which the genetic code within the DNA of a gene is transcribed into RNA. Since transcription itself is tightly controlled, a predominant part of the regulation of gene expression occurs during this stage. Consequently, correct transcription is critical to an organism's health, since its misregulation is associated with a range of diseases, including cancer and developmental disorders [1].

Transcription of protein-coding genes in eukaryotic cells in carried out by RNA-polymerase II (Pol2), the enzyme which synthesizes the RNA molecule (or transcript), from the genomic DNA template. For transcription to occur, Pol2 binds to the core promoter of genes alongside general transcription factor (GTFs), which together form the pre-initiation complex (PIC) [2] (Fig. 1.1). Upon initiation, transcription subsequently begins from the transcription start site (TSS) within the core promoter of a gene.

However, the presence of the transcriptional machinery at the core promoter alone is generally not sufficient to drive efficient transcription. Rather, initiation and rate of transcription are largely dependent on the action of regulatory proteins known as transcription factors. Transcription factors typically exert their function by binding to regulatory DNA elements within the genome and subsequently recruiting co-regulatory factors [3, 4]. The combined action of genome-bound transcription factors and co-regulatory factors thus affects the assembly or activity of the PIC at promoters of associated genes [5] (Fig. 1.1). Interestingly, transcription factor binding sites can be found at varying distances, either upstream or downstream, from promoters of target genes [3, 4]. Moreover, in addition to regulating initiation of transcription, transcription factors can also influence the activity of Pol2 while it is actively transcribing, *i.e.* during the elongation stage of transcription [6].

Hence, due to their ability to control transcriptional initiation and activity, transcrip-

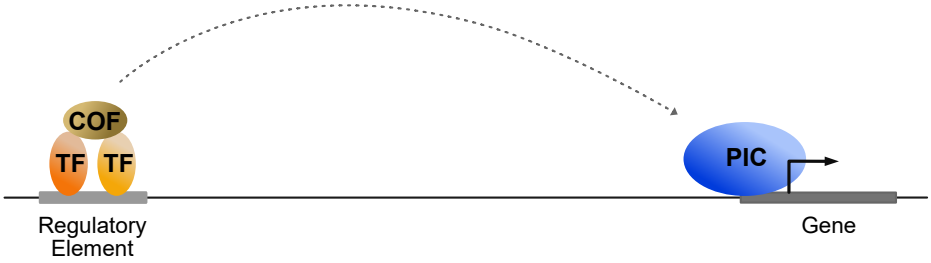

Fig. 1.1: Regulation of transcription by transcription factors. In the nucleus, transcription factors (TFs) bind to specific DNA regulatory elements and recruit cofactors (COFs), which together assert their regulaty effects on the pre-initation complex (PIC) at the promoter of target genes to affect transcription.

tion factors are the central regulators of transcription in cells. Notably, their actions increase the complexity of transcriptional regulation, which becomes particular apparent when considering that approximately 1,600 transcription factors are included within the human proteome [7]. Therefore, studying the action of individual transcription factors is an essential step in unraveling the regulatory processes shaping the transcriptional programs of cells.

1.2 The Glucocorticoid Receptor – a Hormone-Activated Transcription Factor

The glucocorticoid receptor (GR) is one of the most-studied transcription factors. GR is hormone-inducible, which means that it is activated upon binding to its ligand, *i.e.* glucocorticoids. Particular interest in researching the actions of GR, stem from the fact that this transcription factor is expressed in the majority human cell types [8]. Consequently, GR action affects various biological processes, including metabolism, inflammation, development and cognition [9, 10]. These properties have also made GR a very important therapeutic target, as synthetic glucocorticoids are widely applied in the treatment of chronic or acute inflammations [11, 12]. Moreover, GR has become a useful model system to study general mechanisms of transcriptional regulation. Due to its inducibility, measuring GR's direct effects on transcription is facilitated, since its activity can easily be controlled through the presence or absence of hormone.

Overall, GR's application as a powerful tool in molecular genetics as well as its broad physiological functions make GR an important and interesting transcription factor to study.

1.2.1 Glucocorticoids

Glucocorticoids are members of the steroid hormone family and are the primary stress hormones in mammals. Acting on numerous cell types, the effects of glucocorticoids are central to major biological processes, including glucose and lipid metabolism, inflammation, cognition, reproduction and development [9, 13, 14]. In particular due to their metabolic effects, which include enhanced gluconeogenesis and thus increased levels of blood glucose, glucocorticoids also play a notable role in the response to stress in mammals, as their actions provides the necessary energy to orchestrate the 'fight or flight' response [9, 13, 14].

In humans, the predominant glucocorticoid is cortisol which is synthesized in the *zona fasciculata* of the adrenal cortex. As is the case for all classic steroid hormones, cortisol is synthesized from a cholesterol precursor in a series of enzymatic reactions [15]. Under resting physiological conditions, cortisol is released from the adrenal cortex as short bursts in a near-hourly manner, resulting in oscillating plasma glucocorticoid levels [16, 17]. In addition to the rhythmic release, cortisol secretion also follows a circadian pattern with highest levels of secretion occurring at the beginning of the active period of the day [18]. This release pattern is established through the feedback loop of the hypothalamic-pituitary-adrenal (HPA) neuroendocrine axis (Fig. 1.2) [16–18]. The HPA axis establishes a negative feed-forward loop, in which corticotrophin-releasing hormone (CRH), secreted by the hypothalamus, triggers the release of adrenocorticotrophic hormone (ACTH) by the pituitary gland which subsequently stimulates glucocorticoid release from the adrenal cortex. Glucocorticoids, in turn, inhibit the production and secretion of CRH and ACTH. Moreover, the HPA neuroendocrine axis also becomes stimulated by physiological and psychological stressors resulting in increased glucocorticoid synthesis and secretion [16–19].

Furthermore, due to their potent inflammatory and immunosuppressive effects, synthetic glucocorticoids, *eg.* dexamethasone, are widely administered to treat patients suffering from inflammatory and autoimmune conditions, such as asthma or rheumatoid arthritis [11, 12]. However, long-term exogenous treatment with glucocorticoids can lead to severe side effects, such as osteoporosis, delayed wound healing and impaired glucose metabolism [13, 20]. In addition, glucocorticoid resistance can emerge in some patients in response to prolonged glucocorticoid therapy [20, 21]. Hence, since the molecular mechanisms underlying these adverse effects are incompletely understood, research into the actions of glucocorticoids remains critical.

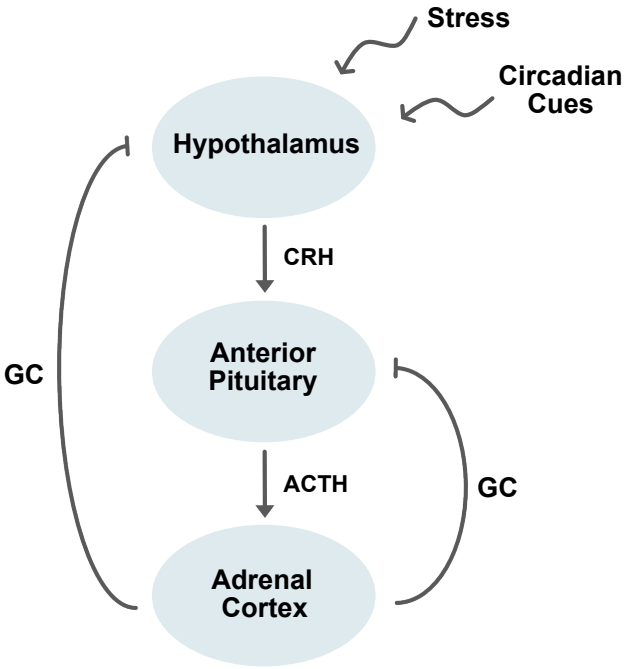

Fig. 1.2: Schematic illustration of the HPA neuroendocrine axis controlling glucocorticoid release. The negative feed-forward loop of the HPA axis establishes the oscillating pattern of glucocorticoid (GC) release. The hypothalamus secretes corticotrophin-releasing hormone (CRH), which stimulates the anterior pituitary gland to secrete adrenocorticotrophic hormone (ACTH). ACTH stimulates the adrenal cortex to secrete GC, which, in turn, inhibit the hypothalamus and the anterior pituitary. The HPA axis is also stimulated by circadian cues and stress, resulting in the release of GC.

1.2.2 GR - a Member of the Steroid Receptor Family

Glucocorticoids exert their biological functions by binding to and thereby activating GR, a hormone-inducible transcription factor and member of the steroid hormone receptor family.

Structurally, GR is composed of an N-terminal transactivation domain, a central DNA-binding domain, a short and flexible hinge region, and a C-terminal ligand-binding domain [22, 23]. Notable structural similarities are shared between GR and the other classical steroid receptors, *i.e.* the androgen receptor (AR), the mineralocorticoid receptor (MR) and the progesterone receptor (PR). This nuclear receptor subfamily is characterized by a highly conserved DNA-binding domain and therefore each receptor recognizes a very similar DNA sequence, the consensus motif of which is composed of two inverted repeats of the halfsite 5'-AGAACA-3', joined by a three-base pair spacer (Fig. 1.3) [23]. GR and the other steroid receptors generally bind to their DNA recognition sequence as homodimers in a head-to-head arrangement (Fig. 1.3) [23, 24].

Even though the binding preferences of the classical steroid receptors are highly similar, each receptor performs functionally distinct roles. Activation of AR, for instance, is critical in driving the male phenotype [26], while MR and PR are prominently involved

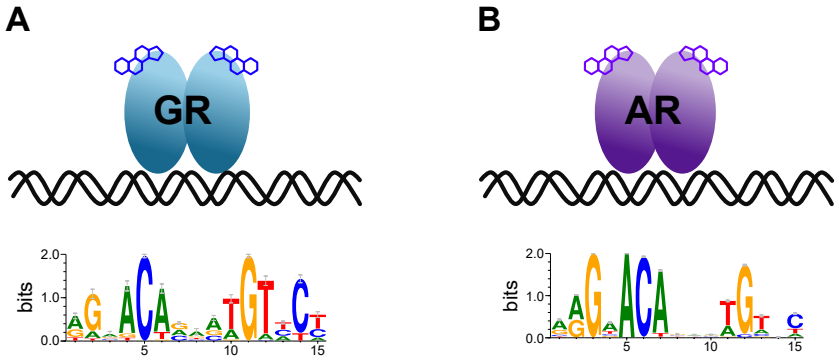

Fig. 1.3: Cartoon representation of GR and AR binding to DNA as homodimers. **(A)** Glucocorticoid-bound GR binds DNA as a homodimer is a head-to-head fashion. GR's consensus recognition sequence from JASPAR is shown below (MA0113.2; [25]). **(B)** Same as (A), but androgen-bound AR is shown. AR's consensus recognition sequence from JASPAR is shown below (MA0007.2; [25])

in blood pressure regulation [27] and the development of mammary glands [28], respectively. This functional diversification of related transcription factors, which recognize and bind to the same DNA consensus sequence, appears initially paradoxical and has been the topic of extensive research.

Particular interest has arisen in comparing genomic binding sites of GR to AR. Functionally, the two related receptors exhibit opposing roles, for instance, with GR action leading to muscle wasting [29] and AR action to muscle growth [30]. In part, the differing functional roles are likely to arise due to differences in genomic binding, since previous studies comparing the binding patterns of GR and AR found that, in the same cell types, the two receptors showed overlapping, yet also receptor-specific binding sites [31–33]. The fact that GR and AR have very similar DNA binding preferences and have structurally near-identical DNA-binding interfaces [34], raises the question of how the receptors achieve binding specificity at certain genomic sites.

Different explanations have been put forward to account for the observed binding specificities. Previous studies have identified a role of composite binding with the forkhead transcription factor FoxA1 to influence receptor-specific binding [33, 35]. Furthermore, there appear to be subtle differences in the exact motif sequence which GR and AR preferentially bind to. Specifically, AR exhibits the ability to bind more degenerate consensus sequences and also shows a preference for sites flanked by poly(A) sequences [32, 34]. Unlike GR, AR also seems to be capable of binding sequences composed of direct repeats of the 5′-AGAACA-3′ halfsite [36, 37], to which it binds in a head-to-head orientation [38].

Together, these findings suggest that GR and AR do show subtle differences in their binding preferences. However, it remains unclear whether the above-described differences account for all the observed binding specificities between GR and AR or whether other factors also play a role in shaping divergent genomic binding. Notably, since tran-

scription factors do not bind to 'naked' DNA in the nucleus, but rather bind to it in its 'packaged' or chromatinized form (as discussed in section 1.3), chromatin structure is a major determining factor which restricts or enables transcription factor binding [39–41]. This raises the question to what extent chromatin context also contributes to shaping differential binding of GR and AR.

1.2.3 GR - an Activator and Repressor of Transcription

Being expressed in most human cell types [8], GR regulates the transcription of a large number of target genes central to processes, such as metabolism, inflammation, development and cognition [9, 10].

In the absence of glucocorticoids, inactive GR is predominantly situated in the cytosol forming part of multi-protein complex consisting of heat shock proteins and other factors [42, 43]. This multi-protein complex aids in stabilizing GR, increases its ligand affinity and is also important in nuclear transport of GR [42, 43]. GR becomes activated upon glucocorticoid binding, causing it to translocate into the nucleus where it associates with various genomic loci and a multitude of other transcriptional regulatory factors. Interestingly, hormone-bound GR can act as both an activator and a repressor of transcription [44]. To gain a better understanding of how GR is able to activate some genes while repressing others, studying the mechanism by which GR regulates target gene expression is essential.

As an activator of transcription, GR is classically thought to directly bind DNA as a homodimer at its consensus recognition sequence (Fig. 1.3) [24, 45]. GR binding subsequently results in the recruitment of co-activators which, together with GR, affect the assembly or activity of the transcriptional machinery at the promoter of target genes. While this mode of action has frequently been put forward as the main mechanism by which GR mediates gene activation, GR-induced repression of transcription appears to be more complex, as a variety of potential mechanisms have been proposed.

Similar to activation, it has been suggested that GR can act as a repressor by directly binding to DNA. In this case, GR binding is thought to occur at repressive DNA motifs which are commonly referred to as the negative glucocorticoid response elements (nGREs) [46, 47]. However, there are ongoing discussions as to whether GR binding to such repressive sequences is, in itself, sufficient to repress transcription, since nGREs were identified in equal amounts near up- and downregulated genes in macrophages [48]. Moreover, GR is also thought to downregulate genes by tethering to other transcription factors, such as nuclear factor-κB (NFκB) or activator protein 1 (AP1), and thereby inhibit their functions [49–53]. However, recent studies oppose the notion that GR represses transcription via tethering, since there is increasing evidence that GR is able to directly bind to DNA at sites where it supposedly only tethers to [54–56]. Furthermore, GR binding to composite motifs together with other transcription factors has also been suggested as

mechanisms explaining downregulation of GR target genes [57]. In addition to models in which GR action directly represses transcription, there is also accumulating evidence that downregulation might be a consequence of the indirect effects of GR binding, since previous studies have reported repression which was not dependent on nearby GR occupancy [58–60]. Along these lines, the notion of 'cofactor squelching' has been proposed as a mechanisms for GR-induced repression, in which the redistribution of cofactors and other transcription factors away from genes results in their downregulation [58–62]. Taken together, multiple mechanisms by which GR mediates repression have been proposed, and the above described findings are summarized in Fig. 1.4. Thus, repression by GR might be inherently more complex than activation and therefore further research is required to better understand how GR represses transcription.

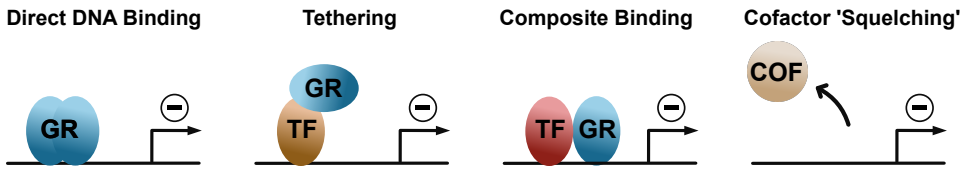

Fig. 1.4: Summary of proposed mechanisms by which GR represses transcription. Different mechanisms have been suggested to explain GR-mediated transcriptional repression, including (1) direct binding near repressed genes to negative response elements known as nGREs, (2) tethering to other transcription factors (TFs) and thereby inhibiting their activity, (3) composite binding together with other TF, and (4) indirect repression via cofactor (COF) 'squelching' or redistribution, in which GR competes for COFs of limited availability.

Experimentally, one of the most prominent methods to study transcriptional changes is RNA-sequencing (RNA-seq) [63], in which all RNA molecules of a population are sequenced, enabling their identification and quantification. A typical RNA-seq workflow involves the enrichment of mature transcripts, also known as messenger RNAs (mRNAs). However, studying transcriptional changes using this approach comes with its limitations. Specifically, active transcription cannot be captured accurately due to the presence of pre-existing mRNAs, whose levels are strongly influenced by their stability. To obtain a more accurate picture of the acute transcriptional processes, previous studies have proposed the analysis of intronic RNA sequences obtained from a total RNA-seq experiment, which does not enrich for mRNAs and therefore allows capturing intron-containing RNAs [64–66]. Since transcripts are generally co-transcriptionally spliced to remove intronic sequences [67], intron-containing molecules thus represent freshly-transcribed RNAs. Moreover, another limitation of classical RNA-seq is the fact that this method measures population averages and does not provide information on individual cells. To address this limitation, single-cell RNA sequencing has emerged as a powerful tool to study transcription of single cells [68]. In addition, non-sequencing-based methods to study single-cell transcription are available, such as RNA fluorescence *in situ* hybridization (FISH) [69], in

which transcripts-of-interest are targeted with fluorescently-labelled probes and can thus be detected using fluorescent microscopy.

1.3 The Role of Chromatin in GR-Mediated Transcriptional Regulation

In the nucleus of eukaryotic cells, DNA forms a complex with different proteins known as chromatin. Chromatin is composed of an array of nucleosomes, which represent the structural units of chromatin. Nucleosomes, in turn, consist of 146 base pairs (bp) of DNA tightly wound around a histone octamer consisting of two copies each of the core histone proteins H2A, H2B, H3 and H4 [70, 71]. This array of nucleosomes is further folded in the three-dimensional (3D) space forming higher-order chromatin structures [72]. As discussed in the following sections, the structure of chromatin does not only allow packaging of the DNA, but also adds an additional layer of regulation to the transcriptional processes of a cell.

1.3.1 Chromatin Accessibility

The packaging of DNA into an array of nucleosomes plays an important role in transcriptional regulation, as nucleosomes might cover regulatory DNA elements and thereby block transcription factors from binding [39–41]. Unsurprisingly, accessible chromatin sites, which are generally nucleosome-depleted, coincide with regulatory DNA sequences, such as promoters or transcription factor binding sites [73–75]. Further, chromatin accessibility has been described to be cell type-specific [74, 76, 77], underlining its regulatory importance in shaping differential transcriptional programs between cell types.

Experimentally, a wide range of methods have been established to measure chromatin accessibility in cells [78]. Recently, Assay for Transposase-Accessible Chromatin using sequencing (ATAC-seq), which is based on the usage of the Tn5 transposase that will insert itself into, and thereby fragment, accessible DNA [79], has emerged as one of the most powerful methods to profile chromatin accessibility.

Transcriptional regulation by GR is greatly influenced by chromatin accessibility. Specifically, GR binding to the genome largely follows the accessible chromatin landscape, as GR preferably associates to accessible sites [77, 80, 81]. Therefore, the differences in chromatin accessibility between cell types is one of the driving factors involved in establishing cell type-specific gene regulation by GR [77, 80, 81].

Not only is GR binding affected by chromatin accessibility, but GR binding, itself, also affects levels of chromatin accessibility. More specifically, GR has been described to induce increases in accessibility at its binding sites, a process often mediated through action

of the SWI/SNF chromatin remodeling complex [82–85]. Interestingly, this opening of chromatin has been shown to enable increased binding of other regulatory factors, a process commonly referred to 'assisted loading' [86]. Hence, GR-induced changes in chromatin accessibility influence gene expression, by making its binding sites more accessible to other regulatory factors which, in turn, can also affect transcription.

In addition to the notion that GR mainly binds previously accessible chromatin sites, there has been evidence that GR binding might also occur at 'closed' genomic regions, as GR has been shown to bind nucleosomal chromatin *in vitro* [87–89]. Interestingly, other studies have further suggested that GR can bind nucleosomal DNA and induce chromatin opening *in vivo* [90, 91]. These results indicate that GR can potentially act similar to a pioneer factor. Pioneer factors are a small group of transcription factors which are able to bind to DNA sequences within closed chromatin and subsequently induce chromatin remodeling [92]. Thus, pioneer factors play an important role during development, since their actions enable binding of other regulatory factors to sites which were previously inaccessible, thereby establishing novel transcriptional programs [92]. However, regarding GR and its potential to act in a pioneer-like fashion, further research is needed to characterize GR's ability to bind inaccessible DNA *in vivo* and to investigate the functional implications of such an ability.

In summary, gene regulation by GR and the accessible chromatin landscape are dynamically interconnected. While chromatin accessibility largely influences GR binding in a given cell type, GR binding, in turn, induces genome-wide changes in chromatin accessibility, thereby changing the availability of accessible binding sites for other transcription factors.

1.3.2 Histone Modifications

The histone proteins of the chromatin can be post-translationally modified by a variety of covalent modifications. These marks are dynamically deposited or removed by different enzymes [93, 94]. Notably, the types and levels of histone marks have been shown to correlate with the functional as well as transcriptional state of the DNA. For instance, the histone marks H3K27ac (acetylation at lysine 27 on histone 3), H3K4me1 (monomethylation at lysine 4 on histone 3) and H3K4me3 (trimethylation at lysine 4 on histone 3) are associated with transcriptionally active chromatin found at distal regulatory elements (H3K27ac, H3K4me1) or promoter regions (H3K4me3) [95, 96]. Marks, such as H3K27me3 (trimethylation on lysine 27 of histone 3) and H3K9me3 (trimethylation on lysine 9 of histone 3), on the other hand, are associated with transcriptional repression and heterochromatin [97, 98]. Rather than just correlating with various regulatory elements of the genome, histone modifications also directly affect transcription by recruiting or blocking regulatory proteins or altering chromatin accessibility [94].

One of the main experimental methods to study levels of histone modifications has

been by chromatin immunoprecipitation (ChIP) followed by sequencing (ChIP-seq) or quantitative polymerase chain reaction (ChIP-qPCR). In particular, this method relies on the usage of antibodies recognizing specific histone modifications (or any protein) on crosslinked and fragmented chromatin to immunoprecipitate the histone proteins of interest and any bound DNA sequences. After de-crosslinking, the co-precipitated DNA fragments are identified and quantified by sequencing or qPCR.

GR binding to the genome is positively correlated with the enhancer marks H3K27ac and H3K4me1, yet its binding does not exclusively occur at genomic sites harboring these marks [81, 91]. Furthermore, GR binding often results in changes in histone modification levels at its binding sites, particularly increases in H3K27ac and H3K4me1, through the action of recruited cofactors [99–101]. For instance, the histone acetyltransferase p300, which deposits H3K27ac across the genome [102], is frequently recruited to GR binding sites [61, 99, 103].

Together, similar to chromatin accessibility, GR binding is likely affected by the levels and types histone marks at its binding sites. In turn, GR binding can induce changes in histone modification levels through cofactor recruitment, reflecting the changes in functional state of its binding sites.

1.3.3 3D Genome Organization

In recent years, the importance of the structural organization of the genome in transcriptional regulation has become increasingly appreciated. The 3D structural arrangement of chromatin allows transcription factor binding sites, which are often found at long distances away from their target genes within the two-dimensional space, to be brought into physical contact with promoters via the formation of DNA-loops [104–106]. Hence, the 3D chromatin structure plays a major role in correct transcriptional regulation. In fact, changes of the 3D genome organization have been linked to disease. For instance, perturbations of the genome architecture leading to a re-wiring of long-range interactions were reported to cause limp malformations in mice [107].

Experimentally, chromatin conformation capture (3C)-based technologies represent powerful methods to study long-range chromosomal interactions on a genome-wide scale [108]. The classical 3C procedure starts by formaldehyde fixation, which crosslinks chromatin-bound proteins to each other and to DNA, to preserve the 3D interactions of chromatin segments. Subsequently, the fixed chromatin is digested with restriction enzymes and subjected to a DNA ligation step, in which the ends of crosslinked interacting fragments are thought to join at higher frequencies to one another than to non-interacting fragments. After de-crosslinking, PCR is subsequently performed targeting regions-of-interest to identify fragments which were joined to one another and, thus, represent likely interacting fragments. Other 3C-based methods differ from the classical 3C in the way the ligated

fragments are identified and quantified. Circularized chromosome conformation capture (4C), for instance, is a variant of 3C, in which the ligated DNA fragments are subjected to a second round of restriction enzyme digestion and DNA ligation, followed by an inverse PCR to amplify interacting fragments of a genomic region-in-interest. The amplified fragments are subsequently identified on a genome-wide scale by sequencing [109].

Regarding GR and the 3D genome structure, there is increasing evidence that long-range chromatin interactions also play an important role in GR-mediated transcriptional control. Specifically, GR-occupied genomic regions are often found to be several kilobases (kb) away from their target genes. For instance, in A549 cells, a human lung carcinoma cell line, more than 50% of glucocorticoid-activated genes exhibited a distance of >10 kb to their closest GR binding site [60]. In fact, in the same cell line, the majority of GR-occupied sites were found >3 kb from the TSS of any protein-coding genes [44]. Thus unsurprisingly, GR has been described to activate genes through long-range interactions, in which contacts between GR binding sites and target gene promoters are established through chromatin looping [101, 110, 111]. The importance of the 3D genome organization in shaping GR-mediated transcriptional processes becomes especially apparent with regards to a previous study which found that cell type-specific differences in pre-established 3D promoter-enhancer contacts determined of a GR-occupied enhancer regulated a nearby gene or not [112].

Regarding structural changes of the 3D chromatin organization induced by GR binding, previous studies, in which the authors applied sequencing-based 3C methods, showed that glucocorticoid treatment increased the interactions frequencies of pre-established long-range chromatin contacts [85, 110, 113]. Additionally, Jubb et al. [114] observed glucocorticoid-induced chromatin unfolding by DNA FISH.

Thus, transcriptional regulation by GR is influenced by the 3D structure of the chromatin and it appears that GR, in turn, is also able to induce structural chromatin changes upon activation.

1.4 Transcriptional Memory of Transient Stressors

Transcription is not a static, but rather a very dynamic process. Further, cells are capable of responding to changes in the environment by transiently altering their transcriptional output to maintain homeostasis. For example, exposure to excessive heat causes the well-studied heat shock response in cells, which results in transient changes in gene expression to protect the cells against the heat stress [115, 116]. To adapt to the occurrence of new stressors, some cells have evolved mechanisms to prime stress-responsive genes upon exposure to an initial stress signal. Consequently, this poised state results in an improved transcriptional response once the stressor is re-encountered, which can be

achieved through an altered expression rate or strength of primed genes upon reinduction [117, 118]. Hence, in these instances cells appear to be able to 'remember' exposure to an initial signal resulting in adaptation to environmental stressors at the transcriptional level.

This type of transcriptional memory in response to transient stressors has repeatedly been described in plants [119, 120]. Due to their inability to escape environmental stresses, transcriptional memory represents as essential coping mechanisms by which plants 'learn' to elicit more efficient transcriptional responses to upcoming stress [119, 120]. In mammalian cells, examples of transcriptional memory have been shown to occur in response to heat stress [121] as well as in response to interferon signaling of immune cells [122–125]. Interestingly, the stress memory in the mentioned examples can be maintained for a few days or even weeks [119–125]

A number of studies have highlighted a mechanistic role for chromatin in establishing transcriptional memory. In particular, gene priming can involve changes in the chromatin state which may be sustained through cell divisions in the absence of ongoing transcription [117]. Specifically, maintained increases in H3K4me2 and H3K4me3 at promoters of primed genes have been implicated in transcriptional memory [119, 120, 122, 123, 126] as well as the presence of poised Pol2 at promoters of primed genes [119–122]. In addition, there has also been evidence showing that signal-induced increases in chromatin accessibility underly transcriptional memory in T cells [124].

In summary, transcriptional memory of transient stressors is a coping strategy which allows cells to adapt to changes in their environment. An important player involved in gene priming appears to be chromatin which, due to its dynamically adjustable nature, allows the memory of environmental signals to be stored. With regards to GR and its ability to induce changes to the chromatin state, as discussed in section 1.3, the apparent question emerges at what point, or if at all, such changes can be propagated through cell divisions resulting in potential gene priming and, thus, transcriptional memory.

1.4.1 Transcriptional Memory upon GR Activation

Binding of GR to the genome results in epigenetic changes, involving histone modifications, chromatin accessibility and 3D chromatin organization, as discussed in previous sections (section 1.3). Previous studies have addressed the question of what happens to GR-induced chromatin changes after hormone is removed and GR becomes inactivated [85, 114, 127]. Interestingly, these studies have uncovered evidence that GR activation can result in long-term structural chromatin changes, indicating that a GR binding event can be 'remembered' by the chromatin.

Firstly, long-lasting changes to chromatin structure following GR activation have been described at the level of chromatin accessibility. At a mouse mammary tumour virus (MMTV)-derived sequence stably integrated into the genome of mouse L cells, GR bind-

ing resulted in increased DNase I-hypersensitivity which was detectable for more than 9 days after hormone washout [127]. Taking a genome-wide approach by DNase-seq, a more recent study found that GR binding resulted in increased levels of chromatin accessibility which, at some of its binding sites, was sustained after removal of hormone for 40 minutes [85]. Secondly, GR has also been described to induce more large-scale chromatin structural changes. Specifically, GR binding has been reported to induce chromatin decompaction near a small number of investigates genes, including the GR-target gene *FKBP5*, which was detected by DNA FISH in mouse macrophages [114]. These structural changes were found to be maintained for another 5 days, even though *FKBP5* transcription levels had returned to pre-hormone levels [114].

Together, these results suggest that GR binding can lead to long-lived chromatin-based changes. However, the findings of the above-mentioned studies were either reported after a very short hormone-washout period (*i.e.* 40 minutes, [85]) or at a small number of loci [114, 127]. Thus, further research is needed to assess GR's potential to induce long-term structural chromatin changes on a genome-wide scale and to determine whether any such changes can be maintained throughout cellular divisions.

1.5 Aim of the Thesis

The present thesis focuses on transcriptional regulation by GR and is aimed to provide a deeper understanding of the genomic effects of GR activation.

In the first part of the thesis, I explored the short and long-term effects of GR activation on chromatin and transcription. To this end, I studied changes in chromatin accessibility upon exposure to glucocorticoids and linked these to GR-induced transcriptional changes. To assess GR's potential to induce long-lived changes in chromatin accessibility, I studied levels of accessibility upon GR binding and following hormone washout. Additionally, I wanted to investigate if GR is capable of inducing transcriptional memory and to study the molecular mechanisms underlying potential gene priming.

In the second part, I investigated how transcription factors with near-identical DNA-binding domains and consensus DNA recognition sequences none-the-less bind to distinct genomic loci. To this end, I compared binding between GR to its related steroid receptor AR. Since both receptors have highly similar binding preferences, yet do not occupy exactly the same genomic regions, my objective was to explore to what extent chromatin accessibility and sequence composition affect receptor binding and contribute to driving receptor-specific binding.

2 Materials and Methods

2.1 Materials

2.1.1 General Labware

Laboratory consumables and general chemicals were purchased from the companies Eppendorf, Sarstedt, Thermo Fisher Scientific, Greiner Bio-One, Sigma-Aldrich, Carl Roth, Gibco, and Merck, unless stated otherwise.

2.1.2 Cell Lines

A549 (ATCC CCL-185): Human epithelial cell line established from the lung carcinoma of a 58-year-old patient (male, Caucasian).

U2OS-GR: The cell line was derived from the U2OS cell line, which is a human bone epithelial cell line established from the osteosarcoma of a 15-year-old patient (female, Caucasian). U2OS cells were genetically engineered to express rat GRα [128].

U2OS-AR: The cell line was derived from the same parental cell line as the U2OS-GR cells. U2OS cells were genetically engineered to express human AR. The cell line was generated by Marina Kulik [129].

2.1.3 Antibodies

Anti-GR (N499): polyclonal antibody recognizing residues 1-499 of the N-terminus of human GR (generated by R. M. Nissen, B. Darimont and K. R. Yamamoto)

Anti-H3K27ac: polyclonal antibody recognizing the acetylation at lysine 27 on histone 3 (Diagenode, Cat. No. C15410196).

Anti-H3K4me3: polyclonal antibody recognizing the trimethylation at lysine 4 on histone 3 (Diagenode, Cat. No. C15410003)

Anti-H3K27me3: polyclonal antibody recognizing the trimethylation on lysine 27 of histone 3 (Diagenode, Cat. No. C15410195)

Anti-RNA Polymerase II (8WG16): monoclonal IgG antibody recognizing the heptapeptide repeat of the C-terminal domain of the largest Pol2 subunit (Covance, Cat. No. MM2-126R)

Anti-phospho-RNA Pol II CTD (Ser5) (4H8): monoclonal IgG antibody recognizing phosphorylated Serine-5 of the C-terminal heptapeptide repeat of the largest Pol2 subunit (Thermo Fisher Scientific, Cat. No. MA1-46093)

2.2 Experimental Methods

2.2.1 Cell Culture

Culturing of Human Cell Lines

A549 and U2OS-GR cells were grown in Dulbecco's Modified Eagle Medium (DMEM, Gibco) containing 5% fetal bovine serum (FBS, Gibco). Culture conditions were maintained in a humidified incubator at 37°C and 5% CO2.

Hormone Treatments

Hormone Reinduction

A549 and U2OS-GR cells were subjected to two subsequent rounds of hormone or vehicle treatment, separated by a 24-hour (or 48-hour) washout period. To this end, cells were treated with 100 nM hormone (dexamethasone or hydrocortisone) or 0.1% ethanol for 4 hours. To remove the hormone, cells were washed twice with phosphate buffered saline (PBS) and grown for 24 hours (or 48 hours) in hormone-free medium. After the 24-hour (or 48-hour) washout period, cells were treated again with 100 nM hormone (dexamethasone or hydrocortisone) or 0.1% ethanol for 4 hours. Cells were 80-90% confluent upon harvest.

For the hormone reinduction treatment involving three rounds of hormone treatment, cells were treated as described above, but washed again with PBS after the second treatment and further cultured in hormone-free medium. 48 hours after the initial washout, cells were treated for a third time with 100 nM hormone (dexamethasone or hydrocortisone) or 0.1% ethanol for 4 hours.

For the hormone reinduction treatment involving a time-course treatment, cells were treated with 100 nM dexamethasone or 0.1% ethanol for 4 hours. Subsequently, cells were washed twice with PBS and cultured for 24 hours in hormone-free medium. Next, cells were treated with 0.1% ethanol for 4 hours or 100 nM dexamethasone for 0, 1, 2, 3 or 4 hours.

Hormone Washout
A549 cells were treated for 20 hours with 100 nM dexamethasone, 100 nM hydrocortisone or 0.1% ethanol and (1) harvested directly upon treatment or (2) washed twice with PBS to remove hormone and grown for 24 hours in hormone-free medium. Cells were 80-90% confluent upon harvest.

For the hormone washout treatment in U2OS-GR cells, cells were treated for 4 hours with 100 nM dexamethasone or 0.1% ethanol and (1) harvested directly upon treatment or (2) washed twice with PBS to remove hormone and grown for 24 hours in hormone-free medium.

2.2.2 Quantification of Gene Expression by Quantitative Reverse Transcription Polymerase Chain Reaction

RNA Isolation

A549 and U2OS-GR cells were grown in 6-well cell culture plates. Following hormone re-induction treatment (see section 2.2.1), 1 million cells were harvested for RNA isolation with the RNeasy Mini Kit (QIAGEN), following the manufacturer's protocol.

cDNA Synthesis

cDNA was synthesized with the PrimeScript RT Reagent Kit (TaKaRa) according to the manufacturer's instructions, using the supplied random 6-mers and oligo dT primer for reverse transcription of 500 ng RNA.

Quantitative Reverse Transcription Polymerase Chain Reaction

DNA content was quantified by quantitative reverse transcription polymerase chain reaction (RT-qPCR) using a home-made qPCR master mix of the following composition: 100 mM Tris-HCl pH 8.3, 6 mM $MgCl_2$, 1 mg/ml bovine serum albumin, 4 mM dNTP mix, 0.66x SYBR Green, 1x ROX reference dye, 0.2 U/µl perpetual Taq DNA polymerase (EURx). cDNA samples were diluted 1:10 and the qPCR reaction was prepared as shown in Table 2.1.

Table 2.1: qPCR Reaction

Template DNA	2 µl
Primer Mix (0.66 µM)	3 µl
qPCR Master Mix	5 µl
Reaction Volume	10 µl

Primers used for gene expression analysis are shown in Table 5.1. For each sample, two technical duplicates were included. The reactions were run on a real-time PCR machine (ABI 7900 HT or QuantStudio 7 Flex by Applied Biosystems) with thermal cycling conditions as shown in Table 2.2. For each sample, expression results were normalized to the housekeeping gene *RPL19*.

Table 2.2: qPCR Thermal Cycling Conditions

Initial Denaturation	95 °C	10 min	100 % ramp rate
Cycles 40x			
Denaturation	95 °C	15 sec	100 % ramp rate
Amplification	60 °C	1 min	100 % ramp rate
	95 °C	15 sec	100 % ramp rate
Dissociation Curve	60 °C	15 sec	100 % ramp rate
	95 °C	15 sec	2 % ramp rate

2.2.3 Total RNA-seq

A549 cells were grown in 6-well cell culture plate and treated according to the hormone reinduction treatment (section 2.2.1). After hormone treatment, 1 million cells were harvested and total RNA was isolated with the RNeasy Mini Kit (QIAGEN), following the manufacturer's protocol. Samples were submitted to the Sequencing Core Facility of the Max Planck Institute for Molecular Genetics where the RNA was further processed using the KAPA RNA HyperPrep Kit with RiboErase (Roche) to deplete ribosomal RNA (rRNA) and prepare sequencing libraries. Libraries were subsequently sequenced on an Illumina HiSeq4000 (paired-end).

2.2.4 Chromatin Immunoprecipitation

For chromatin immunoprecipitation (ChIP) experiments, the following antibodies and amounts were used per 2.5 million cells: 2 µl of anti-GR antibody (N499), 1.4 µg of anti-H3K27ac antibody (Diagenode, Cat. No. C15410196), 1.4 µg of anti-H3K4me3 antibody (Diagenode, Cat. No. C15410003), 1.4 µg of anti-H3K27me3 antibody (Diagenode, Cat. No. C15410195), 2 µg of anti-RNA Polymerase II (8WG16) (Covance, Cat. No. MM2-126R), 2 µg of anti-phospho-RNA Pol II CTD (Ser5) (4H8) (Thermo Fisher Scientific, Cat. No. MA1-46093). For ChIP experiments intended for subsequent quantification by qPCR (ChIP-qPCR), 2.5 million cells were harvested, while for ChIP experiments followed by sequencing (ChIP-seq), 30 million cells were harvested.

Technical assistance for the steps from crosslink to purification was received from Edda Einfeldt.

Cell Harvest and Crosslink

Cells were grown in 10 cm cell culture dishes and subjected to the appropriate hormone treatment as described in section 2.2.1. Directly following hormone treatment, cells were crosslinked for 3 minutes at room temperature by the addition of formaldehyde to a final concentration of 1%. The crosslinking reaction was quenched with 125 mM glycine at 4°C for 10 minutes. Having discarded the medium, the cross-linked cells were rinsed with ice-cold PBS and subsequently incubated with 10 mL PBS at 4°C for 5 minutes. For harvest, cells were scraped off the cell culture dish and transferred to a Falcon tube containing ice-cold PBS. Cells were centrifuged at 645 g at 4°C for 5 minutes. Finally, the supernatant was aspirated before snap-freezing and storing the cells at -80°C.

Cell Lysis and Chromatin Fragmentation

To lyse the cells, pellets were resuspended with 2 mL ice-cold IP lysis buffer (50 mM HEPES-KOH pH 7.4, 1 mM EDTA, 150 mM NaCl, 10% (v/v) glycerol, 0.5% (v/v) Triton X-100) supplemented with 0.5% (v/v) proteinase inhibitor cocktail set III (EDTA-free, Merck) and 0.5 mM PMSF. Following nutation at 4°C for 30 minutes, the suspension was centrifuged at 645 g at 4°C for 5 minutes and the resulting pellets were resuspended in 1 ml ice-cold RIPA buffer (10 mM Tris-HCl pH 8.0, 1 mM EDTA, 150 mM NaCl, 5% (v/v) glycerol, 0.1% (v/v) sodium deoxycholate, 0.1% (w/v) sodium dodecyl sulfate (SDS), 1% (v/v) Triton X-100) supplemented proteinase inhibitors and PMSF as before. The samples were subsequently split into three parts by transferring 330 µl to one of three 1.5 ml tubes. To fragment the chromatin, a Biorupter (Diagenode) placed at 4°C was used to sonicate the sample at high intensity for 24 cycles (30 seconds on, 30 seconds off). The three parts per sample were re-combined into one. As a next step, the fragmented chromatin was centrifuged at maximum speed at 4°C for 20 minutes and the resulting supernatant was transferred to a new 1.5 ml tube. Having added 400 µl RIPA buffer supplemented proteinase inhibitors and PMSF to the cellular lysate, 50 µl per sample were transferred to a new tube and stored at 4°C to serve as genomic input control at a later stage.

Immunoprecipitation

Immunoprecipitation was carried out by adding the indicated amount of antibody (see above) to each sample and nutating the tubes overnight at 4°C. To prepare the Protein A/G Agarose Beads (50% slurry, Santa Cruz Biotechnology), 33 µl beads per ChIP were pelleted by centrifugation (1000 g, 1 minute), washed twice with 1 ml RIPA buffer (supplemented proteinase inhibitors and PMSF as before), and left to incubated overnight at 4°C in 1 ml RIPA buffer. The next day, the beads were centrifuged (1000 g, 1 minute) and the RIPA buffer was removed. To each sample, 30 µl beads were added and the tubes were nutated at 4°C for 4 hours. After the incubation period, the beads were centrifuged (1000

g, 1 minute) and the supernatant removed before subjecting the beads to six washes with 1 ml RIPA buffer containing 500 mM NaCl. After the last wash, the beads were pelleted (1000 g, 1 minute) and all supernatant was carefully removed.

Crosslink Reversal and Purification

To reverse the crosslink, 75 µl crosslink reversal solution (10 mM Tris-HCl pH 8.0, 1 mM EDTA, 0.7% (w/v) SDS, 0.22 mg/ml proteinase K) was added to each sample. At the same time, 60 µl cross-link reversal solution was added to the genomic input control which had been set aside after sonication. The samples were incubated at 55°C for 3 hours and subsequently at 65°C overnight. DNA was purified using the Wizard® SV Gel and PCR Clean-Up System kit (Promega).

Quantification by qPCR and Sequencing

For ChIP-qPCR, ChIP samples were diluted 1:4 and the qPCR analysis was essentially performed as described in section 2.2.2, but using the SYBR Green PCR Master Mix (Thermo Fisher Scientific). Primers used for ChIP-qPCR are shown in Table 5.3.

ChIP samples for sequencing were submitted to the Sequencing Core Facility of the Max Planck Institute for Molecular Genetics where ChIP-seq libraries were generated using the Kappa HyperPrep Kit (Roche). Libraries were subsequently sequenced on an Illumina HiSeq4000 (single-end).

2.2.5 Assay for Transposase-Accessible Chromatin

Assay for Transposase-Accessible Chromatin using sequencing (ATAC-seq) was essentially performed as described in [130].

Cell Harvest and Lysis

Cells were grown in 6-well cell culture dishes and subjected to the appropriate hormone treatment as described in section 2.2.1. After hormone treatment, cells were trypsinized and 100,000 cells were resuspended in DMEM and pelleting by centrifugation at 500 g for 5 minutes at 4°C. Having removed the supernatant, cells were resuspended in 50 µl ice-cold Resuspension Buffer Plus (10 mM Tris-HCl pH 7.4, 10 mM NaCl, 3 mM $MgCl_2$, 0.1% (v/v) Tween-20, 0.1% (v/v) Igepal CA-630, 0.01% (w/v) Digitonin) by pipetting up and down three times, and subsequently incubated for 3 minutes on ice. Next, 1 ml ice-cold Resuspension Butter (10 mM Tris-HCl pH 7.4, 10 mM NaCl, 3 mM $MgCl_2$, 0.1% (v/v) Tween-20) was added and the components were carefully mixed by inverting the tube three times. The lysed cells were centrifuged at 500 g for 10 minutes at 4°C and the supernatant was removed.

Transposition Reaction and Purification

The Transposition Mix was freshly prepared by combining the following components: 25 µl 2x TD buffer (Illumina Cat. No. FC-121-1030), 2.5 µl TDE1 (Tn5 Transposase, Illumina Cat. No. FC-121-1030), 16.5 µl PBS, 0.5 µl 1% (w/v) digitonin, 0.5 µl 10% (v/v) Tween-20, 5 µl H_2O). To start the transposition reaction, the nuclei were resuspended in 50 µl Transposition Mix by pipetting up and down six times, and subsequently incubated at 37°C for 30 minutes while shaking at 1000 rpm. During this step, the Tn5 transposase fragments accessible DNA and simultaneously tags it with sequencing adaptors. The transposition reaction was stopped through the addition of 2.5 µl of 10% (w/v) SDS per sample. Finally, the transposed DNA was purified using the DNA Clean and Concentrator Kit (Zymo) as recommended by the manufacturer.

PCR Amplification and Purification

The sequencing libraries were prepared by PCR-amplifying the transposed DNA. The PCR reaction was prepared as shown in Table 2.3, using primers depicted in Table 5.2. The reaction was subjected to thermocycling conditions shown in Table 2.4.

Table 2.3: PCR Reaction for ATAC Library Amplification

Transposed DNA	20 µl
Universal Primer (fw) (25 µM)	2.5 µl
Barcode Primer (rev) (25 µM)	2.5 µl
NEBNext High-Fidelity 2x PCR Master Mix	25 µl
Reaction Volume	50 µl

Table 2.4: Thermal Cycling Conditions for ATAC Library Amplification

Annealing/Extension	75 °C	5 min
Denaturation	98 °C	30 sec
Cycles 11x		
Denaturation	98 °C	10 sec
Annealing	63 °C	30 sec
Extension	72 °C	1 min

The resulting PCR products were purified using the Agencourt AMPure XP beads (Beckman Coulter). Specifically, a double size selection was carried out by (1) using a 0.7x beads-to-sample ratio and keeping the supernatant while discarding the beads to remove large DNA fragments and (2) using a 1.8x beads-to-sample ratio and purifying according to the manufacturer's recommendations to remove primer dimers.

Quantification by Sequencing and qPCR

ATAC-seq libraries were submitted for Illumina sequencing (paired-end) on a HiSeq4000.

For ATAC followed by qPCR (ATAC-qPCR), 2 ng per final sequencing library were quantified by qPCR as described in section 2.2.2 using primers shown in Table 5.3. A genomic DNA (gDNA) control was also included in the qPCR quantification to be used as reference against which the samples were normalized.

2.2.6 Circularized Chromatin Conformation Capture

Circularized Chromatin Conformation Capture (4C) template and sequencing library preparations were essentially carried out as described in [131, 132], respectively.

Hormone Treatment and Crosslinking, Cell Lysis

A549 cells were grown in 10 cm cell culture dishes and treated according to the hormone reinduction treatment (section 2.2.1). After hormone treatment, 5 million cells were harvested and pelleted by centrifugation at 280 g for 5 minutes. To crosslink the cells, cells were resuspended in 10 ml fixation buffer (2% formaldehyde in PBS/10% FBS) and incubated at room temperature for 10 minutes while tumbling. To quench the reaction, ice-cold glycine was added to obtain a final concentration of 125 mM and the tubes were subsequently placed on ice. The fixation buffer was removed by centrifuging the cells at 400 g for 8 minutes at 4°C and aspirating the supernatant. The cells were resuspended in 5 mL of freshly-prepared, ice-cold lysis buffer (50 mM Tris-HCl pH 7.5, 150 mM NaCl, 5 mM EDTA, 0.5% (v/v) NP-40, 1% (v/v) Triton X-100, 0.5% (v/v) proteinase inhibitors) and incubated on ice for 15 minutes. Next, cells were centrifuged at 500 g for 5 minutes at 4°C and the resulting cell pellet resuspended in 1080 µl ddH_2O.

1st Restriction Enzyme Digest

Each sample was split into three parts by transferring 360 µl to three fresh 1.5 ml tubes. From this point onwards, until stated otherwise, the instructions apply to one part of the sample. To each tube, 60 µl of 10x Csp6I restriction enzyme buffer (Thermo Fisher Scientific) was added. Next, 15 µl of 10% (w/v) SDS was added to each tube and samples were incubated for 1 hour at 37°C while shaking at 900 rpm to remove non-cross-linked proteins. To sequester the SDS, 75 µl of 20% (v/v) of Triton X-100 was added and tubes were again incubated for 1 hour at 37°C under constant shaking at 900 rpm. Next, 5 µl per sample were transferred to a new tube and stored at 4°C to serve as an 'undigested control' at a later stage. The digest was started by adding 600 µl of 1x Csp6I restriction enzyme buffer as well as 133 U Csp6I (Thermo Fisher Scientific) and incubating the reaction at 37°C while shaking at 900 rpm. Further 66 U of Csp6I were added for overnight

incubation and again the next morning for another 4-hour incubation, while continuously keeping the tubes at 37°C and shaking at 900 rpm. After the restriction enzyme digest, 5 µl per sample were transferred to a new tube to serve as a 'digested control' and digestion efficiency was determined before continuing with the protocol. For this purpose, the 'undigested' and 'digested' controls were diluted with 90 µl and 40 µl of 10 mM Tris-HCl (pH 7.5), respectively. RNAs were degraded by the addition of 5 µl RNase A (10 mg/µl, Thermo Fisher Scientific) to each control and incubating at 37°C for 1 hour. Next, 2.5 µl of proteinase K (20 mg/µl, Thermo Fisher Scientific) was added per tube, followed by a 1-hour incubation at 65°C. The samples were loaded onto a 1% agarose gel to inspect the DNA fragment size distribution of the 'undigested' and 'digested controls'.

1st Ligation

Before continuing with the ligation, Csp6I was inactivated by incubating the samples at 65°C for 20 minutes. The ligation reaction was assembled in 50 ml Falcon tubes by combining each sample with 700 µl of 10x ligation buffer (660 mM Tris-HCl pH 7.5, 50 mM $MgCl_2$, 10 mM DTT, 10 mM ATP) and filling up with ddH_2O to 7 ml. Finally, 50 U ligase (Roche) was added, and the reaction was incubated at 16°C overnight. The next morning, 100 µl per sample was transferred to a new 1.5 ml tube to check the ligation efficiency. Following an incubation at 37°C for 1 hour after the addition of 5 µl RNase A (10 mg/µl) and a subsequent incubation at 65°C for 4 hours after adding 2.5 µl proteinase K (20 mg/µl), the ligation controls were loaded onto a 1% agarose gel to inspect the DNA fragment size distribution.

Crosslink Reversal and Purification

The ligated DNA was de-crosslinked by adding of 15 µl proteinase K (20 mg/µl) and incubating overnight at 65°C. The next day, 30 µl RNase A (10 mg/µl) was added and the samples were incubated at 37°C for 45 minutes. To extract DNA, each sample was mixed with 7 ml with phenol-chloroform and centrifuged at 3000 g for 15 minutes. Having transferred the water phase to a fresh tube, 7 ml ddH_2O, 1 ml of 3 M NaAC (pH 5.6), 7 ul glycogen (20 mg/µl) and 35 ml of 100% ethanol were added. The samples were places at -80°C until frozen solid. The DNA was pelleted by centrifugation at 8000 g for 20 minutes at 4°C, washed with 10 ml cold 70% ethanol and subsequently centrifuged again at 3000 g for 15 minutes at 4°C. Finally, the resulting DNA pellet was air-dried at room temperature and resuspended in 50 µl of 10 mM Tris-HCl (pH 7.5). The three parts were combined into one again.

2nd Restriction Digest and Ligation

The second restriction digest was performed by adding 60 U of the restriction enzyme DpnII (Thermo Fisher Scientific) and 50 µl of x DpnII restriction buffer (Thermo Fisher Scientific) to each sample, and filling the reaction up with ddH_2O to obtain a final volume of 500 µl. Subsequently, the samples were incubated at 37°C overnight. The next morning, the restriction digestion efficiency was determined by diluting a 10-µl aliquot per sample 1:1 with 10 mM Tris-HCl (pH 7.5) and loading it onto a 1% agarose gel to inspect the DNA fragment size distribution. Next, DpnII was inactivated by incubating the samples at 65°C for 25 minutes, after which each sample was transferred to a 50 ml Falcon tube. To start the 2nd ligation, 1.4 ml of 10x ligation buffer (660 mM Tris-HCl pH 7.5, 50 mM $MgCl_2$, 10 mM DTT, 10 mM ATP), 100 U T4 DNA ligase (Roche) and ddH_2O (filling up to a final volume of 14 ml) were added and the tubes were incubated at 16°C overnight. The ligation efficiency was investigated by loading a 20 µl sample onto a 1% agarose gel and inspecting the DNA fragment size distribution. As a next step, 940 µl of NaAC (pH 5.6, 3 M), 7 µl glycogen (20 mg/µl) and 35 ml of 100% ethanol were added and the tubes were placed at -80°C until frozen solid. DNA was pelleted by centrifugation at 8300 g for 45 minutes at 4°C. After removing the supernatant, 15 ml ice-cold 70% ethanol was added and the samples were centrifuged again at 3300 g for 15 minutes at 4°C. Having air-dried the pellets at room temperature, DNA was dissolved in 150 µl of 10 mM Tris-HCl (pH 7.5) and purified with the QIAquick PCR Purification Kit (QIAGEN) using three columns per sample, but otherwise following the manufacturer's recommendations. The final 4C template was eluted in 50 µl of 10 mM Tris-HCl (pH 7.5) per column and the three parts were re-combined.

Sequencing Library Preparation

The 4C sequencing libraries were prepared by performing two PCR steps per viewpoint to (1) amplify the DNA sequences ligated to the viewpoint and (2) attach the Illumina sequencing adaptors to the fragments.

The first PCR was carried out using the Expand Long Template PCR-System (Roche) and viewpoint-specific primers shown in Table 5.4. Per viewpoint, four PCR reactions were prepared as shown in Table 2.5 and subjected to thermocyling conditions shown in Table 2.6. After the first PCR, the four PCR reactions were combined. Per sample, 50 µL was transferred to a new tube and purified using Agencourt AMPure XP beads (1.5x beads-to-sample ratio, Beckman Coulter).

The second PCR step was performed using primers shown in Table 5.5. The PCR reaction was prepared as depicted in Table 2.7 and subjected to thermocyling conditions as shown in Table 2.8. The PCR products were purified twice with QIAquick PCR Purification Kit (QIAGEN). The final 4C-seq libraries were submitted for Illumina sequencing

(single-end) on a MiSeq.

Table 2.5: PCR Reaction for 4C Library Amplification (1st PCR)

4C Template	200 ng
10× PCR Buffer	5 µl
dNTP (10 mM)	1 µl
Forward Primer (5 µM)	5 µl
Reverse Primer (5 µM)	5 µl
Expand Long Template Polymerase mix	0.7 µl
ddH_2O	X µl
Reaction Volume	50 µl

Table 2.6: Thermal Cycling Conditions for 4C Library Amplification (1st PCR)

Denaturation	94 °C	2 min
Cycles 16x		
Denaturation	94 °C	10 sec
Annealing	55 °C	1 min
Extension	68 °C	3 min
Final Extension	68 °C	5 min

Table 2.7: PCR Reaction for 4C Library Amplification (2nd PCR)

Purified PCR Product	5 µl
10× PCR Buffer	5 µl
dNTP (10 mM)	1 µl
Primer Mix (5 µM)	5 µl
Expand Long Template Polymerase mix	0.7 µl
ddH_2O	X µl
Reaction Volume	50 µl

Table 2.8: Thermal Cycling Conditions for 4C Library Amplification (2nd PCR)

Denaturation	94 °C	2 min
Cycles 20x		
Denaturation	94 °C	10 sec
Annealing	55 °C	1 min
Extension	68 °C	3 min
Final Extension	68 °C	5 min

2.2.7 RNA Fluorescence in situ Hybridization

Probes

RNA FISH was performed targeting mRNA of human *ZBTB16* and *FKBP5*. The probe sets were purchased from Stellaris (Biosearch Technologies, Inc., Petaluma, CA) and hy-

bridized to the dye Quasar 570. The *FKBP5*-probes had been pre-designed by Stellaris (Cat. No. VSMF-2130-5). For *ZBTB16*, the probes were designed to recognize the complete coding sequence (GenBank: BC029812.1) using the Stellaris RNA FISH Probe Designer (Biosearch Technologies, Inc., Petaluma, CA) available online at www.biosearchtech.com/stellarisdesigner (version 4.2).

Cell Culture, Hormone Treatment, Crosslink, Hybridization

A549 cells were grown on cover glasses (18 mm, No. 1, round) placed within 12-well cell culture plates. Cells were treated according to the hormone reinduction treatment described in section 2.2.1. RNA FISH was carried out following the Stellaris RNA FISH Protocol for Adherent Cells (www.biosearchtech.com/stellarisprotocols). Briefly, cells were washed with 1 mL PBS and subsequently crosslinked with 1 mL fixation buffer (3.7% (v/v) formaldehyde in PBS) for 10 minutes at room temperature. Cells were washed twice with PBS and permeabilized by adding 1 ml 70% (v/v) ethanol and incubating at 4°C for a minimum of one hour. After removing the ethanol, the cover glasses were washed in 1 ml Wash Buffer A (10% (v/v) formamide in Stellaris RNA FISH Wash Buffer A (Biosearch Technologies)). Next, the cover glasses were transferred to a humidified chamber and placed (cell-side down) onto 100 µl hybridization buffer (10% (v/v) formamide in Stellaris RNA FISH Hybridization Buffer (Biosearch Technologies)) supplemented with 1 µl probe (12.5 µM stock). The humidified chamber was closed and sealed and incubated overnight in the dark at 37°C. The next morning, the cover glasses were placed in a 12-well plate and incubated in the dark in 1 ml Wash Buffer A (10% (v/v) formamide in Stellaris RNA FISH Wash Buffer A (Biosearch Technologies)) at 37°C for 30 minutes. To counterstain the DNA, the cover glasses were incubated in the dark in 1 ml nuclear counterstain solution (5 ng/µl DAPI (Thermo Fisher Scientific) in Wash Buffer A) at 37°C for 30 minutes. Finally, samples were washed with 1 ml Wash Buffer B (Biosearch Technologies) and mounted with Antifade Mounting Medium (Vectashield).

Image Acquisition

Images were captured using a 100x/1.4 NA Oil Immersion Objective on an Axio Observer.Z1/7 (Zeiss) running under ZEN 2.3. Per sample, 10 replicate tile regions were determined. Z-stacks of 26 slices were acquired, with the center of the stack being the focused image (adjusted visually on the nuclear counterstaining). The distance between slices was set to 0.25 µm, resulting in a total stack thickness of 6.25 µm.

2.3 Computational Methods (Results Part 1)

2.3.1 RNA-seq Analysis

Downloading Additional RNA-seq Data Sets

The following publicly available ChIP-seq data set was downloaded from ArrayExpress:

mRNA-seq in U2OS-GR cells: cells were treated with 1 μM dexamethasone or ethanol for 4 hours (3 replicates); ArrayExpress accession number E-MTAB-6738; generated by Marina Kulik (Meijsing Lab, Max Planck Institute for Molecular Genetics, Berlin); [133]

Data Pre-processing and Visualization

Reads from total RNA-seq data for A549 cells and mRNA-seq data for U2OS-GR cells were mapped to the human reference genome hg19 utilizing the sequence alignment tool *STAR v2.7.0a* [134] under default parameters. *SAMtools v1.10* [135] was subsequently used to convert Sequence Alignment Map (SAM) files to Binary Alignment Map (BAM) format and subsequently discard reads with a mapping quality score of less than 10.

Having merged replicate BAM files using *SAMtools*, the resulting merged BAM files were converted into bigWig format with the *deepTools v3.4.1* [136] function *bamCoverage*. The option *–normalizeUsing RPKM* was set, to obtain sequencing depth-normalized bigWig files, which were subsequently loaded into the Integrative Genomics Viewer (IGV) genome browser [137] for visualization.

Differential Expression Analysis in A549 and U2OS-GR Cells

Previous studies have shown that analyzing intron coverage, rather than exon coverage, from a total RNA-seq experiment provides information on nascent transcription [64–66]. Thus, to capture changes in active transcription in A549 cells, only reads which mapped to intronic regions of genes were counted and used as input for the differential gene expression analysis.

Gene coordinates for the hg19 reference genome were obtained the NCBI RefSeq annotation available from the UCSC Genome Browser [138]. For genes which have more than one transcript variant, only the coordinates of the longest transcript variant were included in the analysis. For this purpose, the information on the longest transcript variants were extracted from the annotation file using *Python v3.7*.

The following steps were performed in *R v3.6.3*: Intron coordinates were extracted from the annotation file using the function *intronicParts* of the *GenomicFeatures v.1.38.2* package [139]. Intronic regions associated with multiple genes were discarded. Similarly, intronic regions overlapping exons were also removed. To this end, exon coordi-

nates of all transcript variants were extracted from the annotation file using the *exonicParts* function (*GenomicFeatures*). The GRanges objects of intron and exon coordinates were combined and the function *disjoin* (*GenomicFeatures*) applied to the combined object. Finally, regions where introns and exons overlapped were discarded using the function *subsetByOverlaps* (*GenomicFeatures*). Reads mapping to the resulting list of intronic regions were subsequently counted using *featureCounts* [140] of the *Rsubread* package [141] and setting the following options: *isPairedEnd=TRUE, primaryOnly=TRUE, requireBothEndsMapped=TRUE, countChimericFragments=FALSE, useMetaFeatures=FALSE*. After counting, the sum of all intronic reads per gene was calculated. Differential gene expression analysis was subsequently carried out with the *DESeq2 v1.26.0* package [142]. MAplots were generated using the *plotMA* function of *DESeq2*.

For U2OS-GR cells, mRNA-seq data was available and, therefore, reads which mapped to exon regions were counted and used as input for the differential gene expression analysis. The list of exon regions from the longest transcript variants per gene was obtained by applying the *exonicParts* function (*GenomicFeatures*) and setting *linked.to.single.gene.only=TRUE*. To remove regions which associated with multiple genes, *disjoin* (*GenomicFeatures*) was called. Counting of the reads, as well as the subsequent differential gene expression analysis were done as detailed above for the A549 cells.

2.3.2 ATAC-seq Analysis

Data Pre-Processing

ATAC-seq paired-end reads were mapped to the hg19 reference genome using the alignment tool *Bowtie2 v2.1.0* [143] and setting the option *–very-sensitive*. Next, *SAMtools v1.10* [135] was utilized to convert the resulting SAM file to a BAM format. To only retain reads of a high alignment quality, reads with a mapping quality score of less than 10 were filtered out using *SAMtools*. Next, duplicated reads were discarded using the *MarkDuplicates* function from *Picard tools v.2.17.0* (http://broadinstitute.github.io/picard/), to remove any PCR duplicates generated during ATAC-seq library preparation. Lastly, reads were shifted using the function *alignmentSieve* from *deepTools v3.4.1* [136] and setting the option *–ATACshift*, to compensate for the 9-bp sequence duplication created at the transposon insertion site [79].

Defining Sites of Increasing, Decreasing, and Non-changing Chromatin Accessibility

Genomic regions were defined which showed increasing ('opening site'), decreasing ('closing site') or unchanging ('non-changing site') chromatin accessibility upon hormone treatment.

For A549 cells, the ATAC-seq data for dexamethasone, hydrocortisone- and ethanol-treated cells (no washout) were used to define these regions. To obtain opening sites,

peak calling was performed using *MACS2 v2.1.2* [144] (*–broad –broadcutoff 0.001*), by separately calling peaks in the dexamethasone-treatment over ethanol-treatment as well as in the hydrocortisone-treatment over ethanol-treatment. To obtain closing sites, the same *MACS2* settings were used to call peaks in the ethanol-treatment over dexamethasone-treatment as well as in the ethanol-treatment over hydrocortisone-treatment. To remove peaks which showed only small increases or decreases in chromatin accessibility, called peaks were additionally filtered for a 'fold_enrichment' score from the *MACS2* output of >2. To acquire the final lists of high-confidence opening and closing peaks, peaks were only considered if they showed increases or decreases in chromatin accessibility for both hormones. For this purpose, the *intersect* function of the *BEDTools suite v2.27.1* [145] was used to extract overlapping (minimum overlap of 1 bp) opening/closing peaks between dexamethasone- and hydrocortisone-treated samples. Lastly, from the resulting list of opening and closing peaks in A549 cells, sites were removed if they were situated within a window of +/- 500 bp around the TSS of any transcript variant of upregulated and downregulated genes, respectively. This last step was performed to ensure that opening/closing sites are not the consequence of the presence/absence of the transcriptional machinery at regulated genes.

For U2OS-GR cells, sites of increasing, decreasing and non-changing chromatin accessibility were defined based on the ATAC-seq data for dexamethasone- and ethanol-treated U2OS-GR cells (no washout). These sites were obtained similarly as described above for the A549 cells. However, since no hydrocortisone treatment was available (which was treated as a 'replicate' sample in the A549 cells to obtain high-confidence peaks), peaks were filtered for a more stringent 'fold_enrichment' of >3. Otherwise, closing and opening sites were defined as describe above for A549 cells.

To obtain a list of accessible sites which do not show changes in accessibility upon hormone treatment ('non-changing sites') for A549 and U2OS-GR cells, *MACS2* was used to call peaks on all treatment samples independently (*–broad –broadcutoff 0.001*, 'no control'). To further ensure that these regions show relatively high accessibility, peaks with a 'fold_enrichment' score of less than 8 were removed. Next, overlapping peaks between hormone- and vehicle-treatments were obtained using the *intersect* function from *BEDTools*. Finally, to ensure that the non-changing peaks do not show changes in chromatin accessibility upon hormone treatment, *BEDTools intersect* (*-v*) was applied to subtract opening and closing peaks from the final list of non-changing regions.

Additionally, regions showing persistently increased or decreased accessibility before and after washout were determined by peak calling on the ATAC-seq 'after washout' data. For persistent increases in chromatin accessibility, peaks were called in 'hormone-treatment after washout' over the 'vehicle-treatment after washout' samples. Similarly for persistent decreases, peaks were called in the 'vehicle-treatment after washout' over the 'hormone-treatment after washout'. These 'after washout' peaks were determined for

A549 and U2OS-GR cells in the same way as the opening and closing sites (no washout), as described above. Lasty, the final peak set of opening or closing sites 'before and after washout' was obtained by using *BEDtools intersect* to extract the overlap between peaks which opened/closed upon hormone treatment and peaks showing persistent opening/closing after washout.

All defined sites of increasing, decreasing or non-changing chromatin accessibility were filtered by discarding sites that overlap with regions blacklisted by ENCODE for hg19 [146] as well as sites found within mitochondrial DNA or unplaced contigs.

ATAC-seq Normalization for Genome Browser and Heatmaps Visualizations

ATAC-seq samples were normalized by calculating scaling factors for each sample, to compensate for the different signal-to-noise ratios that ATAC-seq samples commonly exhibit. To this end, a high-confidence list of accessible sites was defined per experiment which was subsequently used for read-counting. Thus, *MACS2* [144] was utilized to call peaks for each sample (*–broad –broadcutoff 0.01*, 'no control') and the overlapping peaks for all samples were obtained using *BEDtools intersect* [145]. Thus, these peaks represent sites which are accessible in all treatments. After removing ENCODE hg19 blacklisted sites [146], *featureCounts* (*allowMultiOverlap=TRUE, isPairedEnd=TRUE*) [140] was used to count reads per sample on the list of accessible peaks. The scaling factor for each sample was subsequently calculated using the *DESeq2 v1.26.0* [142] function *estimateSizeFactorsForMatrix*. Next, scaled bigWigs were generated with *bamCoverage* (*deepTools*) [136], by specifying the reciprocal of the calculated scaling factors. The resulting bigWig files were used for genome browser visualizations with IGV [137] as well as for the generation of heatmaps using *computeMatrix* (*reference-point*) and *plotHeatmap* from *deepTools*.

2.3.3 ChIP-seq Analysis

Downloading Additional ChIP-seq Data Sets

The following publicly available ChIP-seq data sets were downloaded from the Gene Expression Omnibus (GEO), the Sequence Read Archive (SRA) or ArrayExpress:

GR ChIP-seq in A549 cells (2 replicates): cells were treated with 100 nM dexamethasone to ethanol for 3 hours; GEO accession number GSE79431; generated by the Reddy Lab; [101]

H3K27ac ChIP-seq in A549 cells: cells were treated with 100 nM dexamethasone for 0 or 4 hours; GEO accession number GSM2421694/GSM2421873; generated by the Reddy Lab; [147]

H3K4me3 ChIP-seq in A549 cells: cells were treated with 100 nM dexamethasone for 0 or 4 hours; GEO accession number GSM2421504/GSM2421914; generated by the Reddy Lab; [147]

H3K27me3 ChIP-seq in A549 cells: cells were treated with 100 nM dexamethasone to ethanol for 1 hours; GEO accession number GSM1003455/GSM1003577; generated by the Broad Institute; [147]

p300 ChIP-seq in A549 cells: cells were treated with 100 nM dexamethasone for 0 or 4 hours; GEO accession number GSM2421805/GSM2421479; generated by the Reddy Lab; [147]

GR ChIP-seq in U2OS-GR cells (replicate 1): cells were treated with 1 μM dexamethasone for 90 minutes; SRA accession number SRX256867/SRX256891; generated by the Yamamoto Lab; [148]

GR ChIP-seq in U2OS-GR cells (replicate 2): cells were treated with 1 μM dexamethasone for 90 minutes; ArrayExpress accession number E-MTAB-9616; generated by Dr. Verena Thormann (Meijsing Lab, Max Planck Institute for Molecular Genetics, Berlin); [129]

H3K27ac ChIP-seq in U2OS-GR cells: cells were treated with 1 μM dexamethasone or ethanol for 90 minutes; ArrayExpress accession number E-MTAB-9617; generated by Dr. Alisa Fuchs (Chung Lab, Max Planck Institute for Molecular Genetics, Berlin); [129]

Data Pre-Processing and Visualization

ChIP-seq reads were aligned to the hg19 reference genome with *Bowtie2 v2.1.0* [143]. *Bowtie2* was run using the option *–very-sensitive* for all data sets and additionally setting the options *-X 600 and –trim5 5* for the GR ChIP-seq reads for replicate 1 (SRP020242, [148]). The resulting SAM files were subsequently converted to BAM format and sorted with *SAMtools v1.10* [135]. To ensure high quality of aligned reads, reads with a mapping quality score of less than 10 were discarded using *SAMtools*. To reduce the potential effects of the PCR amplification bias during ChIP-seq library generation, duplicated reads were discarded with *MarkDuplicates* from *Picard tools v.2.17.0* (http://broadinstitute.github.io/picard/). BAM files were subsequently converted to sequencing-depth-normalized bigWig files using the *deepTools v3.4.1* [136] function *bamCoverage* (*–normalizeUsing RPKM*). The resulting bigWig files were used to visualize the ChIP-seq coverage tracks in the IGV genome browser [137]. To visualize ChIP-seq signal as a heatmap at peak regions-of-interest, the *computeMatrix* (*reference-point*) and *plotHeatmap* functions of the *deepTools* suite were ap-

plied.

Calling GR ChIP-seq Peaks

To identify GR peaks, peak calling was carried out using *MACS2 v2.1.2* [144]. The minimum false discovery rate (FDR) threshold was set to 0.01. To acquire a final list of GR peaks of high confidence, only peaks which were called in both replicates were considered. For this purpose, overlapping peaks (minimum overlap of 1 bp) were obtained utilizing function *intersect* (*-u*) of the *BEDTools suite v2.27.1* [145]. Further, the final peaks were filtered by discarding peaks which fell within the regions blacklisted by ENCODE for hg19, since these regions show increased sequencing signal caused by genome assembly artefacts [146]. Finally, peaks were also discarded if they were found within mitochondrial DNA or unplaced contigs.

2.3.4 Linking Changes in Chromatin Accessibility and GR Binding to Gene Regulation

Differential expression analysis for A549 and U2OS-GR cells was performed as described in section 2.3.1. The resulting output was subsequently filtered to obtain lists of differentially expressed or non-regulated genes. Genes were considered to be upregulated or downregulated with a $\log_2$ fold change of >1 or $<$-1, respectively, and were further filtered for an adjusted p-value of <0.05 and a baseMean (which represents the average expression of a gene) of >40. Nonregulated genes were defined by a $\log_2$ fold change between 0.1 and -0.1 and a baseMean of >40. Nonregulated genes were further randomly downsampled to 500 genes for A549 cells and to 1000 genes for U2OS-GR cells to obtain sample sizes which were closer to the sizes of up- and downregulated genes.

To correlate peaks of increasing, decreasing, or nonchanging chromatin accessibility as well as GR ChIP-seq peaks with gene regulation, the percentage of genes within each group (up-, down- or non-regulated) which had at least one peak of a type within a region +/- 50 kb around the TSS was calculated. For genes with multiple transcript variants, the TSS of the longest transcript variant was chosen. Specifically, the information on TSS coordinates was obtained from the NCBI RefSeq annotation available from the UCSC Genome Browser [138]. Using *Python v3.7*, a bed file was generated containing the coordinates of +/- 50 kb around the TSS of the longest transcript variants for up-, down- or non-regulated genes. The overlap between this 100 kb region and the peaks was determined with *BEDtools intersect* (*-wa -wb*) [145]. The output generated with *BEDtools intersect* was subsequently filtered with a *Python* script to ensure that peaks which intersected the +/- 50 kb region around the TSS of more than one gene would only be assigned to the closest one. The data was visualized with *ggplot2 v.3.3.2* in *R v3.6.3*. A Fisher's exact test was performed to determine if there was a significant association between peaks and

up-, down- or non-regulated genes.

2.3.5 4C-seq Analysis

For the analysis of the 4C-seq data, the *pipe4C* tool [132] was used which in available at GitHub (https://github.com/deLaatLab/pipe4C). Briefly, the tool takes fastq files as input and trims away sequences 5′ of the first Csp6I motif. Sequences missing the first Csp6I motif are discarded. Reads are subsequently mapped to the hg19 reference genome, counted per 5′ fragment ends, normalized by sequencing depth and smoothed.

Default settings were applied, and the output was specified to be generated in WIG (wiggle) format. The resulting WIG file of smoothed and normalized reads was visualized in the IGV genome browser [137].

2.3.6 Image Analysis of RNA FISH

RNA FISH images underwent image analysis using the software ZEN 3.0 (Zeiss) to automatically detect individual transcripts and potential sites of transcription. The analysis was set up in collaboration with Dr. René Buschow.

The raw images were pre-processed to generate 2D images from the full Z-stack of 26 slices. To this end, a Maximum Intensity Projection was applied which projects the brightest pixels from each slice to the final 2D image. The maximum intensity projections were used for the automatic detection analysis of transcripts and transcription sites. The nuclei were identified by the counterstain using fixed intensity thresholds after segmentation (watershed: 10) and a faint smoothing (Gauss: 2.0). To remove cells undergoing mitosis or partially captured cells, nuclei were further filtered by size (75-450 μm^2), circularity (0.5-1) and intensity (mean intensity of maximum=4200). Since the software cannot automatically detect the cytoplasm, a uniform circular area (width 30 pix = 3.96 μm) was defined around each nucleus to serve as a substitute cytoplasmic region. Having applied a Rolling Ball Background Subtraction (radius=5 pix, fixed fluorescence threshold), individual transcripts per cell were identified within the nucleus and the 'cytoplasm'. Transcription sites were detected within the nucleus using the same parameters as for the transcripts. A distinction between transcripts and transcription sites within nuclei was achieved by additionally filtering for a size less than 0.33 μm^2 or greater than 0.38 μm^2, respectively.

The transcript and transcription site counts per cell from 3 biological replicates were merged and the data visualized using *ggplot2 v.3.3.2* in *R v3.6.3*.

2.4 Computational Methods (Results Part 2)

2.4.1 ChIP-seq Analysis

Data Sets

The following ChIP-seq data sets in U2OS-GR and U2OS-AR cells were used:

GR ChIP-seq in U2OS-GR cells (replicate 1): described in section 2.3.3

GR ChIP-seq in U2OS-GR cells (replicate 2): described in section 2.3.3

AR ChIP-seq in U2OS-AR cells (2 replicates): cells were treated with 5 nM R1881 for 4 hours; ArrayExpress accession number E-MTAB-9616; generated by Marina Kulik (Meijsing Lab, Max Planck Institute for Molecular Genetics, Berlin); [129]

H3K27ac, H3K4me1, H3K27me3 and H3K9me3 ChIP-seq in U2OS-GR cells: cells were treated with 1 μM dexamethasone or ethanol for 90 minutes; ArrayExpress accession number E-MTAB-9617; generated by Dr. Alisa Fuchs (Chung Lab, Max Planck Institute for Molecular Genetics, Berlin); [129]

H3K27ac, H3K4me1, H3K27me3 and H3K9me3 ChIP-seq in U2OS-AR cells: cells were treated with 5 nM R1881 or DMSO for 4 hours; ArrayExpress accession number E-MTAB-9617; generated by Dr. Alisa Fuchs (Chung Lab, Max Planck Institute for Molecular Genetics, Berlin); [129]

Data Pre-Processing and Visualization

ChIP-seq reads were processed and data visualization performed as described in section 2.3.3.

Additionally, to generate mean ChIP-seq signal plots for the histone modifications, the *computeMatrix* (*reference-point*) and *plotProfile* functions of the *deepTools suite v3.4.1* [136] were applied, using RPKM-normalized bigWig files as input.

Defining GR and AR Binding Sites

GR and AR binding sites were determined by peak calling with *MACS2 v2.1.2* [144], applying an FDR threshold of 0.05. Each replicate was called over its associated input control. To be considered a final peak, a peak had to be called in both replicates. To this end, *BEDTools v2.27.1* [145] *intersect* function was used to obtain overlapping peaks (minimum overlap of 1 bp) between replicates. Lastly, peaks falling within regions blacklisted

by ENCODE for hg19 [146], mitochondrial DNA or unplaced contigs were filtered out from the final set of peaks. Subsequently, *BEDTools intersect* was used on the final GR and AR binding sites, to extract peaks occupied by both receptors (minimum overlap of 1 bp required) and receptor-specific peaks.

2.4.2 ATAC-seq Analysis

Data Sets

The following ATAC-seq data sets in U2OS-GR and U2OS-AR cells were used:

ATAC-seq in U2OS-GR cells: the experiment was performed by myself as described in section 2.2.5; cells were treated with 1 μM dexamethasone or ethanol for 90 minutes; ArrayExpress accession number E-MTAB-7746; [111]

ATAC-seq in U2OS-AR cells: cells were treated with 5 nM R1881 or DMSO for 4 hours; ArrayExpress accession number E-MTAB-9606; generated by Marina Kulik (Meijsing Lab, Max Planck Institute for Molecular Genetics, Berlin); [129]

Data Pre-Processing and Heatmap Visualization

ATAC-seq data were pre-processed as described in section 2.3.2. The resulting processed BAM files were used as input to generate sequencing-depth-normalized bigWig files using *bamCoverage* (*–normalizeUsing RPKM*) from *deepTools v3.4.1* [136]. ATAC-seq signal at receptor-specific and shared binding sites was subsequently visualized as heatmaps or as mean signal plots +/- 2 kb around the peak center utilizing the *deepTools* functions *computeMatrix* (*reference-point*) followed by *plotHeatmap* or *plotProfile*, respectively.

2.4.3 Motif Enrichment Analysis at GR- and AR-Specific Binding Sites

To identify which motifs were enriched at GR- and AR-specific binding sites, motif enrichment analysis was carried out using *AME* (Analysis of Motif Enrichment, [149]) of the *MEME suite* (Multiple Expectation Maximizations for Motif Elicitation, [150]).

To remove chromatin accessibility as a potential confounding factor, all AR-specific sites were included in the analysis as well as GR-specific sites showing the highest chromatin accessibility. This was done, since many GR binding sites were found to reside within relatively inaccessible chromatin, while AR binding sites occurred at relatively accessible regions (Fig. 3.28). To this end, GR-specific peaks (+/- 250 around the peak center) were sorted by ATAC-seq signal (ethanol treatment in U2OS-GR cells) using the *computeMatrix* function from *deepTools v3.4.1* [136]. Subsequently, the 6593 GR-specific

sites with highest ATAC-seq signal were extracted to equal the number of all AR-specific binding sites.

For the motif enrichment analysis, all input GR- and AR-specific binding sequences had an equal length of 500 bp (+/- 250 around the center of the peak). Sequences were scanned for the clustered JASPAR 2018 CORE vertebrates motif collection [25]. In addition, the sequences were also scanned for the presence of the direct repeat version of the GR/AR consensus motif (shown in Fig. 3.30). This version of the direct repeat motif was generated by using position weight matrix of GR consensus motif from JASPAR (MA0113.2, [25]) as a template and copying the weights from the first half-site into the second half-site. As control sequences for the motif enrichment analysis *AME* utilized the shuffled input sequences. Most highly enriched motifs, *i.e.* motif hits exhibiting an E-value of $<10^{-30}$ for either GR- or AR-specific sequences, were included in the heatmap representation of enriched motifs, which was plotted using *ggplot2 v.3.3.2* in *R v3.6.3*. Motif logos were generated using *WebLogo3* [151].

2.4.4 ChIP-exonuclease Footprints

For AR, ChIP-exonuclease (ChIP-exo) footprints were generated for LNCaP cells at sequences containing JASPAR AR consensus motif MA0007.2 [25] and the direct repeat motif (shown in Fig. 3.30). To this end, publicly available AR ChIP-exo data in LNCaP cells (GSE43791) [152] was downloaded. The ChIP-exo data was processed by aligning the reads to the hg19 reference genome using *Bowtie2 v2.1.0* [143] and discarding reads with a mapping quality score of less than 10 with *SAMtools v1.10* [135]. Further, pre-processed AR binding sites in LNCaP cells were downloaded (GSE43791) [152]. To generate the AR footprint profiles at the above-mentioned motifs, the *ExoProfiler* package [153] was applied, providing the processed ChIP-exo data and the AR peaks as input.

For GR, ChIP-exo footprints were generated for U2OS-GR cells at sequences containing the JASPAR GR consensus motif MA0113.2 [25] and the direct repeat motif (shown in Fig. 3.30). Pre-processed GR ChIP-exo data in U2OS-GR cells was downloaded (ArrayExpress E-MTAB-2955) [153]. Using the *ExoProfiler* and setting GR binding sites and the ChIP-exo data as input, GR footprint profiles were generated at the above-mentioned motifs.

A p-value of $< 10^{-4}$ was set as the threshold for motif hits. Motif logos were generated using WebLogo3 [151].

2.4.5 GC-Content Analysis

To obtain the mean GC-content for bins of 50 bp for the entire genome, the *makewindows* function of the *BEDTools suite v2.27.1* [145] was utilized to divide the hg19 reference genome into 50-bp bins. The GC-content for each bin was then calculated with the

BEDTools function *nuc*. The output of *BEDTools nuc* is a bedgraph file, which was subsequently converted into a bigWig file using the *bedGraphToBigWig* command-line tool [154]. To plot the mean GC-content at all GR- and AR-specific binding sites, the resulting bigWig file was used as input for the *computeMatrix* function (*reference-point*) from *deepTools v3.4.1* [136] followed by the *plotProfile* function, to generate mean plots covering a 10 kb window (*i.e.* +/- 5 kb around the peak center). Additionally, mean GC-content plots of receptor-specific binding sites of high chromatin accessibility were plotted. To this end, GR- and AR-specific peaks (+/- 250 bp around the center) were sorted by ATAC-seq signal in their respective vehicle-treated cell lines using *computeMatrix* and the 3296 peaks per receptor with the highest signal were extracted. A Mann-Whitney-U test was performed to determine statistical significance between GR- and AR-specific binding sites.

To plot the mean GC-content for GR- and AR-specific peaks in the cell lines VCaP and LNCaP-1F5, pre-processed ChIP-seq peaks were downloaded for AR (100 nM dihydrotestosterone for 2 hours) and GR (100 nM dexamethasone for 2 hours) (GSM980657, GSM980658, GSM980660, GSM980662, GSM980664, [33]). Final peak lists were obtained by extracting overlapping peaks between replicates with *BEDTools intersect* and subsequently removing peaks which fell within regions blacklisted by ENCODE for hg19 [146], mitochondrial DNA or unplaced contigs. Shared as well as GR- and AR-specific binding sites for VCaP and LNCaP-1F5 cells were obtained using *BEDTools intersect*. Mean GC-content plots were generated as described above.

3 Results

3.1 Part 1: Transcriptional Memory in Response to GR Activation

The first part of the results section aims at investigating the link between glucocorticoid-induced transcriptional and chromatin structural changes, and further explores the long-term genomic effects of GR activation. In particular, GR's ability to induce transcriptional memory was assessed, and to what extent a previous GR-binding event can be 'remembered' by cells to induce lasting effects at the chromatin and transcriptional level. The following section forms part of a publication (Bothe et al., BioRxiv Preprint, [155]), which has been submitted as of the time of writing.

3.1.1 Glucocorticoid Treatment Induces Genome-Wide Increases and Decreases in Chromatin Accessibility

Upon binding to the genome, GR has repeatedly been described to induce higher levels of chromatin accessibility at its binding sites, a process mediated through the action of recruited chromatin remodeling factors [82–85].

To study the effects of GR activation on chromatin accessibility in A549, a human lung carcinoma cell line, ATAC-seq was performed. To this end, cells were treated with the natural glucocorticoid hydrocortisone, the synthetic glucocorticoid dexamethasone or vehicle (ethanol) for 20 hours, prior to harvest for ATAC-seq. Previous research has largely focused on glucocorticoid-induced increases in chromatin accessibility [82–85]. To gain a better understanding of the global chromatin structural changes, I also included sites of decreasing accessibility in the present analysis. Thus, sites were defined to be 'opening' or 'closing' if they showed increases or decreases in chromatin accessibility, respectively, in response to dexamethasone and hydrocortisone treatment when compared to vehicle treatment. Further, accessible genomic regions which did not show changes in their levels of accessibility ('non-changing sites') were defined and included in the analysis to serve as a control group. The ATAC-seq results showed that GR activation resulted in the opening and closing of thousands of genomic sites (Fig. 3.1 A, B). Overall, the number of opening sites was found to be approximately equal to the number of closing sites, with a slightly higher prevalence of closing sites. To validate the ATAC-seq results and ensure the experiments worked as desired, some sites which were expected to show

increasing, decreasing or unchanging chromatin accessibility were analyzed by ATAC-qPCR. The ATAC-qPCR results further confirmed the sequencing results, as the candidate sites investigated showed the expected changes in chromatin accessibility (Fig. 3.1 C).

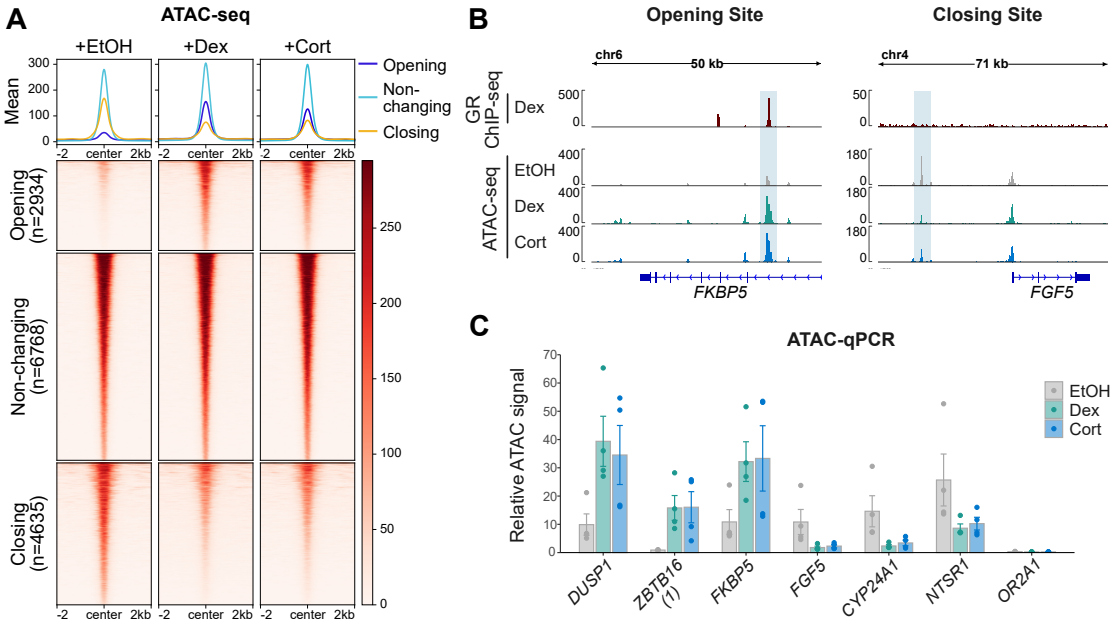

Fig. 3.1: GR activation induces genome-wide changes in chromatin accessibility. (**A**) Heatmap and mean signal plot (top) of normalized ATAC-seq read coverage in A549 cells at genomic regions (+/- 2 kb around center) exhibiting increasing ('opening'), non-changing ('non-changing') and decreasing ('closing') levels of chromatin accessibility in response to glucocorticoid treatment. A549 cells were treated for 20 hours with ethanol ('EtOH'), dexamethasone (100 nM, 'Dex') or hydrocortisone (100 nM, 'Cort'). (**B**) Genome browser view showing read coverage tracks of GR ChIP-seq (100 nM dexamethasone, 3 h; RPKM-normalized; data from [101]) and ATAC-seq (normalized, cells treated as described in (A)) at the *FKBP5* and *FGF5* loci in A549 cells. Genomic regions opening or closing upon glucocorticoid treatment are highlighted in blue. (**C**) ATAC-qPCR analysis targeting opening or closing genomic regions in A549 cells in response to glucocorticoid treatment near indicated genes. Cells were treated as described in (A). Mean ATAC signal normalized to gDNA is shown (n = 4). Error bars represent ± SEM.

Next, I wanted to investigate if GR binds opening or closing sites to determine whether its presence is required for the chromatin accessibility changes to occur. Therefore, available GR ChIP-seq data [101] in A549 cells were downloaded and intersected with the ATAC-seq results. GR occupancy was detectable at most sites which exhibited increases in chromatin accessibility Fig. 3.2, which is expected as GR is known to induce chromatin opening at its genomic binding sites [82–85]. For closing sites, only a small subset of sites showed detectable GR ChIP-seq signal Fig. 3.2. In fact, intersection analysis of the genomic coordinates between opening/closing sites and GR peaks revealed that, while 49% of opening sites overlapped with a GR peak, only 10% of closing sites were occupied by GR. Thus, it appears that GR occupancy is largely not required at regions losing chromatin accessibility and closing might be consequence of indirect effects of GR activation.

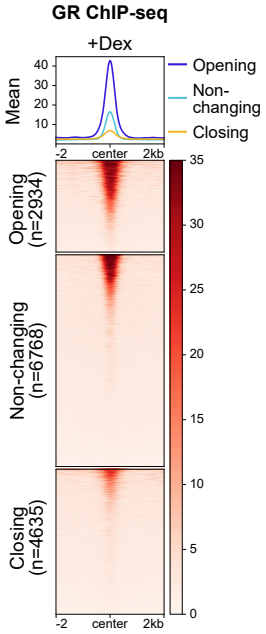

Fig. 3.2: GR occupancy at genomic regions exhibiting increasing, non-changing or decreasing levels of chromatin accessibility upon glucocorticoid exposure. Heatmap and mean signal plot (top) of RPKM-normalized GR ChIP-seq read coverage in A549 cells (100 nM dexamethasone, 3 h, data from [101]) at genomic regions (+/- 2 kb around center) exhibiting increasing ('opening'), non-changing ('non-changing') or decreasing ('closing') levels of chromatin accessibility in response to glucocorticoid treatment (same sites as shown in Fig. 3.1 A)).

To explore GR-induced changes in chromatin accessibility in another cell line, ATAC-seq was performed in U2OS cells, human osteosarcoma cell line stably expressing GRα (U2OS-GR cells) [128]. Prior to harvest for ATAC-seq, U2OS-GR cells were treated with vehicle (ethanol) or dexamethasone for 4 hours. As previously observed in the A549 cells (Fig. 3.1 A, B), thousands of genomic regions in the U2OS-GR cell line showed increases and decreases in chromatin accessibility levels (Fig. 3.3 A). However, unlike the accessibility changes in A549 cells, opening of genomic regions compared to closing was significantly more prevalent in U2OS-GR cells (Fig. 3.3 A). To investigate GR occupancy at opening and closing sites in U2OS-GR cells, available GR ChIP-seq data [148] was analyzed and integrated with the ATAC-seq results. Similar to the results in A549 cells, GR occupancy was detectable at most opening sites, yet largely absent at closing sites (Fig. 3.3 B). These results were further confirmed by an intersection analysis between opening/closing sites and GR peaks in U2OS-GR cells, which revealed that 54% of opening sites overlapped with a GR peak, yet only 0.2% of the closing sites did.

In summary, glucocorticoid treatment induces genome-wide increases as well as decreases in chromatin accessibility. Since sites of increasing accessibility were found to be associated with GR occupancy, chromatin opening is likely a direct consequence of GR binding to many of those sites. Conversely, closing sites were not found to be enriched for GR occupancy, and thus, conceivably lose accessibility due to indirect mechanisms of

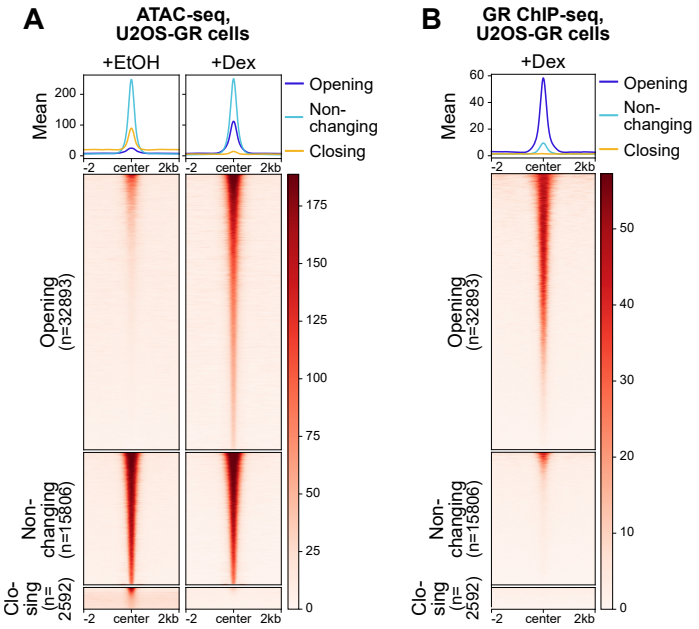

Fig. 3.3: Genome-wide changes in chromatin accessibility and GR occupancy upon dexamethasone treatment in U2OS-GR cells. **(A)** Heatmap and mean signal plot (top) of normalized ATAC-seq read coverage in U2OS-GR cells at genomic regions (+/- 2 kb around center) exhibiting increasing ('opening'), non-changing ('non-changing') or decreasing ('closing') levels of chromatin accessibility in response to glucocorticoid treatment. U2OS-GR cells were treated for 4 h with ethanol ('EtOH') or dexamethasone (100 nM, 'Dex'). **(B)** Heatmap and mean signal plot (top) of RPKM-normalized GR ChIP-seq read coverage in U2OS-GR cells (1 µM dexamethasone, 1.5 h, data from [148]) at genomic regions (+/- 2 kb around center) exhibiting increasing ('opening'), non-changing ('non-changing') or decreasing ('closing') levels of chromatin accessibility in response to glucocorticoid treatment (same sites as shown in (A)).

associated with GR activation.

3.1.2 Opening and Closing Chromatin Regions Are Enriched near Activated and Repressed Genes, Respectively

Since sites which show decreasing chromatin accessibility upon glucocorticoid treatment have not been described much in the literature so far, I wanted to further investigate their potential role in glucocorticoid-induced transcriptional changes.

Thus, to investigate how changes in chromatin accessibility connect to GR-induce transcriptional responses, the ATAC-seq results were intersected with gene expression data. To this end, total RNA-seq was performed in A549 cells and differentially expressed genes were defined to be upregulated (295), downregulated (110) or nonregulated (randomly sampled 500 genes) in response to dexamethasone treatment. To determine whether changes in chromatin accessibility and transcriptional responses are correlated, sites of changing accessibility were assigned to genes based on genomic proximity. Specifically, a region of +/- 50 kb around the TSS of differentially regulated genes was scanned for

the presence of sites showing increasing, decreasing or non-changing chromatin accessibility upon glucocorticoid treatment. This 100 kb window was chosen based on previous findings in A549 cells which showed that GR binding generally occurred 10-100 kb away from upregulated genes [60]. Furthermore, it needs to be noted that opening and closing of chromatin, in particular at the start of genes, might be a consequence of the presence or absence of the transcriptional machinery at promoters of up- or downregulates genes, respectively. Therefore, the final list of opening sites was filtered to not contain regions which overlap promoters of upregulated genes, while closing sites were filtered not to contain regions which overlap promoters of downregulated genes.

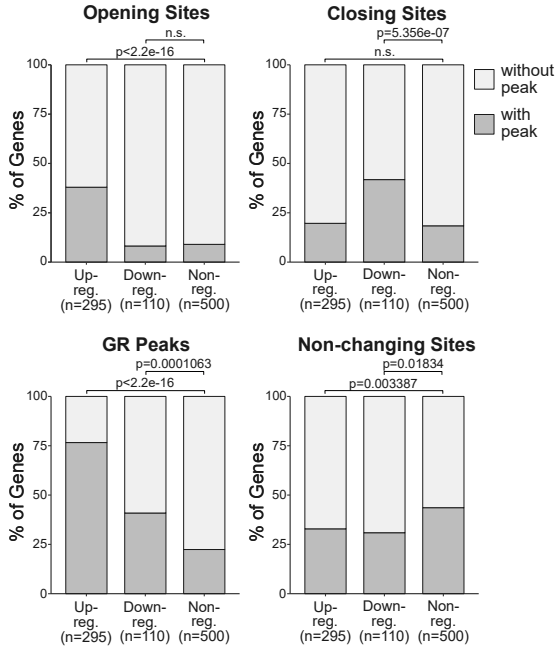

Fig. 3.4: Connecting transcriptional responses in A549 cells with changes in chromatin accessibility and GR binding. Stacked bar graphs depicting the percentage of upregulated, downregulated and nonregulated genes in A549 cells which have one or more 'peaks' in a region +/- 50 kb centered on the TSS. 'Peaks' were grouped into regions of increasing ('opening sites'), decreasing ('closing sites') or non-changing chromatin accessibility ('non-changing sites') as well as GR binding sites ('GR peaks'). P-values were derived from a Fisher's exact test. GR ChIP-seq data is from [101]. n.s.: not significant.

The results showed that there was a significant association between the presence of nearby opening sites and activation of genes (Fig. 3.4). Interestingly, repressed genes were significantly associated with nearby closing sites (Fig. 3.4). As I have previously found that opening sites are typically occupied by GR while closing sites are not (Fig. 3.2), these findings suggest transcriptional repression might not be dependent on nearby binding of GR. To further investigate GR occupancy near activated and repressed genes, I repeated the above analysis by scanning the +/- 50 kb region around the TSS of regulated genes for the presence of a GR binding site. As expected, GR peaks were found to

be enriched near activated genes (Fig. 3.4). Interestingly, GR binding peaks were also significantly associated with repressed genes, though to a much lesser degree than with activated genes (Fig. 3.4). Thus, since downregulated genes showed an enrichment for nearby closing sites and only slight enrichment for GR peaks, it is conceivable that repression of many GR target genes is the result of indirect effects of GR binding rather than active repression by GR.

Further, since a recent study working in mouse mammary epithelial adenocarcinoma cells showed that p300 levels became depleted near repressed genes upon glucocorticoid treatment [61], I wanted to investigate whether a similar phenomenon also occurs in A549 cells. To this end, available p300 ChIP-seq data [147] were analyzed to assess p300 occupancy at sites of changing chromatin accessibility. The results showed that p300 levels increased upon hormone treatment at opening sites, whereas they decreased at closing sites (Fig. 3.5 A). Hence, it is conceivable that a loss of co-factors, such as p300, at closing sites upon hormone treatment, causes the decrease in chromatin accessibility and subsequent downregulation of nearby genes. Moreover, since p300 is a histone acetyl transferase, changes in acetylation of histone 3 on lysine 27 (H3K27ac) were investigated using available ChIP-seq data [147]. H3K27ac ChIP-seq signal was found to increase and decrease upon dexamethasone exposure at opening and closing sites, respectively (Fig. 3.5 B), which correlated with changes in p300 occupancy (Fig. 3.5 A). Notably, H3K27ac levels were also found to decrease at genomic regions of non-changing chromatin accessibility (Fig. 3.5 B), arguing for global changes in H3K27ac upon glucocorticoid treatment.

To investigate if the observed enrichment of closing sites, which are not occupied by GR, near repressed genes in A549 cells was a cell type-specific effect or not, I repeated the above analysis in U2OS-GR cells. Having analyzed available mRNA-seq data in U2OS-GR cells [133], genes were again defined to be upregulated (838), downregulated (534) or nonregulated (randomly samples 1000). As for A549 cells, upregulated genes were significantly associated with opening regions and GR peaks, whereas downregulated genes were significantly associated with closing regions and, to a lesser extent, with GR peaks (Fig. 3.6).

Together, the above results suggest glucocorticoid-induced gene activation and repression occur through direct and indirect effects of GR activation, respectively. GR appears to actively upregulate genes through nearby binding to genomic regions which, in turn, exhibit increases in chromatin accessibility. Downregulation of target genes, on the other hand, frequently seems to occur through indirect effects of GR activation, possibly due to cofactor redistribution away from sites, which consequently exhibit decreasing chromatin accessibility.

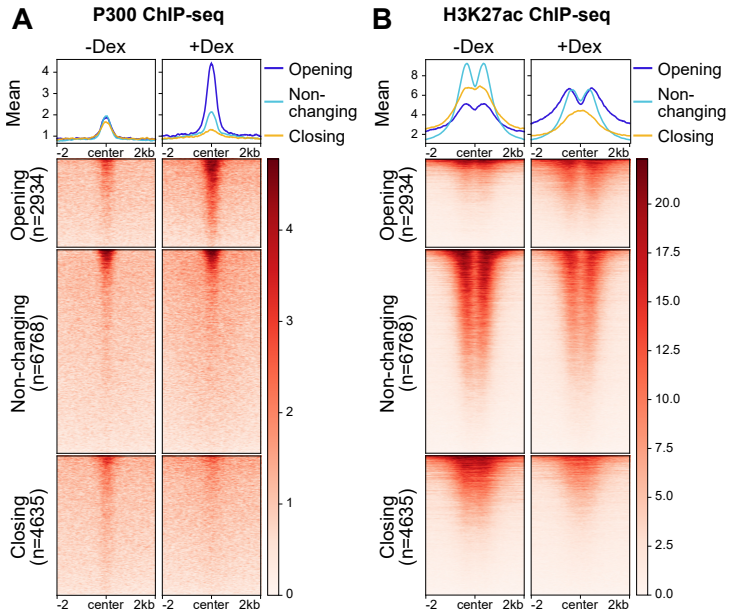

Fig. 3.5: p300 and H3K27ac levels at genomic regions of changing chromatin accessibility. (**A**) Heatmap and mean signal plot (top) of RPKM-normalized p300 ChIP-seq read coverage in A549 cells (+/- 100 nM dexamethasone, 4 h; data from [147]) at genomic regions (+/- 2 kb around center) exhibiting increasing ('opening'), non-changing ('non-changing') or decreasing ('closing') levels of chromatin accessibility in response to glucocorticoid treatment (same sites as shown in Fig. 3.1 A). (**B**) Analogous to (A), but RPKM-normalized H3K27ac ChIP-seq read coverage in A549 cells (+/- 100 nM dexamethasone, 4 h; data from [147]) is shown.

3.1.3 Changes in Chromatin Accessibility upon GR Activation Are Universally and Rapidly Reversible

Previous studies found GR-induced increases in chromatin accessibility to be long-lived at certain genomic regions [85], [127]. Specifically, in a genome-wide investigation, Stavreva et al. [85] found that a subset of sites showed increases in chromatin accessibility which persisted for 40 minutes after hormone washout in mouse mammary adenocarcinoma cells. Strikingly, Zaret and Yamamoto [127] studying an individual locus identified maintained increases in chromatin accessibility for more than 9 days at a stably integrated viral sequence in mouse L cells.

To address the question if long-lived changes in chromatin accessibility are commonly observed in response to GR activation, ATAC-seq was performed in A549 cells which were treated with dexamethasone, hydrocortisone or ethanol for 20 hours and subsequently subjected to washes to remove residual hormone and cultured for 24 hours in hormone-free medium (Fig. 3.7). The hormone treatment time of 20 hours was chosen, since Zaret and Yamamoto [127], who observed persistent changes for more than 9 days, applied the same treatment time in their study. Additionally, the washout period of 24 hours was chosen to determine whether chromatin accessibility can persist beyond one cell cycle in A549 cells. Further, since I had previously observed that GR induced wide-spread decreases in

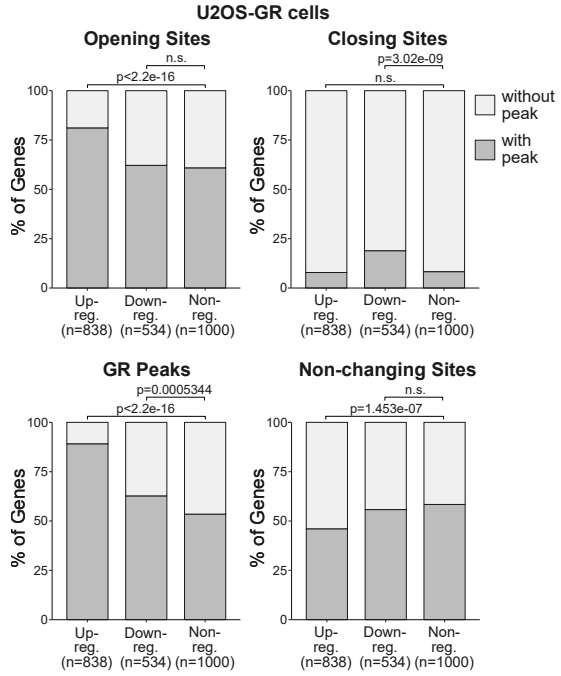

Fig. 3.6: Connecting transcriptional responses in U2OS-GR cells with changes in chromatin accessibility and GR binding. Stacked bar graphs depicting the percentage of upregulated, downregulated and nonregulated genes in U2OS-GR cells which have one or more 'peaks' in a region +/- 50 kb centered on the TSS. 'Peaks' were grouped into regions of increasing ('opening sites'), decreasing ('closing sites') and non-changing chromatin accessibility ('non-changing sites') as well as GR binding sites ('GR peaks'). P-values were derived from a Fisher's exact test. RNA-seq data is from [133] and GR ChIP-seq data is from [148]. n.s.: not significant.

chromatin accessibility (Fig. 3.1), I therefore not only investigated chromatin accessibility changes after hormone washout at sites opening upon glucocorticoid treatment, but extended the analysis to include closing genomic regions.

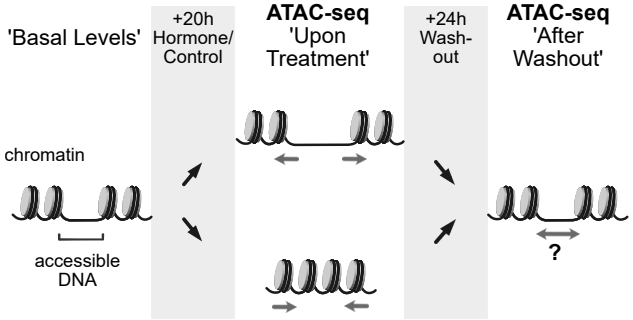

Fig. 3.7: Experimental setup to study changes in glucocorticoid-induced chromatin accessibility after hormone washout. Cartoon representation of the experimental procedure performed to study changes in chromatin accessibility in response to glucocorticoid treatment and subsequent washout. A549 cells were treated for 20 hours with dexamethasone (100 nM), hydrocortisone (100 nM) or ethanol, after which cells were either harvested for ATAC-seq or subjected to washes and cultured in medium in the absence of hormone for 24 hours and then harvested for ATAC-seq.

The ATAC-seq results showed that most opening sites fell back to basal accessibility levels 24 hours after hormone withdrawal (Fig. 3.8). Likewise, most closing sites gained accessibility again after hormone washout (Fig. 3.8). Strikingly, persistently increased or decreased accessibility was only observed at 1.9% and 0.9% of sites, respectively, though the ATAC-seq signal at those regions after washout was lower on average compared to the signal before washout (Fig. 3.8).

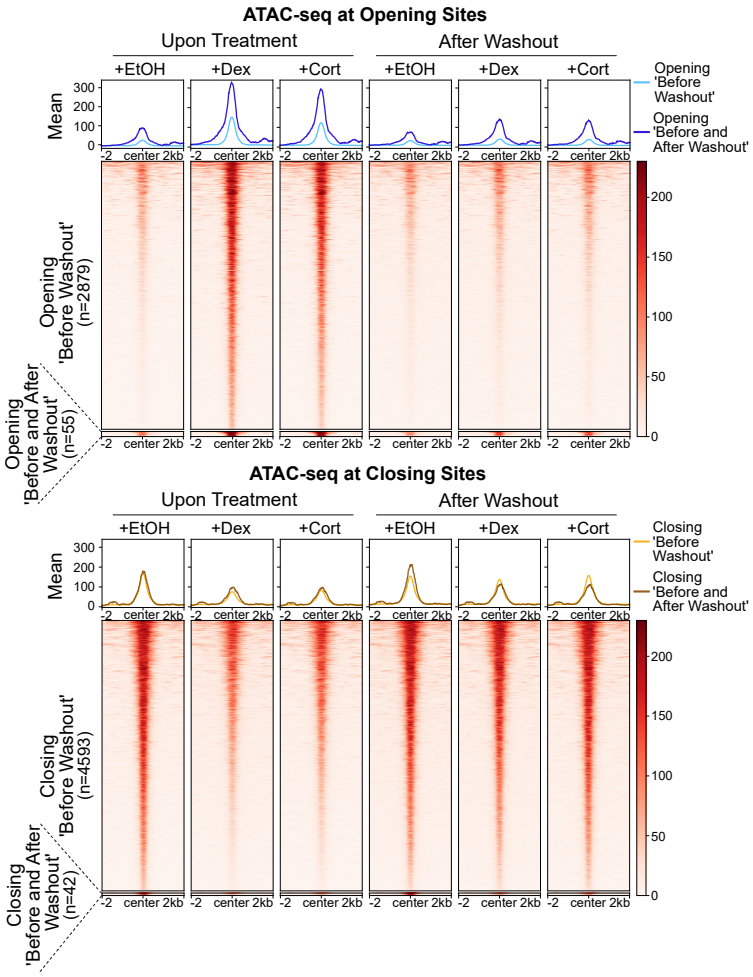

Fig. 3.8: Genome-wide increases and decreases in chromatin accessibility upon glucocorticoid treatment are not long-lived at most genomic regions in A549 cells. Heatmap and mean signal plot (top) of normalized ATAC-seq coverage in A549 cells at genomic regions (+/- 2 kb around center) exhibiting increasing ('opening', top) or decreasing ('closing', bottom) levels of chromatin accessibility in response to glucocorticoid treatment. A549 cells were treated as detailed in Fig. 3.7. Sites are split into genomic regions showing no persistently increased or decreased accessibility after hormone washout, and genomic regions showing maintained increased accessibility after hormone washout.

To validate whether the long-lived accessibility at opening sites was reproducible, ATAC followed by qPCR was performed targeting a few candidate opening sites which showed the most promising persistent increases in chromatin accessibility based on the

sequencing results (Fig. 3.9 A, B). However, persistently increased accessibility could not be confirmed by ATAC-qPCR, as only subtle differences were observed between hormone- and vehicle treated samples after washout (Fig. 3.9 B). It needs to be noted the ATAC experiment, as such, appears to have worked as expected, since expected chromatin opening upon hormone treatment and subsequent closing following hormone removal were observed at control regions (Fig. 3.9 B). Thus, the small fraction of regions which showed residual accessibility based on the ATAC-seq results (Fig. 3.9 A, B) might have been false-positives, which are commonly present in genome-wide sequencing data.

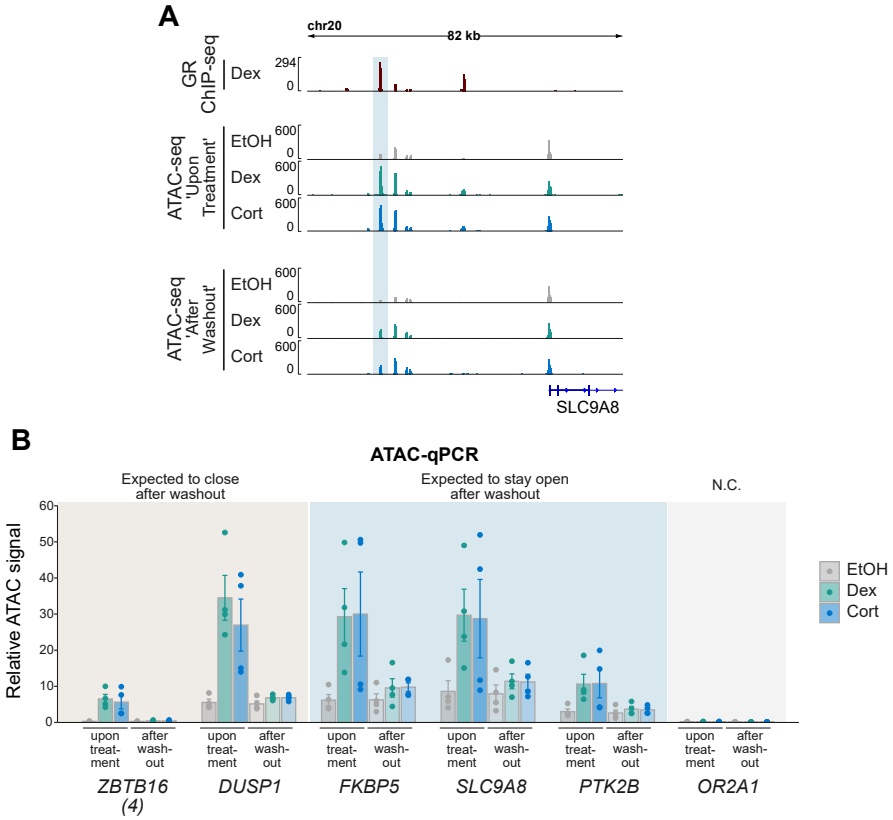

Fig. 3.9: Genomic regions showing persistently increased chromatin accessibility by ATAC-seq are not validated by ATAC-qPCR. (**A**) Genome browser view showing read coverage tracks of GR ChIP-seq (100 nM dexamethasone, 3 h; RPKM-normalized; data from [101]) and ATAC-seq (normalized, cells treated as described in Fig. 3.7) at the *SLC9A8* locus in A549 cells. Genomic region showing residual increased chromatin accessibility after hormone withdrawal is indicated. (**B**) ATAC-qPCR analysis targeting genomic regions in A549 cells which open in response to glucocorticoid treatment near indicated genes. Cells were treated as described in Fig. 3.7. Mean ATAC signal normalized to gDNA is shown (n=4). Error bars represent ± SEM. N.C. negative control.

Taken together, GR activation results in genome-wide increases and decreases in chromatin accessibility which are largely lost 24 hours after hormone washout, suggesting that such hormone-induced structural chromatin changes are not propagated beyond one cell cycle in A549 cells.

3.1.4 Long-Lived Increases in Chromatin Accessibility in U2OS-GR Cells Are a Consequence of Residual GR Binding

As I described above, I found that long-lived increases in chromatin accessibility in response to GR activation were not reproducibly observable in A549 cells (Fig. 3.8, Fig. 3.9). However, it is possible that long-term chromatin structural changes, as previously described in [85], [127] are cell type-specific.

Thus, I assessed chromatin accessibility changes following glucocorticoid treatment and subsequent withdrawal in another cell type, namely the U2OS-GR cell line. For this purpose, U2OS-GR cells were treated with dexamethasone or ethanol for 4 hours. Hormone was subsequently washed-out and the cells were cultured in medium in the absence of hormone for 24 hours prior to harvest for ATAC-seq. As previously observed in A549 cells, increases or decreases in chromatin accessibility upon dexamethasone treatment were lost 24 hours after hormone washout, with only a small subset of regions showing maintained changes (Fig. 3.10 A, B). To determine whether the sequencing results were reproducible, ATAC-qPCR was performed targeting candidate sites which showed the most promising (based on ATAC-seq data) residual increases in accessibility following hormone washout (Fig. 3.10 B, C). Interestingly, persistent increases were found to be reproducible by ATAC-qPCR (Fig. 3.10 C), suggesting that GR induces long-lived increases in chromatin accessibility in U2OS-GR cells.

To determine whether persistent increases in chromatin accessibility in U2OS-GR cells occur in the absence of GR binding, in which case these long-lived changes would represent a true 'memory' of GR activation, GR ChIP-qPCR was performed on dexamethasone-treated cells as well as on cells following a 24-hour hormone washout. Upon hormone treatment, GR binding was detectable at all genomic regions investigated (Fig. 3.11 B). Following hormone washout, GR occupancy was no longer observed at sites exhibiting reversible chromatin accessibility (Fig. 3.11 B). However, GR binding was detectable after hormone washout at the genomic regions of persistent increased accessibility (Fig. 3.11 B). Further, H3K27ac ChIP-qPCR revealed that GR binding at 'persistent' sites after washout was accompanied by maintained increased levels of H3K27ac (Fig. 3.11 B). These findings suggest that the long-lived opening of certain genomic regions in U2OS-GR cells is likely the result of residual GR binding. This hypothesis was further confirmed by a genome-wide analysis of GR occupancy 24 hours after hormone removal by ChIP-seq, which revealed that residual GR binding was observable at most regions of 'persistent' accessibility, yet absent at reversible sites (Fig. 3.11 A).

Consequently, it is conceivable that low levels of GR remain active after washout due to potential residual dexamethasone. To investigate GR binding when cells are exposed to different hormone amounts, U2OS-GR cells were treated with a range of dexamethasone concentrations and subsequently subjected to GR ChIP-qPCR analysis. At higher concentration, GR was observed to bind to sites which close after hormone washout and

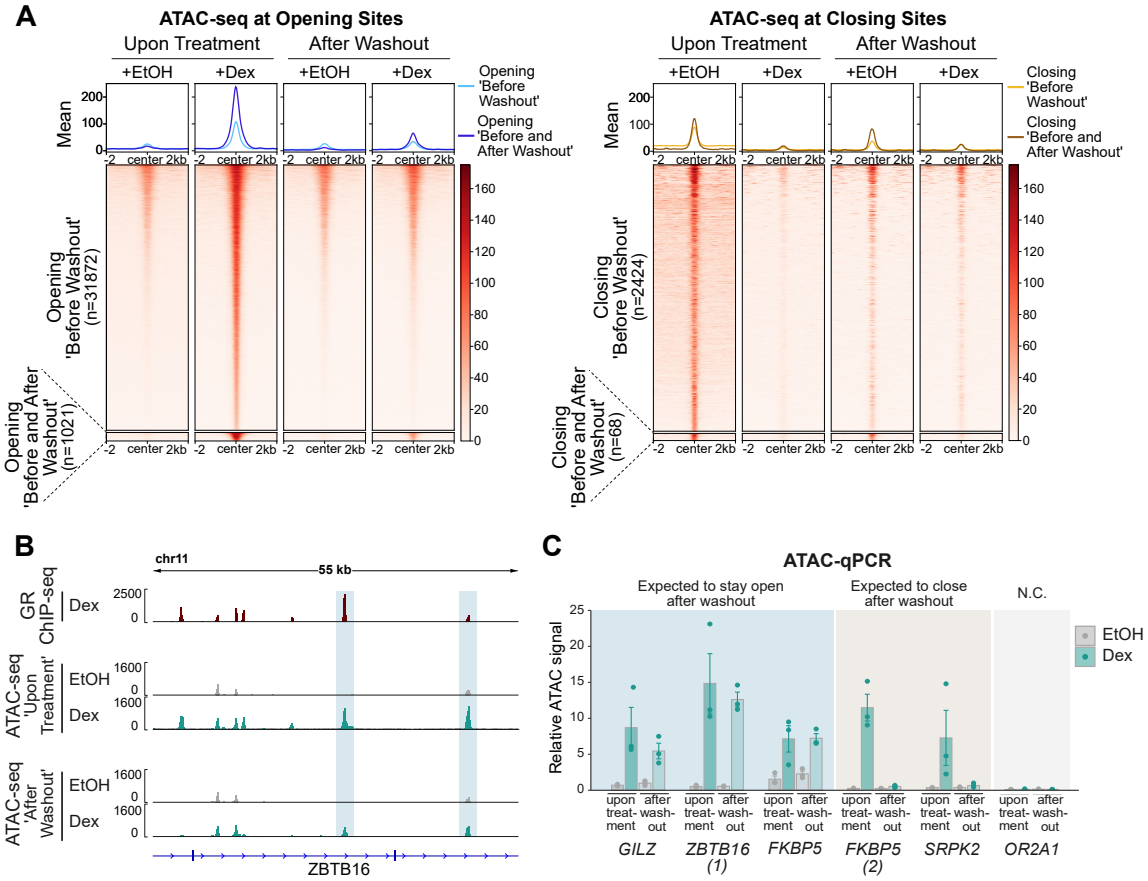

Fig. 3.10: Persistent increases and decreases in chromatin accessibility upon glucocorticoid treatment in U2OS-GR cells. (**A**) Heatmap and mean signal plot (top) of normalized ATAC-seq coverage in U2OS-GR cells at genomic regions (+/- 2 kb around center) exhibiting increasing ('opening', left) or decreasing ('closing', right) levels of chromatin accessibility in response to glucocorticoid treatment. U2OS-GR cells were treated similarly as detailed in Fig. 3.7, with the modification that cells were treated for 4 hours with dexamethasone (100 nM) or ethanol, before being either harvested for ATAC-seq or washed and cultured in hormone-free medium for 24 hours and then harvested for ATAC-seq. Sites are split into genomic regions which do not show persistently increased or decreased accessibility after hormone washout, and genomic regions showing sustained increased accessibility after hormone washout. (**B**) Genome browser view showing coverage tracks of GR ChIP-seq (1 µM Dex, 1.5 h; RPKM-normalized; data from [148]) and ATAC-seq (normalized, cells treated as detailed in (A)) at the *ZBTB16* locus in U2OS-GR cells. Genomic regions showing residual increased chromatin accessibility after hormone withdrawal are indicated. (**C**) ATAC-qPCR analysis targeting opening genomic regions in U2OS-GR cells near indicated genes. Cells were treated as detailed in (A). Mean ATAC signal normalized to gDNA is shown (n=3). Error bars represent ± SEM. N.C. negative control.

to those showing persistent accessibility. At the low dexamethasone concentration of 0.1 nM, on the other hand, GR binding was only detectable at 'persistent' sites (Fig. 3.12). Thus, these findings suggest that genomic regions showing sustained increases in chromatin accessibility are, in fact, sites where GR preferentially binds upon very low hormone concentrations. Consequently, it appears likely that residual increases in chromatin accessibility are the result of low levels of hormone-bound GR binding to those sites, possibly

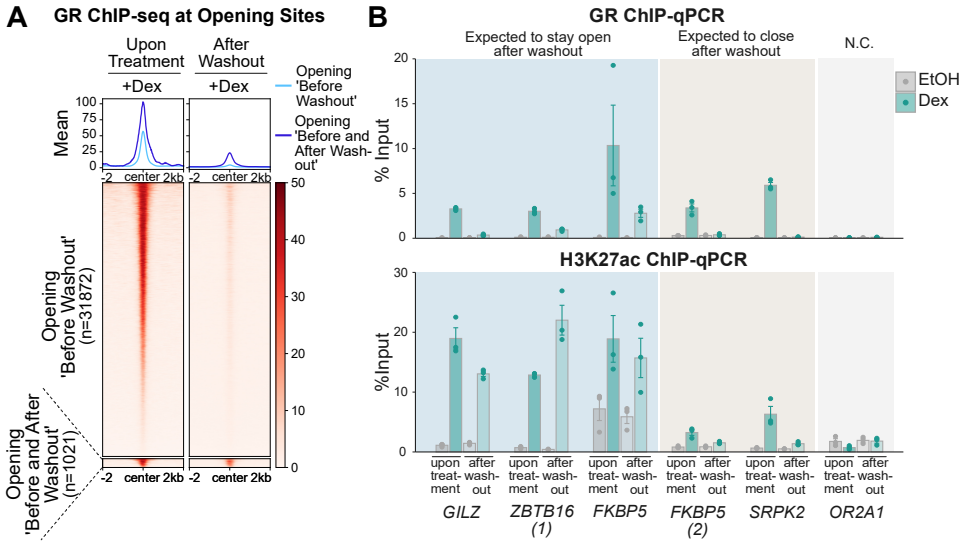

Fig. 3.11: GR binding detectable at genomic regions showing long-lived increases in chromatin accessibility 24 hour after hormone washout. (**A**) Heatmap and mean signal plot (top) of RPKM-normalized GR ChIP-seq coverage at genomic regions (+/- 2 kb around center) exhibiting increasing levels of chromatin accessibility in response to glucocorticoid treatment in U2OS-GR cells (same regions as shown in Fig. 3.10 A). 'Upon treatment': U2OS-GR cells were treated with dexamethasone (1 µM) for 90 minutes (data from [148]. 'After washout': U2OS-GR cells were treated with dexamethasone (100 nM) for 4 hours, subjected to washes and cultured for 24 hours in medium the absence of hormone. (**B**) ChIP-qPCR analysis in U2OS-GR cells targeting GR (top) and H3K27ac (bottom) at opening genomic regions in response to glucocorticoid treatment near indicated genes (same sites as shown in Fig. 3.10 C). Cells were treated as detailed in Fig. 3.10 A. Mean percentage of input is shown (n = 3). Error bars represent ± SEM. N.C. negative control.

due to incomplete hormone washout.

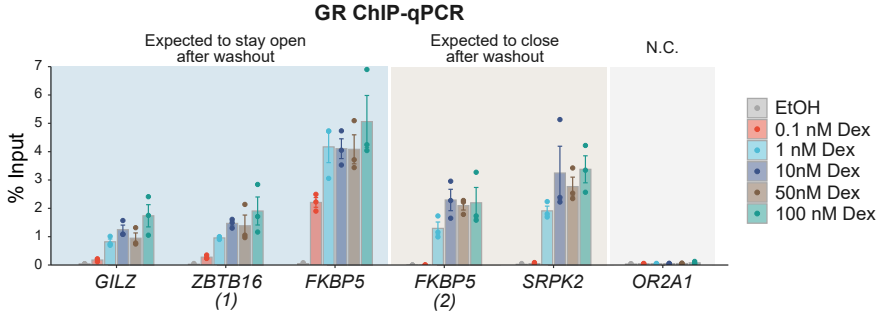

Fig. 3.12: GR binds to genomic regions showing 'persistent' opening of chromatin in the presence of low hormone concentrations. GR ChIP-qPCR at opening genomic regions in response to glucocorticoid treatment near indicated genes in U2OS-GR cells (same sites as shown in Fig. 3.10 C). U2OS-GR cells were treated with ethanol or dexamethasone at concentration of 0.1 nM, 1 nM, 10 nM, 50 nM and 100 nM for 4 hours. Mean percentage of input is shown (n = 3). Error bars represent ± SEM. N.C. negative control.

Taken together, long-lived increases in chromatin accessibility in U2OS-GR cells are likely the consequence of residual GR occupancy, due to the presence of low residual hormone concentrations. Hence, the above results do not provide evidence that the local

chromatin environment retains a true 'memory' of GR activation, as long-term structural chromatin changes in U2OS-GR cells in the absence of GR binding are not observed.

3.1.5 Measuring Changes in Transcriptional Output after Repeated GR Activation

The above-described results revealed that GR activation does not induce increases or decreases in chromatin accessibility which persist throughout cell divisions in A549 and U2OS-GR cells. However, I wanted to further investigate whether GR action can be 'remembered' by cells at the transcriptional level.

Thus, to investigate whether transient GR activation can induce long-term transcriptional memory resulting in an altered transcriptional response upon GR re-activation, total RNA-seq was performed in A549 cells. Specifically, the cells received two rounds of treatment, separated by a 24-hour washout period ('hormone reinduction treatment') Fig. 3.13. In each treatment round, cells were exposed to either dexamethasone or vehicle (ethanol) for 4 hours. Cells which were subjected to vehicle for the first treatment represent a 'naïve' state when receiving the second treatment, whereas cells which were exposed to hormone in the first treatment represent a 'primed' state upon the second treatment. Moreover, it is important to note that total RNA-seq involves the sequencing of total cellular RNA depleted of ribosomal RNAs (rRNAs) and thus includes the sequencing of intron-containing RNAs, such as nascent RNAs and pre-mRNAs. Previous studies have shown that the quantification of intronic reads from total RNA-seq data provides information about active transcription [64–66]. Hence, gene expression changes in response to the 'hormone reinduction treatment' (Fig. 3.13) were obtained by performing a differential gene expression analysis based on the quantification of reads which align to intronic regions. This approach allows capturing acute transcriptional changes upon hormone reinduction and avoids including stable transcripts in the analysis which might have been generated during the first hormone treatment.

Unsurprisingly, dexamethasone treatment of naïve cells resulted in the up- and downregulation of many genes (Fig. 3.14 A). Comparing the transcript levels after vehicle treatment between primed and naïve cells showed no significant differences between the cell states (Fig. 3.14 B), which suggests that the transcriptional output of primed cells is restored to pre-hormone treatment levels after the washout period. The fact that the transcriptional output falls back to 'basal' conditions after hormone washout is an essential prerequisite for a direct comparison of the transcriptional dexamethasone-response between primed and naïve cells. Next, I compared the transcriptional response upon dexamethasone treatment between primed and naïve cells and found that overall transcript levels were very similar (Fig. 3.14 C), indicating that priming does not occur for the majority of genes. Interestingly, this was different for the GR-target gene *ZBTB16* (zinc finger and BTB domain containing gene 16), which exhibited higher expression in primed cells

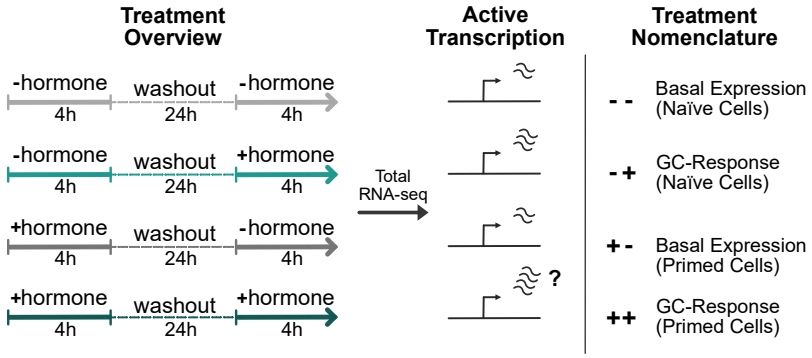

Fig. 3.13: Hormone reinduction treatment. Cartoon representation of the experimental design to assess transcriptional responses upon glucocorticoid (GC) reinduction. Cells were first treated with 100 nM dexamethasone ('primed') or ethanol ('naïve') for 4 hours, after which a washout was performed, and cells were cultured in hormone-free medium for 24 hours. For the second treatment, cells received the second treatment of 100 nM dexamethasone or ethanol for 4 hours and were subsequently harvested for total RNA-seq analysis.

compared to naïve cells (log2 (fold change) = 1.27; adjusted p-value = 3.68e-07) (Fig. 3.14 C).

To validate the total RNA-seq results, RT-qPCR was performed in A549 cells which had been treated according to the hormone reinduction plan (Fig. 3.13). Consistent with the RNA-seq results, *ZBTB16* exhibited increased upregulation upon dexamethasone treatment in primed cells (Fig. 3.15 A). Other GR target genes *GILZ* (glucocorticoid induced leucine zipper) and *FKBP5* (FK506 binding protein 5) did not show this expression pattern (Fig. 3.15 A), indicating that priming by prior glucocorticoid exposure is specific to the *ZBTB16* gene.

To explore *ZBTB16* transcription following a third round of dexamethasone treatment, A549 cells were treated similarly to the hormone reinduction treatment (Fig. 3.13), however, after the second treatment, the cells were washed again and cultured in hormone-free medium and subjected to another dexamethasone- or vehicle-treatment. Interestingly, *ZBTB16* expression was further increased upon the third treatment (Fig. 3.15 B). It needs to be noted that, upon vehicle treatment, *ZBTB16* transcription levels always returned to pre-hormone treatment levels, indicating that the higher transcript levels do not simply reflect RNA accumulation, but rather a more robust response upon a second and third exposure. Additionally, the genes *GILZ* and *FKBP5* also showed a slightly increased upregulation after the third dexamethasone treatment compared to the first, though to a much lesser extent than *ZBTB16* (Fig. 3.15 B).

To test if transcriptional memory persists beyond 24 hours, and possibly beyond cell division which is likely to occur within a 48-hour period, I examined gene expression changes in A549 cells which were treated according to the hormone reinduction treatment (Fig. 3.13), but applying a hormone-washout period of 48 hours. Notably, analysis by

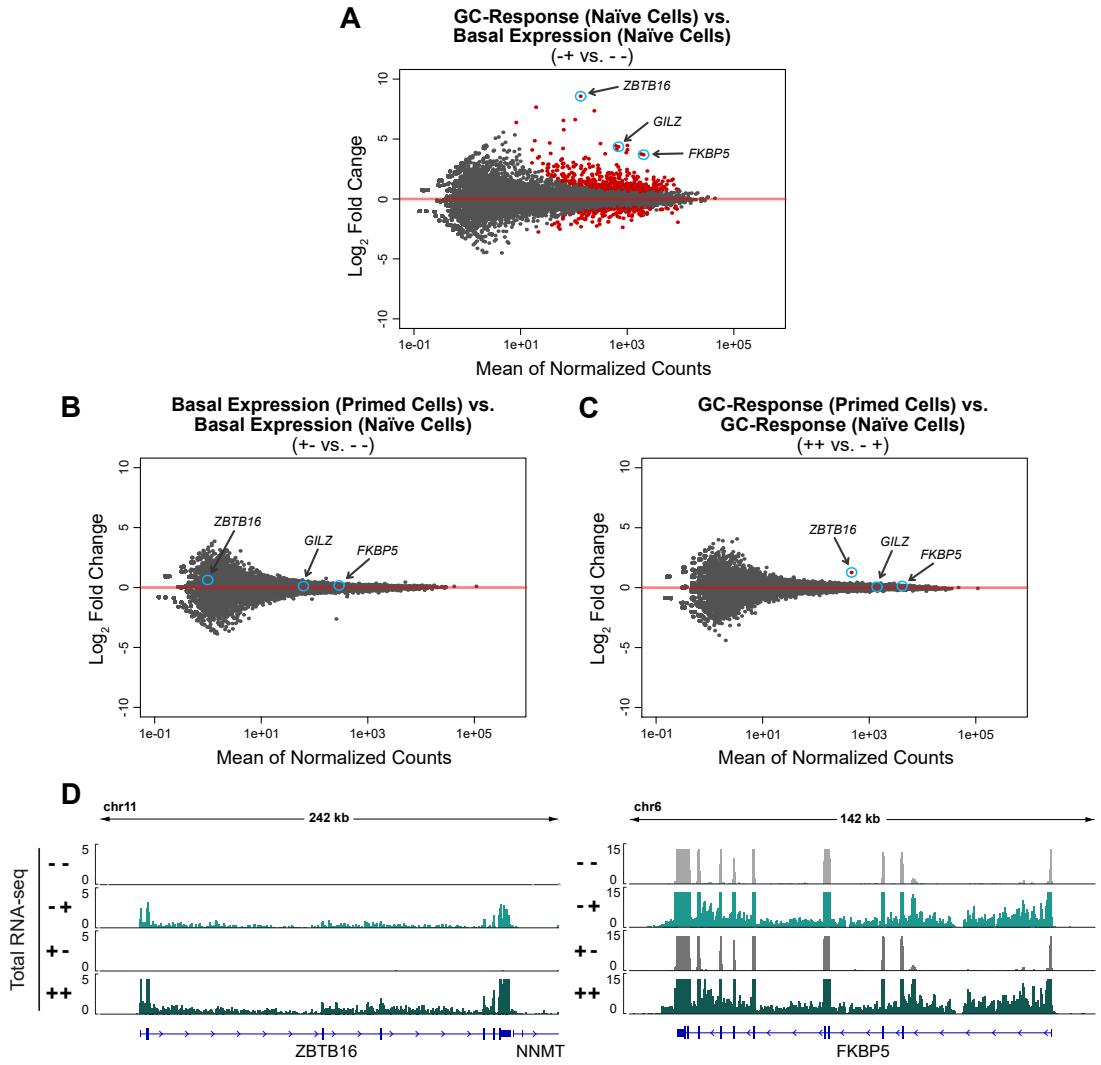

Fig. 3.14: Glucocorticoid (GC) reinduction results in an increased transcriptional response of *ZBTB16*. (**A-C**) MA plots showing the $\log_2$ fold changes and the mean of normalized counts of genes from three biological replicates (A) when comparing dexamethasone-treatment versus vehicle-treatment in naïve cells ('- +' vs. '- -'), (B) basal expression in primed versus naïve cells ('+ -' vs. '- -') and (C) dexamethasone-induction of primed versus naïve cells ('++' vs. '- +'). Differential gene expression analysis was performed based on the quantification of reads which align to intronic regions. Cells were treated as detailed in Fig. 3.13. Dots colored in red indicate genes significantly activated or repressed (FDR < 0.001). (**D**) Genome browser view showing RPKM-normalized RNA-seq read coverage tracks (merge of three biological replicates) in A549 cells at the *ZBTB16* and *FKBP5* genes. A549 cells were treated as detailed in Fig. 3.13.

RT-qPCR showed that the increased upregulation of *ZBTB16* following dexamethasone reinduction was observable even if the time between treatments lasted 48 hours (Fig. 3.15 C), suggesting that the effects of priming persist through at least one cell divisions.

Taken together, priming of A549 cells with dexamethasone results in transcriptional memory of the GR-target gene *ZBTB16*, which shows enhanced upregulation upon hormone reinduction. However, the majority of genes do not become primed upon gluco-

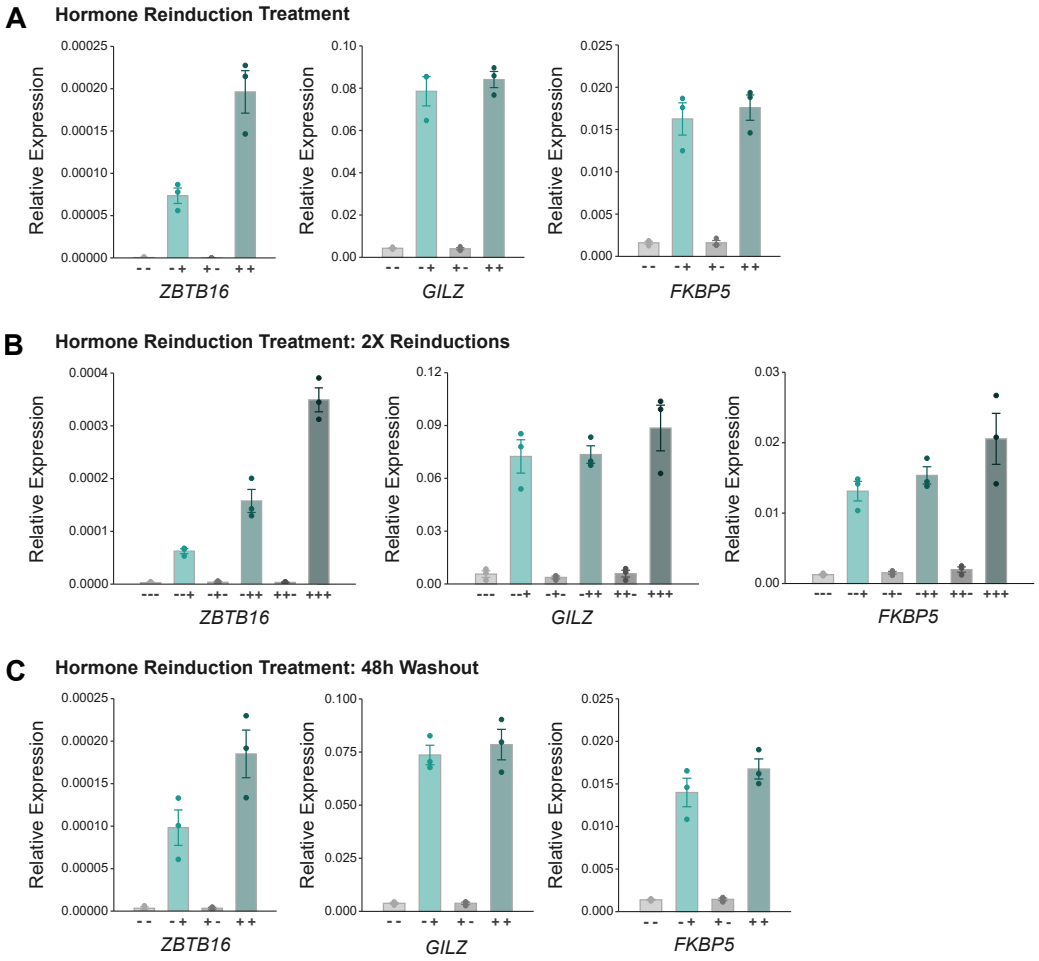

Fig. 3.15: *ZBTB16* expression increases upon repeated glucocorticoid treatment. (**A**) RT-qPCR results showing expression levels of *ZBTB16*, *FKBP5* and *GILZ* in A549 cells. Cells were treated as detailed in Fig. 3.13. Mean expression relative to *RPL19* is shown (n = 3). Error bars represent ± SEM. (**B**) RT-qPCR results showing expression levels of *ZBTB16*, *FKBP5* and *GILZ* in A549 cells. Cells were treated similarly as described in Fig. 3.13, with the modification that they were washed again after the second treatment and grown in medium without hormone, before being treated for a third time with dexamethasone (100 nM) or ethanol for 4 hours. Mean expression relative to *RPL19* is shown (n = 3). Error bars represent ± SEM. (**C**) RT-qPCR results showing expression levels of *ZBTB16*, *FKBP5* and *GILZ* in A549 cells. Cells were treated as detailed in Fig. 3.13, expect that the washout period between treatments lasted 48 hours. Mean expression relative to *RPL19* is shown (n = 3). Error bars represent ± SEM.

corticoid exposure. These results are in line with my previous findings showing that GR-induced chromatin accessibility changes are universally reversible. Thus, a prior GR activation might not leave many lasting changes at the chromatin and transcriptional level.

3.1.6 Increased ZBTB16 Upregulation upon Glucocorticoid-Reinduction is Cell Type-Specific

Target gene regulation by GR has repeatedly been shown to be cell type-specific [10, 81, 112].

To test whether the observed transcriptional memory of *ZBTB16* expression in A549 cells is a cell type-specific phenomenon or shared with other cell types, *ZBTB16* expression was analyzed in U2OS-GR cells, which were subjected the hormone reinduction treatment (Fig. 3.13). Unlike the results in A549 cells, gene expression levels did not revert to basal levels after hormone washout ('+ -' treatment) for *ZBTB16* and *FKBP5* (Fig. 3.16).

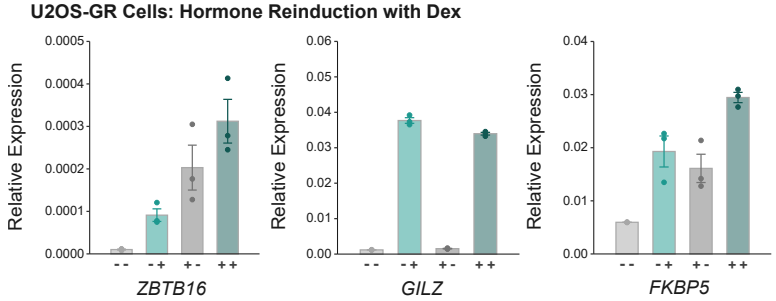

Fig. 3.16: GR-target gene expression in U2OS-GR cells does not revert to basal expression levels after dexamethasone washout. RT-qPCR results showing expression levels of *ZBTB16*, *FKBP5* and *GILZ* in U2OS-GR cells. Cells were treated as detailed in Fig. 3.13, mean expression relative to *RPL19* is shown (n = 3). Error bars represent ± SEM.

Due to the ongoing transcription and, hence, the presence of pre-existing transcripts in primed cells, a valid comparison of active transcription upon hormone induction between naïve and primed cells could not be made. However, this ongoing transcription in U2OS-GR cells is in accordance with the above-described results, in which residual GR occupancy was detected 24-hours after dexamethasone washout (Fig. 3.11). Therefore, U2OS-GR cells were treated according to the hormone re-induction plan (Fig. 3.13) but using the natural glucocorticoid hydrocortisone, since hydrocortisone dissociates from GR faster compared to the synthetic glucocorticoid dexamethasone, which has a dissociation half-life of approximately 10 minutes [156]. RT-qPCR analysis showed gene expression levels for all genes investigated reverted to basal levels after hormone washout when using hydrocortisone, thereby enabling the comparison of hormone-treated naïve and primed cells. Notably, there was no enhanced expression of *ZBTB16* upon hormone reinduction when using hydrocortisone in U2OS-GR cells (Fig. 3.17 B). To test if this effect was due to the different cell type used or the nature of the ligand, I repeated the experiments in A549 cells using hydrocortisone instead of dexamethasone. Interestingly, treating A549 cells with hydrocortisone also resulted in transcriptional memory of *ZBTB16*, and the results showed a similar expression pattern to the results when using dexamethasone (Fig. 3.17 A). Thus, the fact that enhanced *ZBTB16* expression was found in A549 cells, but

not observable in U2OS-GR cells, is not a consequence of the ligand used, but appears to reflect a difference in cell type-specific transcription.

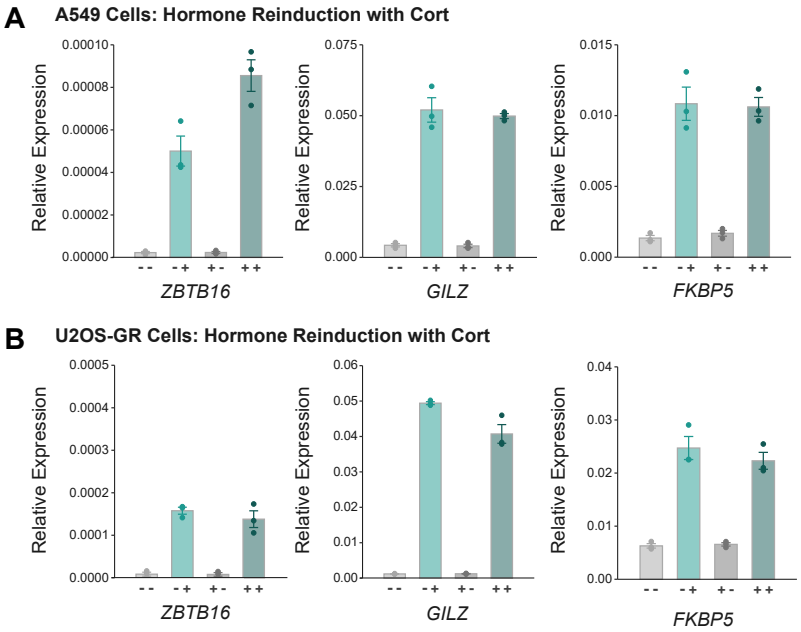

Fig. 3.17: Hormone reinduction using hydrocortisone shows transcriptional memory of *ZBTB16* in A549 cells but not U2OS-GR cells. (**A**) RT-qPCR results in A549 cells showing expression levels of *ZBTB16*, *FKBP5* and *GILZ* in U2OS-GR cells. Cells were treated as detailed in Fig. 3.13, except that hydrocortisone was used instead of dexamethasone. Mean expression relative to *RPL19* is shown (n = 3). Error bars represent ± SEM. (**B**) Same as (A), expect that U2OS-GR cells were used.

In summary, transcription memory of *ZBTB16* gene is observed in A549 cells but not in U2OS-GR cells, suggesting this is a cell type-specific phenomenon.

3.1.7 Enhanced ZBTB16 Expression Is Not a Consequence of a Faster Response to Hormone Treatment in Primed Cells

A more robust expression of signal-inducible genes established through gene priming has previously been shown to be the result of an accelerated onset of transcription [121].

To investigate if the increased *ZBTB16* expression following hormone-re-stimulation is a consequence of faster transcriptional activation, primed and naïve A549 cells were treated with dexamethasone and harvested at different time points. RT-qPCR analysis revealed that *ZBTB16* upregulation was notably detectable 3 hours after dexamethasone treatment in both naïve and primed cells (Fig. 3.18), arguing against a faster onset of transcription. Interestingly, at this time point *ZBTB16* transcript levels were already higher in primed compared to naïve cells (Fig. 3.18). However, faster *ZBTB16* induction cannot be excluded entirely, since it is possible that a slightly faster transcriptional response occurs between the time points of 2 and 3 hours. For *GILZ* and *FKBP5*, dexamethasone-

induced upregulation was comparable between naïve and primed cells at every time point investigated (Fig. 3.18), showing that neither the degree of activation nor the kinetics are changed upon priming for these genes.

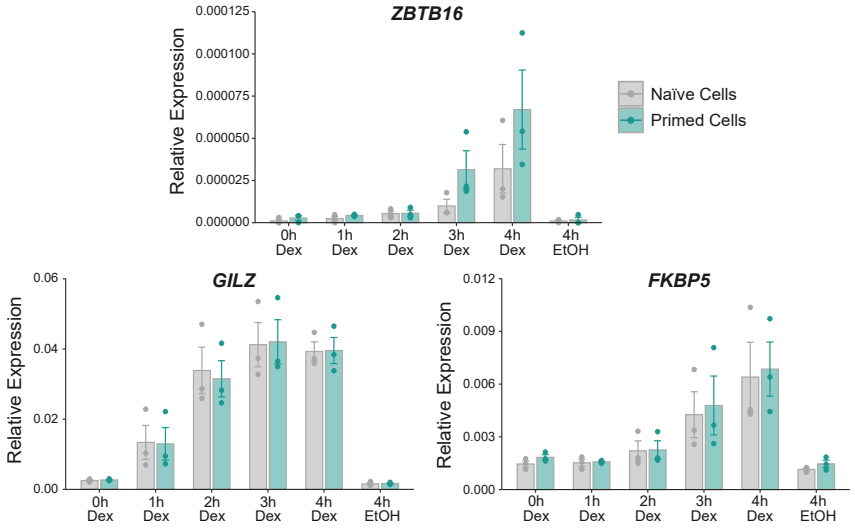

Fig. 3.18: Time-course treatment shows that *ZBTB16* induction is not faster in primed compared to naïve cells. RT-qPCR results showing expression levels of *ZBTB16*, *FKBP5* and *GILZ* in A549 cells. Cells were treated similarly as detailed in Fig. 3.13: for the first treatment cells were treated with 100 nM dexamethasone ('primed') or ethanol ('naïve'), after which cells were subjected to washes and cultured in hormone-free medium for 24 hours. For the second treatment, cells were treated with ethanol for 4 hour or 100 nM dexamethasone for 0, 1, 2, 3 or 4 hours. Mean expression relative to *RPL19* is shown (n = 3). Error bars represent ± SEM.

To conclude, increased *ZBTB16* expression upon dexamethasone re-stimulation does not appear to be the result of an accelerated, but rather a more robust transcriptional response.

3.1.8 Enhanced ZBTB16 Expression in Primed Cells Occurs Due to a Higher Probability of Cells Responding Combined with Individual Cells Showing Enhanced Transcript Levels

Since the enhanced expression of *ZBTB16* upon hormone reinduction was not found to be the result of a faster transcriptional response (Fig. 3.18), I wanted to further investigate how the increased response of *ZBTB16* is achieved by studying transcript levels in single cells. Specifically, my aim was to elucidate whether enhanced *ZBTB16* expression in primed cells was the consequence of stronger transcriptional responses of individual cells or the consequence of a larger number of transcribing cells.

To gain a better understanding of the nature of the increased *ZBTB16* expression at the single-cell level, RNA FISH using probes targeting the coding sequence of *ZBTB16* was performed in A549 cells treated according to the hormone reinduction plan (Fig. 3.13). For comparison, RNA FISH was also performed using probes targeting the coding

sequence of *FKBP5*, a GR-target gene which does not exhibited increased responsiveness upon glucocorticoid reinduction (Fig. 3.14 C, 3.15 A). To enable quantification of *ZBTB16* and *FKBP5* transcript-counts by RNA FISH, automatic detection of transcripts was set up (Fig. 3.19). Initial inspection of the images showed individual transcripts were visible as dots in the nucleus and cytoplasm (Fig. 3.19). In addition, many dexamethasone-treated cells exhibited one or two large dots in the nuclei which possibly are the sites of active transcription (Fig. 3.19).

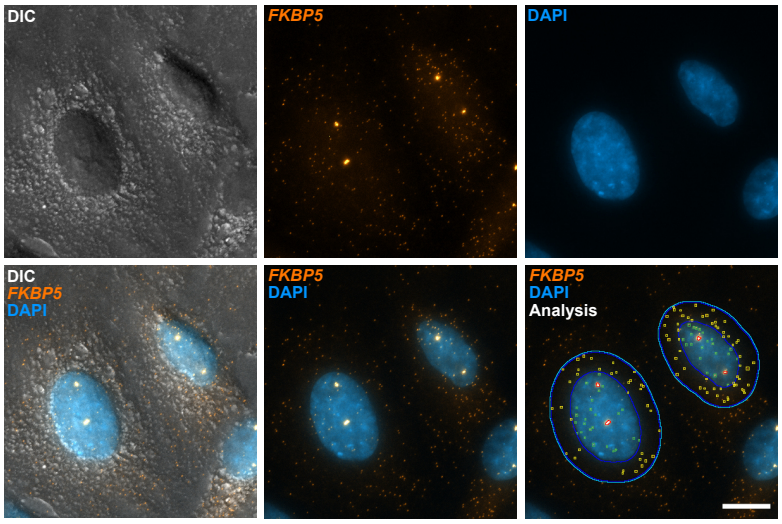

Fig. 3.19: Quantifying the number of transcripts and transcription sites by RNA FISH. Example RNA FISH image of naïve A549 cells upon dexamethasone treatment ('- +' treatment from Fig. 13). Hybridization probes targeting *FKBP5* mRNA (orange) were used and nuclei were counterstained with DAPI (blue). 'Analysis': Transcripts and possible transcription sites were automatically detected using ZEN 3.0 (Zeiss) software which identified the nuclei (dark blue), defined an area for the cytoplasm (light blue) and detected transcripts (yellow in the cytoplasm, green in the nucleus) as well as possible transcription sites (red). The white scale bar equals 10 µm. DIC: differential interference contrast.

RNA FISH using probes targeting *ZBTB16* mRNA was performed in A549 cells treated according to the hormone reinduction plan (Fig. 3.13), including a treatment of three rounds of dexamethasone ('+ + +') as described in Fig. 3.15 B. Overall, the expression changes of *ZBTB16* observed by RNA FISH (Fig. 3.20) were consistent with expression changes seen in the qPCR and total RNA-seq data (Fig. 3.14 C, D, Fig. 3.15 A, B). For vehicle-treated naïve cells, hardly any *ZBTB16* transcripts were detectable (Fig. 3.20 A, B). Upon hormone exposure, 54% of cells showed at least one detectable transcript and 18% of cells exhibited at least one visible site of transcription (Fig. 3.20 A, B, C). After hormone washout ('+ -'), the number of transcripts and transcriptions sites was comparable to basal conditions (Fig. 3.20 A, B, C). Dexamethasone treatment of primed cells resulted in an increase of detectable *ZBTB16* transcripts and transcription sites (Fig. 3.20 A, B, C). Notably, hormone-reinduction of primed cells resulted in a larger proportion of cells (8%) which exhibited two sites of transcription, whereas only 1.5% of naïve cells

showed two transcription sites when exposed to dexamethasone (Fig. 3.20 C). Further, the higher number of detectable *ZBTB16* transcripts upon hormone treatment in primed cells compared to naïve cells appears to be the results of a larger fraction of cells responding and showing detectable transcripts and, on the other hand, individual cells showing increased transcript levels (Fig. 3.20 B). These observations were even more pronounced for the cells which were treated with three rounds of hormone, showing an even larger proportion of responding cells and cells with higher transcriptional activity as well as cells showing more than one transcription site (Fig. 3.20).

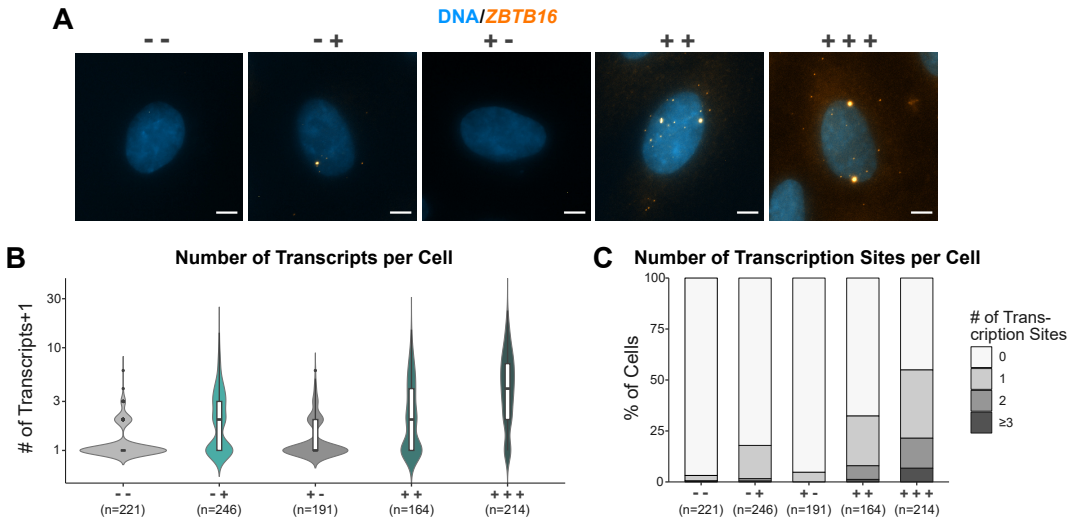

Fig. 3.20: Single-cell expression analysis of *ZBTB16* by RNA FISH. (**A**) Representative RNA FISH images of A549 cells. Hybridization probes targeting *ZBTB16* mRNA (orange) were used and nuclei were counterstained with DAPI (blue). A549 cells were treated as detailed in Fig. 3.13, including a triple dexamethasone treatment (+ + +) as described in Fig. 3.15 B. The white scale bar equals 5 µm. (**B**) Violin plots with included boxplots exhibiting the per-cell *ZBTB16* transcript-count (+1) of A549 cells from the RNA FISH experiment shown in (A). Three biological replicates were performed for each treatment. (**C**) Stacked bar graphs depicting what percentage of A549 cells exhibited 0, 1, 2 or more than 3 transcription sites visible within the nucleus from the RNA FISH experiment shown in (A). Three biological replicates were performed for each treatment.

The RNA FISH results targeting *FKBP5* mRNA showed that, as for the *ZBTB16* results, transcript levels followed the same expression changes as observed in the qPCR and total RNA-seq data (Fig. 3.14 C, D, Fig. 3.15 A, B), with a comparable number of transcripts and transcriptions sites upon hormone treatment between naïve and primed cells (Fig. 3.21). Unlike RNA FISH results for *ZBTB16*, most cells showed detectable *FKBP5* transcripts and transcriptions sites (Fig. 3.21), though cells exhibited notable cell-to-cell heterogeneity.

In summary, analysis of *ZBTB16* expression at the single cell levels by RNA FISH revealed that glucocorticoid-priming of *ZBTB16* in A549 cells results in a higher probability of cells expressing *ZBTB16* as well as individual cells exhibiting enhanced transcript levels upon reinduction.

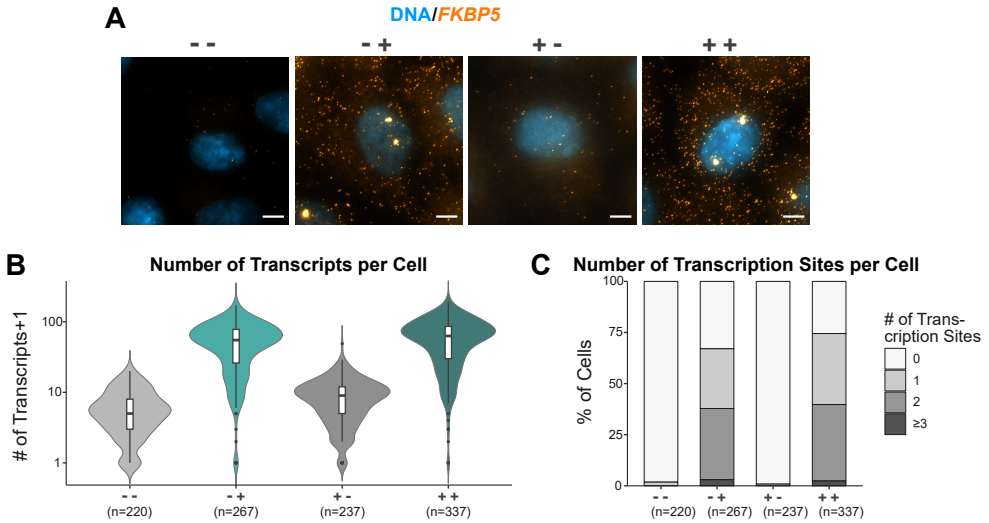

Fig. 3.21: Single-cell expression analysis of *FKBP5* by RNA FISH. (**A**) Representative RNA FISH images of A549 cells. Hybridization probes targeting *FKBP5* mRNA (orange) were used and nuclei were counterstained with DAPI (blue). A549 cells were treated as detailed in Fig. 13. The white scale bar equals 5 µm. (**B**) Violin plots with included boxplots exhibiting the per-cell *FKBP5* transcript-count (+1) of A549 cells from the RNA FISH experiment shown in (A). Three biological replicates were performed for each treatment. (**C**) Stacked bar graphs depicting what percentage of A549 cells had 0, 1, 2 or more than 3 transcription sites visible within the nucleus from the RNA FISH experiment shown in (A). Three biological replicates were performed for each treatment.

3.1.9 Investigating Epigenetic Changes at the ZBTB16 Locus

Transcriptional memory of signal-inducible genes has frequently been described to be established through long-term epigenetic changes at loci of primed genes [119, 120, 122–124, 126]. Therefore, I wanted to investigate potential epigenetic changes at the *ZBTB16* locus which might mechanistically underly priming of that gene upon glucocorticoid treatment. However, to first gain a better understanding of the epigenetic landscape around the *ZBTB16* gene and identify GR binding sites at this locus, I downloaded available ChIP-seq data sets for GR [101] and different histone modifications [147] for A549 cells to generated signal tracks for visual inspection in the genome browser.

With regards to GR binding, the closest binding sites to the *ZBTB16* promoter are situated approximately 100 kb downstream within intronic regions (Fig. 3.22). Inspection of histone modification ChIP-seq coverage tracks revealed that ZBTB16 is located within a repressed region marked by high levels of the repressive mark H3K27me3 (Fig. 3.22). This is further supported by absence of the active histone mark H3K27ac and low levels of H3K4me3 under basal conditions (Fig. 3.22). Upon hormone treatment, increased levels of H3K27ac are observable at GR binding sites and at the promoter (Fig. 3.22), reflecting the activation of *ZBTB16* after GR activation.

In the following section, I set-out to explore whether the enhanced expression of *ZBTB16* upon hormone re-stimulation coincides with an altered chromatin state after initial prim-

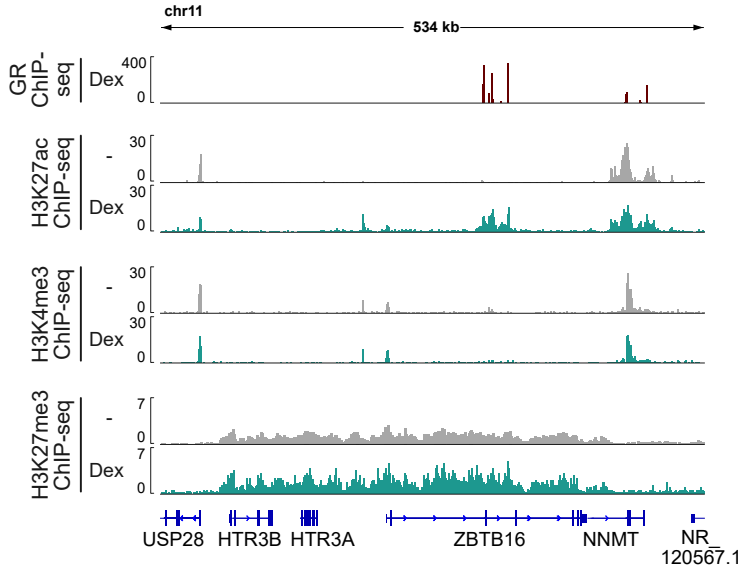

Fig. 3.22: Epigenetic Profiles at the *ZBTB16* Locus. Genome browser view showing the region around the ZBTB16 gene in A549 cells. RPKM-normalized ChIP-seq read coverage tracks are shown for GR, (100 nM dexamethasone, 3 h; RPKM-normalized; data from [101]), H3K27ac (+/- 100 nM dexamethasone, 4 h; data from [147]), H3K4me3 (+/- 100 nM dexamethasone, 4 h; data from [147]) and H3K27me3 (100 nM dexamethasone or ethanol, 1 h; data from [147]).

ing and would thereby give insights into the mechanisms underlying the gene's transcriptional memory. To this end, changes at the *ZBTB16* locus in response to glucocorticoid priming and re-stimulation were studied at the level of chromatin accessibility, 3D chromatin interactions, Pol2 binding, and histone modifications.

Chromatin Accessibility

Previous studies have described GR-induced increases in chromatin accessibility to be long-lived after hormone washout at certain genomic regions [85], [127]. Therefore, I wanted to investigate if maintained increases in chromatin accessibility at GR binding sites occurred at the *ZBTB16* locus and might serve as a priming mechanism upon glucocorticoid exposure.

To test whether GR binding can lead to persistent increases in accessibility at its binding sites at the *ZBTB16* locus, A549 cells were subjected to the hormone reinduction treatment (Fig. 3.13) and subsequently harvested for ATAC-seq. The nearest GR binding sites to the *ZBTB16* promoter are located approximately 100 kb downstream of the promoter within introns of the gene (Fig. 3.22). As expected, hormone treatment resulted in increases in chromatin accessibility at GR binding sites (Fig. 3.23 A). Further, there appeared to be no notable differences in ATAC signal between glucocorticoid treatment in naïve ('- +') and primed cells ('+ +') (Fig. 3.23 A). However, the results revealed similar levels of accessibility between untreated cells ('- -') and primed cells after hormone

washout ('+ -'), suggesting that glucocorticoid-induced increases in accessibility are not maintained after hormone washout for more than 24 hours (Fig. 3.23 A). To confirm these findings, ATAC-qPCR was performed using primers targeting three GR binding sites at the *ZBTB16* locus. The ATAC-qPCR results further validated the ATAC-seq results, as similar accessibility changes were observed (Fig. 3.23 B). Furthermore, the pattern of changes in accessibility at GR binding sites at the *ZBTB16* locus did not differ from the accessibility changes at GR peaks near the GR-target genes *GILZ* and *FKBP5*.

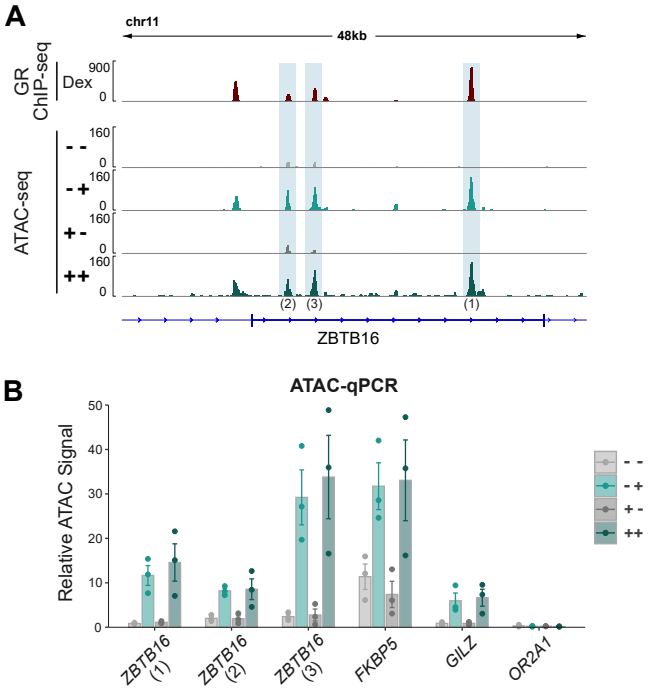

Fig. 3.23: Transient increase in chromatin accessibility at GR binding sites near the *ZBTB16* gene upon glucocorticoid exposure. **(A)** Genome browser view showing coverage tracks of GR ChIP-seq (100 nM dexamethasone, 3 h; RPKM-normalized; data from [101]) and ATAC-seq (normalized, cells treated as detailed in Fig. 3.13) at GR binding sites within introns of *ZBTB16* in A549 cells. Indicated sites were targeted by ATAC-qPCR analysis in (B). **(B)** ATAC-qPCR analysis in A549 cells targeting sites indicated in (A). Cells were treated as detailed in Fig. 3.13. Mean ATAC signal normalized to gDNA is shown (n = 3). Error bars represent ± SEM.

Taken together, these findings show that GR binding at the *ZBTB16* gene results in increased chromatin accessibility, yet the increased accessibility is not sustained after washout and does therefore unlikely to contribute to establishing transcriptional memory of the *ZBTB16* gene.

3D Chromatin Interactions

GR activation has previously been reported to induce large-scale chromatin unfolding at a small number of investigated loci in mouse bone-marrow-derived macrophages [114]. These large-scale chromatin structural changes were found to be maintained for several

days [114].

Therefore, I set out to investigate 3D chromatin interactions at the *ZBTB16* locus in response to GR activation and determine whether any induced changes were long-lived. To this end, I performed 4C-seq which is a derivative 3C method that captures all chromatin interactions from a selected genomic region of interest ('viewpoint'). Thus, 4C-seq assays were performed in A549 cells treated according to the hormone reinduction plan (Fig. 3.13). The *ZBTB16* promoter and an intronic GR binding site were used as viewpoints. The results showed that hormone induction in naïve cells ('- +') causes enhanced interaction levels between the promoter and a group of intronic GR bindings sites, which cluster together approximately 100 kb downstream of the promoter (Fig. 3.24). However, the results from both viewpoints indicate that this increased chromatin interaction was not maintained after hormone washout ('+ -') (Fig. 3.24), suggesting that GR activation does not induce long-lived large-scale structural changes at the *ZBTB16* locus. Additionally, the 4C-profiles of dexamethasone-treated cells exhibited very similar interactions frequencies between naïve and primed cells.

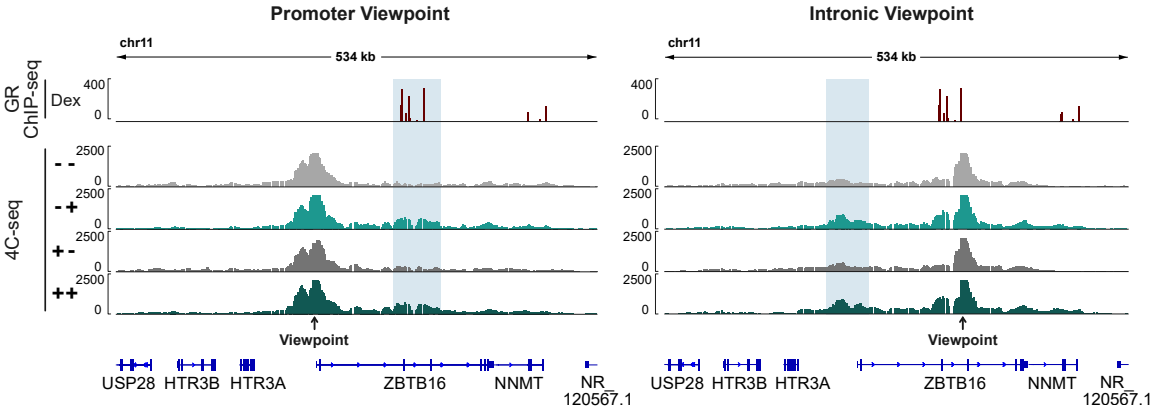

Fig. 3.24: Changes in chromatin interactions in response to hormone reinduction. Genome browser view showing coverage tracks of GR ChIP-seq (100 nM dexamethasone, 3h; RPKM-normalized; data from [101]) and 4C-seq (normalized, cells treated as detailed in Fig. 3.13) at the *ZBTB16* locus in A549 cells. The promoter of *ZBTB16* (left) and an intronic GR binding site (right) were used as viewpoints. Regions exhibiting higher interactions frequencies to the viewpoint upon glucocorticoid treatment are indicated in blue.

Together, the 4C-seq results showed that dexamethasone-induced changes in chromatin interactions frequencies at the *ZBTB16* locus were not maintained after hormone washout and did not differ upon hormone treatment in naïve and primed cells. Hence, persistent changes in 3D chromatin structure at the *ZBTB16* gene are unlikely to play a role in the mechanisms underlying the transcriptional memory of *ZBTB16*.

Pol2 Binding

Previous findings have reported increased promoter-proximal pausing of Pol2 at primed genes following exposure to a stress signal [61].

To test if transcriptional memory of *ZBTB16* is the consequence of altered Pol2 binding at its promoter, ChIP-qPCR was carried out in A549 cells treated according to the hormone reinduction plan (Fig. 3.13). For the ChIP experiments, two Pol2 antibodies were used which bind to hypophosphorylated Pol2, representing total Pol2, and Pol2 phosphorylated at serine-5, representing promoter-proximal paused Pol2 [157]. Upon dexamethasone treatment of naïve cells ('- +'), slightly increased Pol2 occupancy was detectable at the promoter of *ZBTB16* (Fig. 3.25), reflecting the gene's activation. Further, the results showed that there were no differences in Pol2 occupancy at the *ZBTB16* promoter between basal conditions ('- -') and after hormone withdrawal ('+ -') (Fig. 3.25), suggesting that any increases in Pol2 upon hormone treatment are transient. Pol2 levels were further found to be increased at the *ZBTB16* promoter in hormone-treated primed cells ('+ +') compared to naïve cells ('- +') (Fig. 3.25). This observation was made for Pol2 and Pol2 phosphorylated at serine-5 (Fig. 3.25) and thus could be a reflection of the increased transcriptional activity of *ZBTB16* in primed cells. Interestingly, slightly higher Pol2 ChIP levels were also observed in hormone-treated primed cells at the promoters of *GILZ* and *FKBP5* (Fig. 3.25). However, large variability was observed between replicates and therefore additional experiments would be needed to test if the observed trends are real.

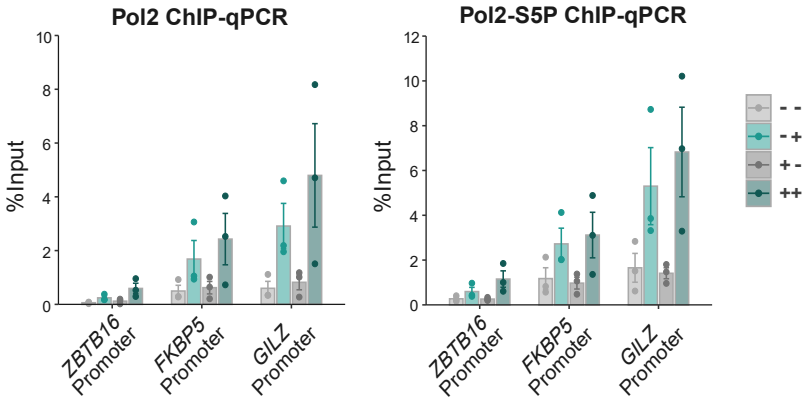

Fig. 3.25: Increased Pol2 binding is not maintained at the *ZBTB16* promoter after hormone washout. Pol2 ChIP-qPCR at promoter of GR target genes in A549 cells. Pol2 antibodies recognize unphosphorylated Pol2 (left) or Pol2 phosphorylated at serine-5 (Pol2-S5P, right). Cells were treated as detailed in Fig. 3.13. Mean percentage of input is shown (n = 3). Error bars represent ± SEM.

To conclude, Pol2 occupancy at the *ZBTB16* promoter accumulates upon glucocorticoid treatment in naïve and primed cells, reflecting changes in transcription. However, there is no indication that the increased occupancy is maintained after washout in the

absence of hormone, arguing against a mechanism in which higher levels of promoter-proximal paused Pol2 are involved in establishing transcriptional memory.

Histone Modifications: H3K27ac, H3K4me3 and H3K27me3

Several studies have previously described sustained changes in histone marks at promoters of primed genes to be involved in the mechanisms underlying transcriptional memory [119, 120, 122, 123, 126].

To determine whether the enhanced expression of *ZBTB16* upon reinduction is accompanied by altered levels of histone marks in primed versus naïve cells, levels of H3K27ac, H3K4me3 and H3K27me3 at the *ZBTB16* were measured by ChIP-qPCR in A549 cells treated according to hormone reinduction treatment (Fig. 3.13). At the promoter region of *ZBTB16*, levels of the active marks H3K4me3 and H3K27ac were found to be elevated upon hormone treatment in naïve and primed cells ('- +' and '+ +') compared to vehicle-treated naïve and primed cells ('- -' and '+ -') (Fig. 3.26). Notably, maintenance of these histone modifications was not observed after washout ('+ -'), with levels comparable to untreated cells ('- -') (Fig. 3.26). For the repressive histone mark H3K27me3, levels were largely unchanged in response to the hormone treatments, though dexamethasone induction appeared to result in slightly reduced levels of H3K27me3 (Fig. 3.26). Similar to H3K27ac and H3K4me3, changes in H3K27me3 did not seem to be maintained after hormone washout compared to basal conditions (Fig. 3.26). Furthermore, the patterns of changes of all three histone marks at the *ZBTB16* locus is very similar to the changes detectable at the *GILZ* and *FKBP5* loci (Fig. 3.26), genes which do not show transcriptional memory.

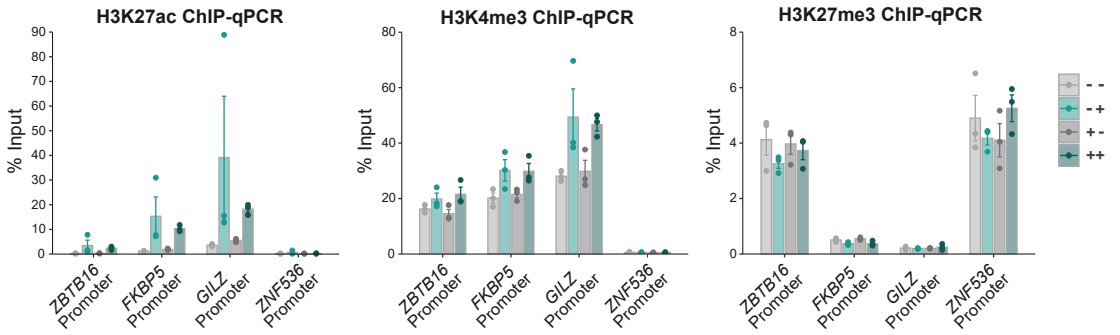

Fig. 3.26: GR-incuded levels in histone marks H3K27ac, H3K4me1 and H3K27ac are not maintained after hormone withdrawal. H3K27ac, H3K4me3 and H3K27me3 ChIP-qPCR targeting promoters of indicated GR target genes in A549 cells. Cells were treated as detailed in Fig. 3.13. Mean percentage of input is shown (n = 3). Error bars represent ± SEM.

Taken together, levels of the histone marks H3K27ac, H3K4me3 and H3K27me3 are not maintained following a prior dexamethasone treatment at the *ZBTB16* promoter and are therefore unlikely to contribute to driving transcriptional memory of *ZBTB16*.

3.2 Part 2: Comparison of AR and GR Binding Preferences in U2OS Cells

The second part of the results sections aims at investigating the mechanisms that underly the distinct genomic binding preferences of GR in comparison to the androgen receptor (AR). The following section is the result of a collaborative project between Marina Kulik and myself, and forms part of our recent publication [129].

3.2.1 Genome-Wide Binding Analysis of GR and AR

GR and AR are related steroid receptors whose DNA-binding domains show a high degree of structural similarity. In fact, the DNA-binding domains of the two receptors have an almost identical amino-acid composition and consequently near-identical structure [23, 34]. As a result, both receptors bind to the same DNA recognition sequence with high affinity [23].

To explore GR- and AR-specific binding preferences in the same cellular context, genomic occupancy of both receptors was studied in the same parental cell line, namely the U2OS cell line. To this end, GR binding in GR-expressing U2OS cells (U2OS-GR cells,[128]) was compared to AR binding in AR-expressing U2OS cells (U2OS-AR cells; cell line generated by Marina Kulik, [129]). Similarly to GR in the U2OS-GR cells, which becomes activated upon treatment with the synthetic glucocorticoid dexamethasone, AR in U2OS-AR cell line is inducible through treatment with the synthetic androgen R1881. To identify GR and AR binding sites, GR ChIP-seq data in glucocorticoid-treated U2OS-GR cells (replicate 1: [148], replicate 2: generated by Verena Thormann, [129]) and AR ChIP-seq data in androgen-treated U2OS-AR cells (2 replicates generated by Marina Kulik, [129]) were analyzed and binding sites determined through peak calling. Genomic regions were defined to be bound by both receptors (shared sites), only bound by GR (GR-specific sites) or only bound by AR (AR-specific sites). The ChIP-seq results showed that many sites were occupied by both receptors, which is to be expected considering their similar binding sequence preferences (Fig. 3.27 A). Additionally, GR-specific as well as AR-specific sites were also identified (Fig. 3.27 A, B). These findings are in line with previous studies which also found a combination of overlapping and receptor-specific binding sites [31–33]. Interestingly, there is a larger number of GR binding sites overall (Fig. 3.27 A). This is likely a consequence of the fact that GR expression levels were found to be approximately three times higher in U2OS-GR cells compared to AR levels in U2OS-AR cells, as quantified by whole-cell [^{3}H] steroid binding assays performed by Marina Kulik (see Fig. 5.1, [129]).

Taken together, GR and AR share a large proportion of their binding sites. However, both receptors are also capable of binding in a receptor-specific manner in the U2OS cell line which, given their structurally near-identical DNA-binding domains, raises the ques-

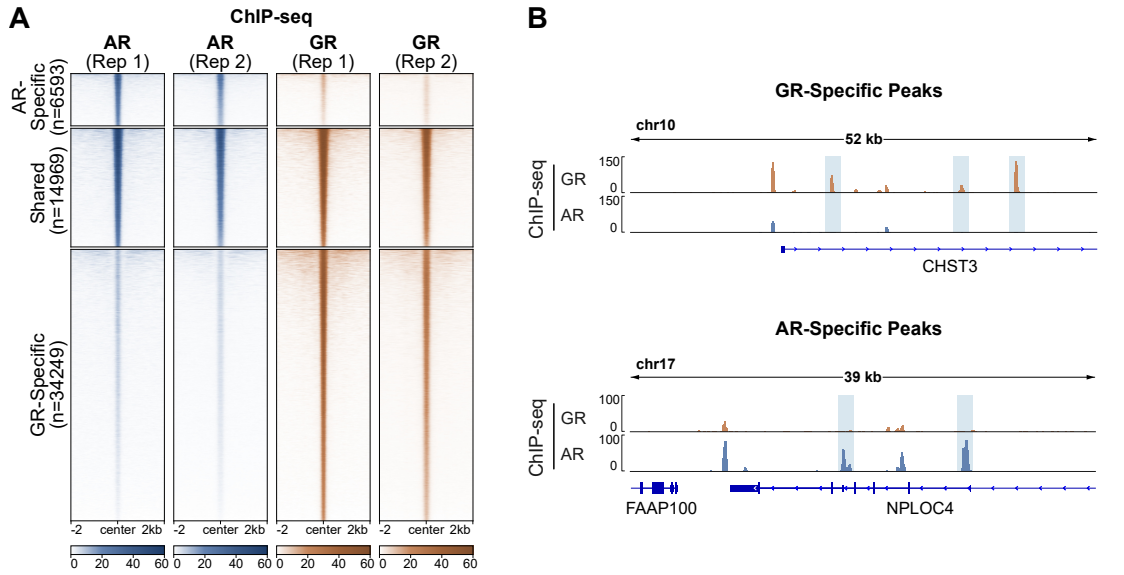

Fig. 3.27: Genome-wide binding of AR and GR in U2OS cells. (**A**) Heatmap of RPKM-normalized ChIP-seq read coverage targeting AR and GR in U2OS-AR (5 nM R1881 for 4 h) and U2OS-GR cells (1 µM dexamethasone for 1.5 h), respectively. Genomic regions shown are sites of shared and AR- or GR-specific binding (+/- 2 kb around center). AR ChIP-seq replicates in U2OS-AR cells performed by Marina Kulik, [129]. GR ChIP-seq replicate 1 data from [148] and replicate 2 performed by Verena Thormann, [129]. (**B**) Genome browser view of RPKM-normalized GR and AR ChIP-seq read coverage tracks showing example GR-specific and AR-specific bindings sites (highlighted in blue). One representative ChIP-seq replicate (same as (A)) is shown.

tion of how this selectivity can be achieved.

3.2.2 GR Is Able to Bind to More Inaccessible Genomic Regions than AR

Chromatin accessibility plays a major role in restricting or enabling binding of transcription factors to DNA [39].

To determine whether chromatin accessibility contributes to binding specificities of GR and AR, ATAC-seq data was generated in vehicle- or hormone-treated U2OS-GR cells (performed by myself) and U2OS-AR cells (performed by Marina Kulik). The data were integrated with the ChIP-seq results to determine accessibility levels before and after receptor binding. The ATAC-seq results showed that both receptors induced increases in chromatin accessibility at the shared binding sites, but also at their respective receptor-specific sites (Fig. 3.28). Interestingly, the average ATAC signal in vehicle-treated conditions is much lower at GR-specific sites than at AR-specific sites. In fact, a large proportion of GR-specific sites exhibit very low levels of accessibility (Fig. 3.28). Hence, GR appears to be capable of binding to relatively inaccessible chromatin compared to AR.

To better characterize the chromatin landscape of GR- and AR-specific binding sites, I next analyzed ChIP-seq data in both cell lines (data generated by Alisa Fuchs) of histone marks associated with euchromatin (H3K27ac, H3K4me1) and heterochromatin

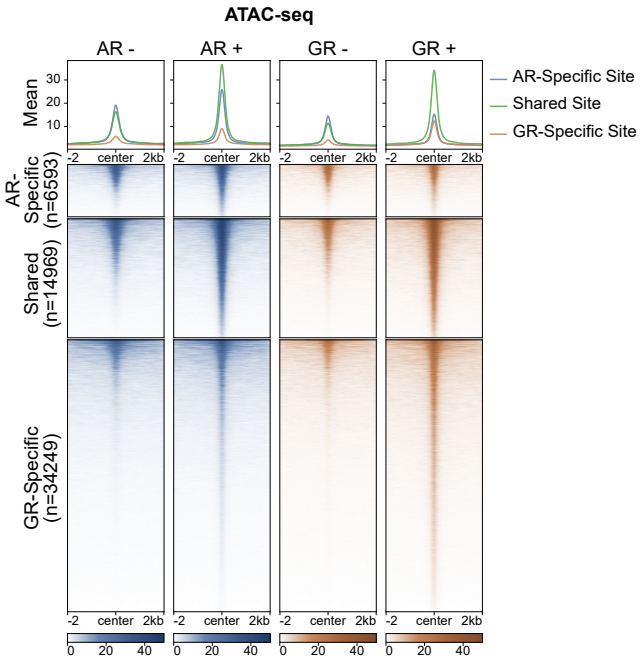

Fig. 3.28: Chromatin accessibility at GR and AR binding sites. Heatmap and mean signal plot (top) of RPKM-normalized ATAC-seq read coverage in U2OS-AR and U2OS-GR cells at genomic regions (+/- 2 kb around center) of shared and AR- or GR-specific binding sites (same sites as shown in Fig. 3.27 A). U2OS-AR cells were treated with DMSO (AR -) or 5 nM R1881 for 4 hours (AR +). U2OS-GR cells were treated with ethanol (GR -) or 1 µM dexamethasone for 1.5 hours (GR +). ATAC-seq in U2OS-AR cells was performed by Marina Kulik.

(H3K9me3, H3K27me3) [95–98]. In accordance with the ATAC-seq results, GR-specific regions were marked by low levels of the active marks H3K27ac and H3K4me1 and relatively high levels of the repressive marks H3K9me3 and H3K27me3 prior to hormone treatment, while AR-specific regions showed the reverse pattern (Fig. 3.29). Interestingly, AR-specific sites also exhibited higher levels of active marks and lower levels of repressive marks than the shared sites (Fig. 3.29), suggesting that these binding sites are situated in particularly active accessible chromatin. Furthermore, regarding changes in histone modifications upon receptor binding, one striking difference between the two receptors was the fact that GR binding induced major increases in H3K27ac, while AR binding resulted in subtle increases of the same mark (Fig. 3.29).

In summary, the above results indicate that GR is able to bind relatively inaccessible genomic regions in U2OS cells, while AR binding seems largely restricted to sites which are very accessible prior to hormone treatment. This suggests that binding specificity of GR and AR is, in part, achieved through their differing abilities to bind inaccessible chromatin.

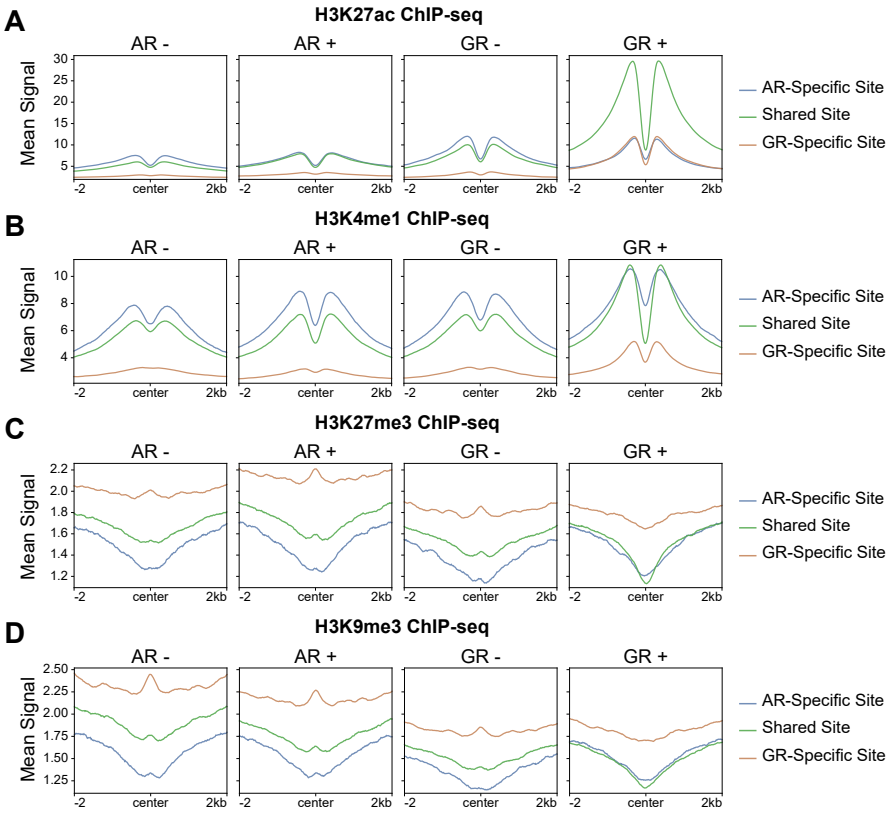

Fig. 3.29: Active and repressive histone marks at GR and AR binding sites. (A-D) Mean RPKM-normalized ChIP-seq read coverage of (A) H3K27ac, (B) H3K4me1, (C) H3K27me3 and (D) H3K9me3 at shared and AR- or GR-specific binding regions (+/- 2 kb around center) (same sites as shown in Fig. 3.27 A). U2OS-AR cells were treated with DMSO (AR -) or 5 nM R1881 for 4 hours (AR +). U2OS-GR cells were treated with ethanol (GR -) or 1 μM dexamethasone for 1.5 hours (GR +). ChIP-seq experiments were performed by Alisa Fuchs.

3.2.3 AR Binds to the Direct Repeat Motif

Next, I wanted to investigate the role of sequence in directing receptor-specific binding, since recent studies provided evidence that AR, but not GR, binds a version of GR/AR consensus motif which is composed of a direct repeat of the 5'-AGAACA-3' halfsite [36, 37]. Hence, AR's ability to bind the direct repeat consensus sequence is likely involved in direct AR-specific binding.

To investigate the differences in the receptors' motif preferences at their binding sites, I performed a motif enrichment analysis using AME (Analysis of Motif Enrichment, [149]) of the MEME suite (Multiple Expectation maximizations for Motif Elicitation, [150]). More specifically, GR- and AR-specific binding sites were scanned for the clustered JASPAR CORE vertebrates motif collection [25]. In this motif collection, very similar motifs, such as the GR and the AR consensus motifs, for instance, have been clustered together, which removes redundancy compared to including all JASPAR motifs. Additionally, a direct repeat version of the GR/AR consensus motif (Fig. 3.30) was also included in

the motif search. Moreover, since many GR-specific binding sites exhibited very low levels of chromatin accessibility prior to hormone treatment, only the 6593 GR-specific sites of highest accessibility (as sorted by vehicle-treated ATAC-seq signal in U2OS-GR cells) were included in the analysis. This was done to exclude chromatin accessibility as a confounding factor, since GC-content is generally higher in accessible chromatin [158–160] and would therefore affect the results from the motif analysis. After carrying out the motif enrichment analysis of GR- and AR-specific sites, I identified a large number of enriched motifs (data not shown). To facilitate a direct comparison of the most enriched motifs for each receptor, I only retained motifs which had a significance E-value threshold of $<10^{-30}$ for either one of the receptors and plotted the results as a heatmap (Fig. 3.30). Notably, the GR/AR consensus motif was found to be enriched at GR- and AR-specific sites, yet was more highly enriched at GR-specific sites (Fig. 3.30). The lower enrichment at AR-specific sites suggests that the consensus motif might be less well-defined at those regions, which is in line with previous results showing that AR is able to bind to more degenerate versions of the consensus motif [32]. As expected, the direct repeat motif was also more enriched at the AR-specific binding sites than GR-specific sites (Fig. 3.30). Hence, it appears that selective binding of AR can, in part, be explained through AR's ability to bind to the direct repeat motif as well as to more degenerate versions of the consensus motif in U2OS cells. With regards to the enrichment of other motifs, a small number of motifs was found to be enriched at GR-specific sites, yet not enriched at all at AR-specific sites (Fig. 3.30). This raises the possibility that composite binding with other transcription factors might also affect receptor binding specificities. One of the motifs which was enriched at GR-specific but not at AR-specific sites was a Fox-like motif (Fig. 3.30). Interestingly, previous studies have described composite binding with FoxA1 to affect GR and AR binding specificities [33, 35].

Since the direct repeat motif showed higher enrichment at AR-specific sites (Fig. 3.30), I wanted to further explore the ability of both receptors to bind to this sequence and to determine whether GR might also be able to bind to this motif *in vivo*. Therefore, I made use of available ChIP-exo data to investigate the receptors' footprints when bound to the direct repeat sequence. ChIP-exo is a modification of ChIP-seq [161], which includes the usage of a lambda exonuclease to digest unbound DNA at the 5' end of the fragment. DNA which bound to protein will be protected from degradation. As a result, ChIP-exo provides information on the exact location of transcription factor binding to DNA with high resolution. To obtain the receptor footprints, I applied the ExoProfiler tool [153]. The ExoProfiler scans a transcription factor's binding sites for the presence of a DNA motif of interest and outputs a footprint of the bound protein to those regions based on ChIP-exo data. To this end, I downloaded ChIP-exo data for GR in U2OS-GR cells [153] as well as available ChIP-exo and ChIP-seq data for AR in LNCaP cells [152]. Next, the ExoProfiler was used to scan receptor binding sites with either the direct repeat motif or

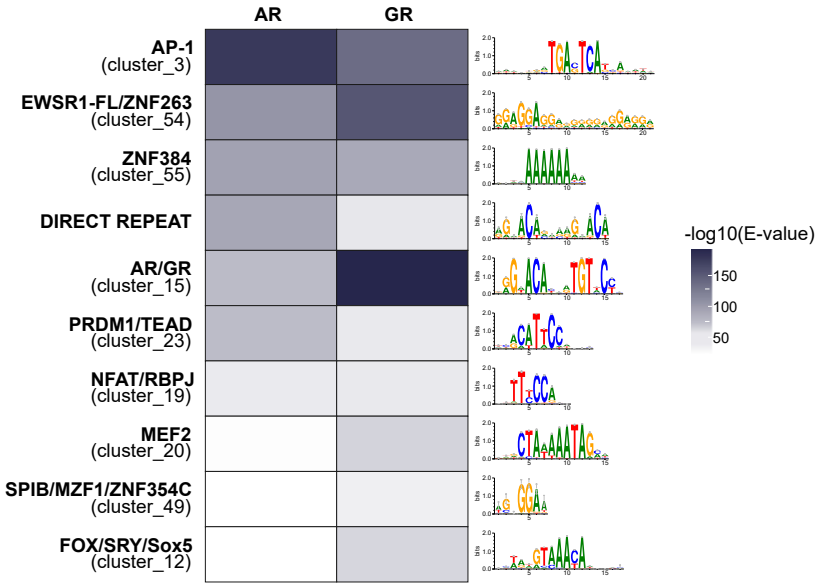

Fig. 3.30: Motif enrichment analysis comparing GR- and AR-specific binding sites. Heatmap showing the enrichment ($-\log_{10}$(E-value)) of JASPAR motif clusters [25] at GR- and AR-specific binding regions (+/- 250 bp around center). All AR-specific sites (6593 regions) were used in the analysis, whereas only the GR-specific sites of highest chromatin accessibility (6593 regions) were used. Motifs which exhibited an E-value score of $<10^{-30}$ for either GR or AR are shown.

the respective consensus motifs for each receptor. For AR, a footprint was observable for the consensus and the direct repeat motif (Fig. 3.31). Interestingly, for GR a footprint was also observable for the direct repeat motif, though not as pronounced as for its consensus sequence (Fig. 3.31). Hence, the more pronounced AR footprint suggests that the direct repeat is preferentially bound by AR, which is consistent with higher enrichment of this motif at AR-specific sites.

Together, the results from the motif enrichment analysis suggest that the exact sequence of the GR/AR recognition motif is one driving factor in determining receptor-specific binding. Binding specificity of AR seems to be partly achieved through its ability to bind the direct repeat motif as well as to more degenerate consensus motifs. Additionally, composite binding with other transcription factors might also play a role in shaping GR binding specificity.

3.2.4 GR Binds to Genomic Regions with a Higher GC-Content than AR

Previous research found that AR, but not GR, prefers occupying sites where the consensus motif is directly flanked by poly(A) sequences [34]. Hence, GC-content appears to influence receptor binding preferences.

To investigate to what extent GC-content influences binding of GR and AR in U2OS cells, the mean GC-content was calculated for the region +/- 5 kb around the center of all AR-specific and GR-specific peaks. Directly at the binding sites, GR-specific regions

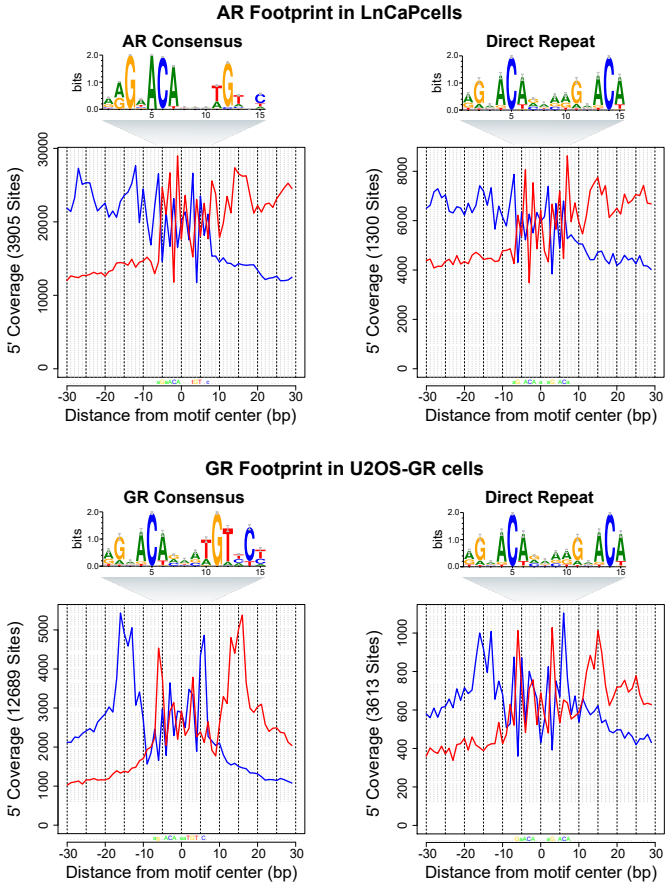

Fig. 3.31: ChIP-exo footprint profiles of AR and GR. AR and GR ChIP-exo footprint profiles in LNCaP cells and U2OS-GR cells, respectively. For both receptor footprints at their respective consensus motifs and the direct repeat motif are shown. The consensus motifs were obatined from JASPAR (GR: MA0113.2; AR: MA0007.2; [25]). Blue signifies the forward and red the reverse strand. GR ChIP-exo data in U2OS-GR cells from [153]. AR ChIP-exo and ChIP-seq data in LNCaP cells from [152].

exhibited a higher GC-content than AR-specific regions (Fig. 3.32 A). Interestingly, the entire 10 kb region investigated showed a higher mean GC-content for GR-specific sites (Fig. 3.32 A), indicating that not just the GC-content directly at the binding site, but also of the larger surrounding areas affects receptor binding preferences. In addition, AR-specific sites also exhibited a drop in GC-content in the areas directly flanking the peaks (Fig. 3.32 A), arguing for the presence of the poly(A) sequences at AR-specific binding sites, as was previously observed *in vitro* [34]. However, since GC-content is generally higher in accessible chromatin [158–160], I wanted to exclude chromatin accessibility as a confounding factor and only include GR- and AR-specific regions in the analysis which exhibited comparable levels of chromatin accessibility. For this purpose, GR- and AR-specific sites were sorted by their ATAC-seq signal prior to hormone treatment and only the 3296 sites per receptor of the highest chromatin accessibility were included in the analysis. The mean ATAC-seq signal of those regions exhibited similar levels prior to

hormone treatment (Fig. 3.32 C). Interestingly, the difference in GC-content between GR-specific and AR-specific peaks was even more striking when investigating the regions of highest accessibility (Fig. 3.32 B).

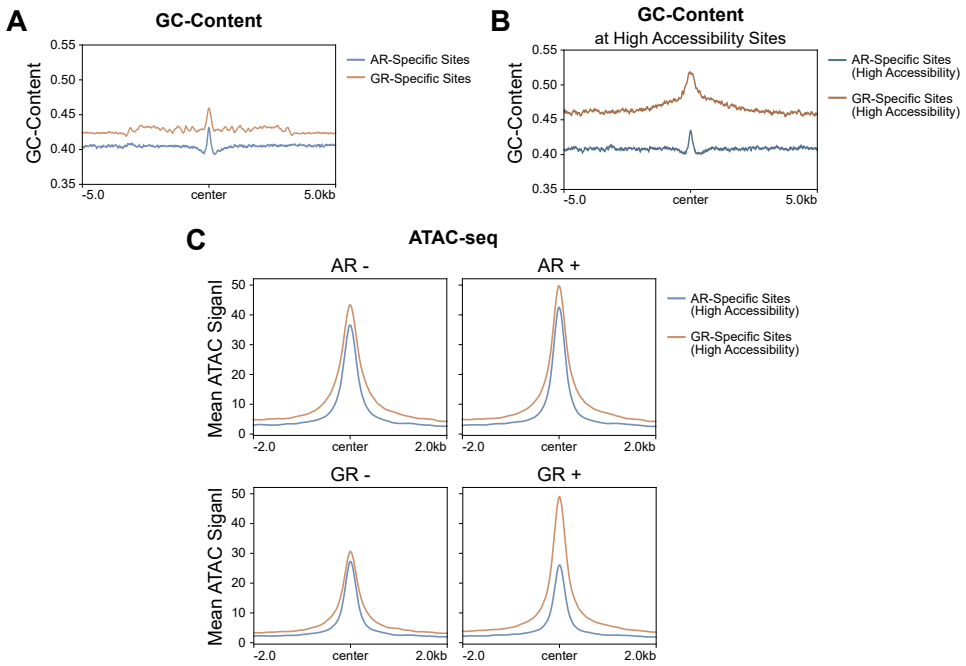

Fig. 3.32: GC-content at AR and GR binding sites. (**A**) Mean GC-content at GR- and AR-specific binding sites. Region +/- 5 kb around the center of the binding sites are shown. (**B**) Same as (A), except that mean GC-content for GR- and AR-specific sites of highest chromatin accessibility (3296 sites per receptor) is shown. GC-content was found to be significantly higher at GR-specific sites for both (A) and (B), with a p-value<2.2e-16 as calculated with a Mann-Whitney-U. (**C**) Mean RPKM-normalized ATAC-seq signal at GR- and AR-specific binding sites of highest chromatin accessibility (same sites as used in the analysis shown in (B)). U2OS-AR cells were treated with DMSO (AR -) or 5 nM R1881 for 4 hours (AR +). U2OS-GR cells were treated with ethanol (GR -) or 1 μM dexamethasone for 1.5 hours (GR +). ATAC-seq in U2OS-AR cells was performed by Marina Kulik.

Furthermore, to determine whether these observations were specific to U2OS cells or a general phenomenon, I downloaded available lists of GR and AR ChIP-seq peaks from two prostate cancer cell lines, namely VCaP and LNCaP-1F5 cells [33], and performed the same analysis. Given AR's role in maintaining prostate cancer function but also in driving prostate cancer progression [162], studying AR binding in those cell types is of notable clinical relevance. Interestingly, the same trends regarding GC-content as previously observed in U2OS cells were also observed in VCaP and LNCaP-1F5 cells (Fig. 3.33), indicating that GR's preference for a high GC-content of its binding sites and the surrounding genomic regions is not a cell type-specific effect, but rather represents a more general mechanism.

Taken together, the GC-content at GR-specific binding sites was found to be higher than at AR-specific sites. Interestingly, the higher GC-content for GR binding sites ex-

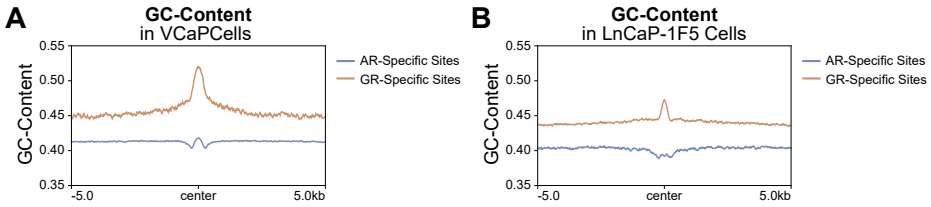

Fig. 3.33: GC-content at AR and GR binding sites in LNCaP and VCaP cells. Mean GC-content at GR- and AR-specific binding sites are shown. Region +/- 5 kb around the center of the binding sites is shown. ChIP-seq data from [33].

tended beyond the binding sites itself, suggesting that receptor selective binding is also driven by the sequence composition of the larger genomic region. Such different preferences in sequence composition for the extended genomic area have previously been described for transcription factors from different families [163]. Notably, the present results possibly provide the first example of this phenomenon occurring for transcription factors of the same family.

4 Discussion

4.1 Transcriptional Repression by GR Partially Due to Indirect Mechanisms

Hormone-bound GR is capable of functioning as an activator as well as a repressor of transcription. In the human cell line A549, for instance, GR action results in the up- and downregulation of a large number of genes [44, 60] (Fig. 3.14). As an activator of transcription, GR binding to its consensus recognition sequence as a homo-dimer has emerged as the predominant mode of action [24, 45]. Conversely, transcriptional repression by GR appears to be more complex, since a range of mechanisms have been put forward by which GR represses its target genes (see section 1.2.3).

In recent years, the notion that transcriptional repression might not depend on local occupancy of GR has been suggested [58, 59]. In fact, Reddy et al [60] observed a median distance of 146 kb between the TSS of downregulated genes and the closest GR binding site in A549 cells, while the median distance between upregulated genes of GR peak was only 11 kb. These findings raise the possibility that, at least in some instances, GR does not actively repress transcription, but rather induces downregulation of target genes through the indirect effects of its action. This notion has been further supported by studies investigating GR's ability to enhance or repress the activity of regulatory sequences using STARR-seq (Self-Transcribing Active Regulatory Region sequencing). STARR-seq is a massively parallel reporter assay in which the regulatory activity of candidate sequences is measured by placing them downstream of a minimal promoter and quantitatively assessing to what extent they can activate their own expression [164]. Analysis of GR binding sequences by STARR-seq showed that GR action either did not repress enhancer activity [101] or, if repression was observed, it was not found to be reproducible [133]. In another study by Johnson et al. [90], the authors did observe repressed enhancer activity following dexamethasone treatment in a STARR-seq experiment carried out in A549 cells. However, the authors observed that these repressed sequences were not enriched for the GR consensus motif and also showed GR occupancy levels that were comparable with non-regulated controls of similar accessibility [90], suggesting that the observed repression does not depend on GR binding.

In the present study, genomic sites of decreasing chromatin accessibility upon hormone treatment, which were largely not occupied by GR (Fig. 3.2, 3.3), were found to be

significantly enriched near downregulated genes (Fig. 3.4, 3.6). It is conceivable that the loss of chromatin accessibility at some of those sites might be the result of regulatory factors, which were bound to those regions prior to hormone treatment, becoming recruited away upon GR activation. Accordingly, at closing regions, p300 levels were found to be reduced after hormone exposure, which was accompanied by a loss in H3K27ac levels (Fig. 3.5). Since the co-activator p300 is known to frequently be recruited by GR to its binding sites [61, 99, 103], it is possible that GR binding causes p300 to be sequestered away from other genomic regions, resulting in the downregulation of nearby genes. A similar observation has previously been made by Portuguez et al [61], who showed that p300 levels were reduced at enhancers near repressed genes following GR activation. Hence, downregulation of GR target genes might occur, in part, through the indirect effects of co-factor 'squelching' (Fig. 4.1). The concept of co-factor squelching, in which transcription factors compete for a finite number of cofactors, has previous been suggested as a possible mechanism of repression for signal-inducible transcription factors [62]. Further research is needed to confirm if closing sites, as described in this thesis, indeed contribute to glucocorticoid-dependent repression of nearby genes. Follow-up experiments could, for instance, involve overexpression of cofactors, such as p300, to determine if repression of genes near closing sites would still be observed if large amounts of the investigated cofactor were available.

However, it needs to be noted that the results from this thesis do not indicate that GR exclusively represses via indirect mechanisms, specifically since GR binding sites were found to be enriched near downregulated genes, yet, to a lesser extent than near upregulated genes (Fig. 3.4, 3.6). This finding suggests that for certain genes GR-induced repression might still be dependent of nearby binding of GR, highlighting that transcriptional repression by GR likely occurs via a range of mechanisms.

In summary, the present thesis provides evidence that GR activation induces decreased chromatin accessibility at a large number of sites that are typically not bound by GR. This is in addition to the increases in accessibility at many genomic regions, which are well-documented in the literature. The present results further support of the notion that GR-induced transcriptional repression of some of its target genes might occur via indirect mechanisms of its action, specifically through 'squelching' of cofactors, such as p300 (Fig. 4.1).

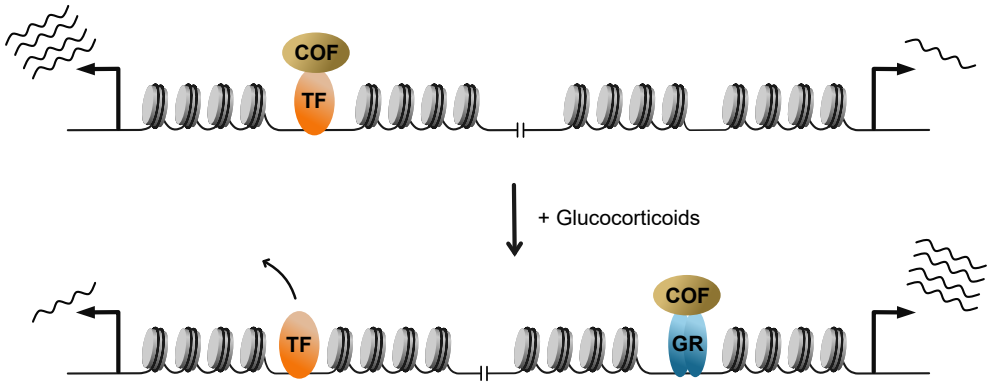

Fig. 4.1: Model of GR-mediated repression via indirect effects of GR action. Upon activation, GR binds to the genome and recruits cofactors (COFs), which results in transcriptional upregulation of nearby target genes. Prior to GR activation, COFs were bound to other transcription factors (TFs) at regulatory elements near actively transcribing genes. The loss of COFs from those regulatory elements results in a loss of chromatin accessibility, possibly also due to the loss of other bound TFs, and subsequent downregulation of nearby genes.

4.2 GR-Induced Changes in Chromatin Accessibility are Reversible 24 Hours after Hormone Washout

Upon binding to the genome, GR has frequently been described to induce an opening of the chromatin at its binding sites [77, 80, 81]. The question of what happens to the increased chromatin accessibility after glucocorticoid withdrawal, and thus in the absence of activated GR, has previously been addressed by Zaret and Yamamoto [127] and Stavreva et al. [85], who observed that certain genomic regions exhibited sustained increases in accessibility after hormone washout. Hence, these findings suggest that a GR-binding event can induce long-lived structural changes of the chromatin. Given the widespread applications of glucocorticoids as therapeutic anti-inflammatory agents [11, 12] and their commonly associated side-effects upon long-term treatments [13, 20, 21], studying the effects of glucocorticoids on chromatin structure might provide valuable clues into some of the mechanisms underlying such adverse effects.

Here, to investigate whether long-term chromatin structural changes are a general feature of GR activation and are therefore observable in different cell systems, I compared levels of chromatin accessibility 24 hours after hormone removal to accessibility levels directly upon hormone treatment in the two human cells lines A549 and U2OS. In A549 cells, GR-induced changes in chromatin accessibility largely reverted to pre-hormone treatment levels (Fig. 3.8, 3.9). In U2OS cells, on the other hand, maintained changes in chromatin accessibility were observed (Fig. 3.10). However, analysis of GR occupancy 24 hours after hormone withdrawal showed that residual receptor binding was found at sites of persistently increased chromatin accessibility (Fig. 3.11). Since GR was found to bind these 'persistent' sites at very low hormone concentrations (Fig. 3.12), it is likely that low dex-

amethasone concentrations were still present in the cells 24 hours after hormone removal resulting in GR binding to those regions. These findings are in line with a previous study which showed that, at very low glucocorticoid concentrations, GR selectively binds to only a small fraction of all its possible binding sites [165]. Thus, the maintained increases in accessibility after hormone washout might not indicate any form of memory, but rather are the consequence of low levels of active receptor preferentially binding to a subset of sites, namely the 'persistent' sites. Hence, GR-induced changes in chromatin accessibility are not sustained in A549 and U2OS cells for 24 hours, and therefore are unlikely to be maintained throughout cell divisions in these cell types.

The fact that the present thesis does not report maintained changes in chromatin accessibility, which had been described in the above-mentioned studies [85, 127], argues that long-term accessibility changes are not a commonly observed feature of GR activation. The study by Stavreva et al. [85] investigated genome-wide chromatin accessibility changes in mouse mammary adenocarcinoma cells. In particular, the authors performed DNase-seq following a 40-minute hormone washout period. Hence, aside from the different cell type that was used, the much shorter washout period applied by the authors might account for the fact that they observed persistently increased accessibility, which could not be confirmed in the present thesis. Thus, the possibility cannot be excluded that I would also observe persistent changes in chromatin accessibility following shorter washout periods. In the study by Zaret and Yamamoto [127], the authors reported GR-induced increases in chromatin accessibility at a stably integrated MMTV sequence in mouse L cells, which were sustained for more than 9 days after hormone washout. Again, aside from the different cell type investigated, Zaret and Yamamoto [127] observed the persistent accessibility at an exogenous sequence, which raises the questions whether this finding is representative of endogenous mammalian loci.

From a physiological perspective, the fact that glucocorticoid-induced changes in chromatin accessibility are of a reversible nature seems expected, given that GR is repeatedly activated throughout the day following the pulsative and circadian release pattern of glucocorticoids from the adrenal glands [16, 17, 166]. However, it needs to be noted that, under resting conditions, each GR-activation period is relatively short, since the release of endogenous glucocorticoids occurs in short bursts of approximately 20 minutes [16, 17]. However, previous studies have reported that GR activation in response to longer hormone exposure times exhibits distinct binding patterns and target gene expression profiles when compared to shorter exposure times [85, 166]. Hence, it is conceivable that longer glucocorticoid exposure times might also have different long-term effects on the chromatin than shorter exposures. Therefore, future experiments should address the duration of the hormone treatments and investigate if persistent chromatin changes are observable as a consequence of longer hormone exposures.

Taken together, chromatin accessibility changes in A549 and U2OS cells were found to

be reversible following a 24-hour hormone washout, suggesting any GR-induced changes in accessibility are unlikely to be maintained throughout cell division. Hence, persistent changes in chromatin accessibility do not appear to be a general feature associated with GR activation. However, it remains unclear if long-lived accessibility changes would be observed under different experimental conditions, such as different hormone concentrations or exposure times. Given the side-effects observed due to long-term treatment with synthetic glucocorticoids in a clinical setting [13, 20], long-lived structural chromatin changes might be more likely to be observed after much longer hormone exposure times. Further research would be required to investigate this.

4.3 Gene-Specific Transcriptional Memory upon GR Reinduction

Repeated exposures to high levels of glucocorticoids over prolonged periods of time can lead to serious health problems. This can occur as a consequence of chronic stress, in which the adrenal glands synthesize and secrete higher levels of cortisol, and result in pathological effects, such as muscle wasting, cognitive decline and severe metabolic effects including glucose intolerance and central fat accumulation [9, 167]. Alternatively, repeatedly high glucocorticoid levels are also encountered in patients undergoing long-term treatment with synthetic glucocorticoids and is often accompanied by severe metabolic side effects or glucocorticoid resistance [13, 20]. At the molecular level, the mechanisms underlying the adverse effects of repeatedly elevated levels of glucocorticoids are highly complex and remain poorly understood.

Since previous studies suggested that GR has the potential to induce long-lived chromatin changes, in particular maintained increases in chromatin accessibility as well as chromatin decompaction [85, 114, 127], I wanted to investigate to what extent GR activation can also have long-lived effects on the transcriptional output. Therefore, I studied the effects of repeated GR activation on the transcriptional response to determine if GR activation can be 'remembered' by the cells in a way that a second GR activation elicits an altered transcriptional response. Overall, I observed that GR-induced transcriptional changes reverted back to basal levels following hormone withdrawal, thus transcriptional responses are not maintained in the absence of active GR (Fig. 3.14 B). Further, comparison of transcriptional output in naïve or primed cells showed the GR-induced changes were very similar, showing no large-scale changes in the transcriptional response (Fig. 3.14 C). In general, it is to be expected that prior GR activation does not cause major transcriptional re-wiring since, under physiological resting conditions, GR activation follows the pulsed pattern of the endogenous glucocorticoids [166], which are secreted from the adrenal glands as hourly pulses throughout the day [16, 17].

However, I did identify a single gene, namely *ZBTB16*, which exhibited enhanced expression upon glucocorticoid treatment in primed cells. ZBTB16, a member of the

POZ and Krüppel-like zinc finger protein family, is a transcription factor which regulates the expression of genes involved in physiological processes including development, spermatogenesis as well as glucose and lipid metabolism [168–173]. ZBTB16's role in metabolic processes [173] make it a potential candidate gene to be mis-regulated as a consequence of long-term treatment with glucocorticoids, since patients often experience metabolic side effects [13, 20]. In fact, Krupková et al. [174] identified a role of ZBTB16 in dexamethasone treatment-induced insulin resistance of skeletal muscles as well as increased glucose and lipid blood levels in rats. In addition, a previous study has also reported that ZBTB16 inhibited transcriptional activation by GR in HeLa cells [175].

Together, repeated activation of GR results in enhanced transcription of *ZBTB16*, indicating that GR is able to induce gene-specific transcriptional memory. Since *ZBTB16* plays a role in metabolic processes, it is an interesting candidate to study in relation to the glucocorticoid-resistance or the side effects commonly associated with long-term glucocorticoid therapy. To this end, experiments involving repeated hormone exposure of physiologically relevant cells and subsequent analysis of *ZBTB16* expression would be important to determine if transcriptional memory of *ZBTB16* also occurs in those settings.

4.4 Potential Mechanisms of ZBTB16 Priming

Transcriptional memory of external signals allows cells to prime signal-inducible genes when a signal is first encountered, leading to an altered, or more efficient, transcriptional response when the signal is re-encountered. This phenomenon, which has frequently been described in plants in response to environmental stress, can thus be seen as an adaptive transcriptional response to the environment. Mechanistically, the way the memory of an external signal is stored has frequently been observed to involve chromatin changes which can be sustained throughout cell divisions [119, 120, 122–124, 126].

In the present thesis, I explored if epigenetic changes at the *ZBTB16* locus to determine if chromatin changes, induced through a first GR activation, could serve as mechanistic explanations for the observed transcriptional memory. Investigation of changes in the histone marks H3K4me3, H3K27me3 and H3K27ac as well as Pol II (unphosphorylated or phosphorylated on serine 5) occupancy, chromatin accessibility and long-range chromatin interactions showed that GR activation induces changes to the chromatin state at the *ZBTB16* locus, yet these changes were not found to persist after hormone washout (Fig. 3.23, 3.24, 3.25, 3.26). Additionally, GR-induced epigenetic changes showed no notable differences between naïve and primed cells (Fig. 3.23, 3.24, 3.25, 3.26). Hence, the investigated features gave no indications of priming mechanisms of *ZBTB16*. However, the methods used to study the chromatin state, i.e. ChIP-seq, ATAC-seq and 4C-seq, provide information of the average levels within a population of cells. Thus, it is possible that changes occurring in single cells might be missed through the use of bulk methods, espe-

cially since *ZBTB16* is only expressed in a small fraction of cells of the entire population, as was shown by RNA FISH (Fig. 3.20). Therefore, future experiments are required to gain more information on chromatin changes in individual cells in order to uncover potential mechanisms underlying the transcriptional memory of *ZBTB16*. For instance, the recently emerged single-cell version of ATAC-seq [176, 177] would be a powerful method to investigate structural chromatin changes in single cells upon repeated hormone exposure.

However, the question remains how the memory of the first round of GR activation can be stored at the *ZBTB16* locus. Another possible epigenetic feature which might be involved in the priming of *ZBTB16* is DNA methylation. DNA methylation is an epigenetic mark that is associated with silencing of transcription [178] and has been shown to play a role in transcriptional memory in plants [179]. In fact, *ZBTB16* has previously been found to exhibit a hypermethylated promoter region in A549 cells, which contributed to the silencing of the gene, since de-methylation resulted in its upregulation [180]. Interestingly, another study by Matsuda et al. [181] found that a 14-day dexamethasone treatment of cultured human trabecular meshwork cells led to de-methylation of the *ZBTB16* promoter. Hence, it is conceivable that GR might induce stable de-methylation of the *ZBTB16* promoter, thus, facilitating enhanced transcription upon GR re-activation. Notably, a similar mechanism has previously been described in rat hepatoma cells, in which a 3-day dexamethasone treatment led to de-methylation of an enhancer of the Tat gene and ultimately enhanced Tat transcription upon glucocorticoid reinduction [182]. However, since the mentioned studies observed de-methylation following several days of glucocorticoid treatment, additional experiments would be required to investigated if a 4-hour dexamethasone treatment, as applied in the present study, is sufficient to induce de-methylation of the *ZBTB16* promoter region.

Furthermore, studying *ZBTB16* transcription in single cells by RNA FISH revealed that the gene's enhanced expression upon glucocorticoid-reinduction is the result of a higher proportion of cells responding within a population Single-cell expression analysis by RNA FISH showed that the increased upregulation of *ZBTB16* is due to an increased probability of cells to transcribe *ZBTB16* but also due to some cells responding more robustly (Fig. 3.20). Consequently, it appears that a prior glucocorticoid exposure increases the probability of a cells to express *ZBTB16*. Additionally, individual cells were also found to exhibit increased transcript levels upon glucocorticoid reinduction, arguing that the transcriptional rate might be increased in these cells. Interestingly, a recent study, which described transcriptional memory in HeLa cells in response to IFNγ stimulation, also found that the enhanced expression of primed genes in a population of cells was the consequence of more cells transcribing but also individual cells transcribing more actively [125]. Hence, a combination between increased probability of a cell to transcribe and an increased transcriptional rate in certain cells, might be a common feature underlying tran-

scriptional memory (Fig. 4.2).

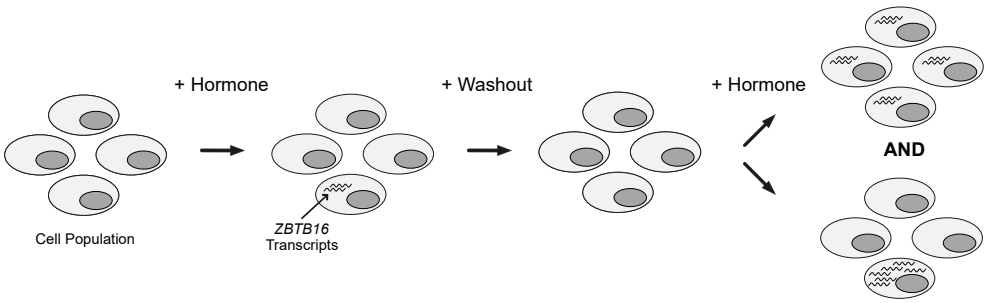

Fig. 4.2: Cartoon representation illustrating the enhanced expression of *ZBTB16* in single cells. Enhanced transcriptional output upon hormone reinduction of *ZBTB16* is the consequence of a larger number of cells responding as well as a higher transcriptional response of single cells.

Taken together, the molecular mechanisms underlying transcriptional memory of *ZBTB16* in response to glucocorticoid exposure remain to be elucidated. Future experiments investigating chromatin changes in single cells as well as DNA methylation at the *ZBTB16* locus might provide useful insights into the mechanisms allowing cells to 'remember' a previous glucocorticoid stimulation.

4.5 The Role of Chromatin and DNA Sequence in Shaping Binding Specificities of Related Transcription Factors

Related transcription factors commonly exhibit similar DNA binding preferences due to their highly similar DNA-binding domains [183]. Such transcription factors families might have evolved from a common ancestral gene through gene duplication, as is the case for the paralogous transcription factors GR and AR [184]. However, recent research is appreciating that even related transcription factors with highly similar DNA recognition sequences can also show differential binding preferences, particularly at regions to which they bind with lower affinity [185].

In the present thesis, I studied genomic binding of GR and AR in the same cellular context. Analysis of receptor binding revealed that GR and AR share a large proportion of binding sites but also occupy receptor-specific regions (Fig. 3.27). The fact that GR and AR, which both have near-identical DNA-binding domains and highly similar DNA recognition motifs [34], can bind differential genomic regions *in vivo*, an observation which has previously also been made by others [31–33], raises the question of how such binding specificity arises.

Firstly, I identified a role of the accessible chromatin landscape in affecting divergent genomic occupancy of GR and AR. Investigation of chromatin accessibility at GR- and AR-occupied regions revealed that a large proportion of GR-specific binding occurs at

relatively inaccessible chromatin regions (Fig. 3.28). Many of these inaccessible GR-specific binding sites likely represent 'closed' or nucleosomal chromatin regions. This is further supported by the fact that GR-specific sites, in comparison to other GR and AR sites, showed relatively high levels of the histone marks H3K27me3 and H3K9me3 (Fig. 3.29), which are commonly associated with heterochromatin [97, 98]. These results are in line with previous studies, which observed GR binding to nucleosomal DNA *in vitro* [87–89]. Furthermore, hormone treatment resulted in an increased ATAC-seq signal at GR-specific sites (Fig. 3.28), suggesting that GR might be capable of binding nucleosomal regions and induce opening of chromatin in a pioneer-like fashion [92]. Similarly, previous studies also provide evidence that GR can bind to and induce opening of closed genomic regions *in vivo*, an action likely achieved through recruitment of chromatin remodelers such as BRG1 [90, 91]. However, in the present study, it needs to be noted that GR expression levels in the U2OS-GR cell line were found to be approximately three times higher than AR expression levels in the U2OS-AR cell line, as determined by whole-cell [^{3}H] steroid binding assays performed by my colleague Marina Kulik (see Fig. 5.1, [129]). Therefore, it is possible that the observed differences stem from the fact that GR expression is higher than AR expression. To exclude this possibility, Marina Kulik assessed GR binding by ChIP-qPCR at a few selected inaccessible GR-specific loci after treating cells with a low dexamethasone concentration of 1 nM. At this concentration only a fraction of all GR would be expected to be active, since 1 nM is less than the previously determined K_d values (dissociation constant) of GR for dexamethasone [186, 187]. At the low hormone concentration of 1 nM GR binding was reduced, though still detectable (data not shown, see [129]). These results suggest that GR binding to inaccessible sites, yet not AR, is not merely a consequence of the higher expression levels of GR in U2OS-GR cells. Together, these findings indicate that binding specificities of GR and AR are shaped by chromatin accessibility and further provide evidence that GR might be able to act in a similar fashion to pioneer factors and induce opening of closed genomic sites.

However, the question arises why GR is able to bind to inaccessible sites while AR is not. It is possible that GR's 'pioneering' ability is based on the fact it can associate to nucleosomal recognition sequences and subsequently recruit chromatin remodelers which induce chromatin opening. Since GR and AR recognize highly similar DNA sequences, a scenario is conceivable in which AR might also briefly associate to nucleosomal sites, yet successful binding is not established due to an inability to recruit the same chromatin remodelers as GR, potentially due to differences in interactions with other proteins.

Moreover, the present thesis provides further evidence that the exact receptor recognition sequence affects GR and AR binding preferences. Motif enrichment analysis of GR- and AR-specific binding showed that the consensus recognition motif for both receptors was more enriched at GR-specific binding sites (Fig. 3.30). These results indicate that

GR might exhibit stricter recognition motif sequence requirements, while AR is able to bind to sequences which are more degenerate. This is in accordance with previous work showing that AR possesses less strict sequence requirements of the recognition motif than GR [32, 34]. Furthermore, AR seems to achieve binding specificity through its ability to bind to a direct repeat version of the GR/AR consensus motif, since this motif was found to be more enriched at AR-specific binding regions, confirming previous findings made by others [36, 37]. Hence, the exact sequence of the GR/AR consensus recognition motif plays an important role in driving receptor binding. Again, given the near-identical DNA-binding interfaces of the receptors, the question arises how such sequence specificity is achieved. The answer may lie in the structural differences in the remaining parts of the proteins, which could influence the affinity with which GR and AR could bind to certain sequences. For instance, both receptors bind as homodimers to their recognition sequences, yet AR monomers dimerize with higher affinity due to structural differences in the dimer interface [188]. Thus, it is conceivable that dimerization affinity affects sequence preferences. However, future experiments would be needed to confirm such a hypothesis.

Moreover, it needs to be noted that the motif analysis performed in the present thesis provided information on whether certain motifs were enriched at GR- and AR-specific binding sites or not. However, distances between enriched motifs as well as motif orientations were not captured. Therefore, follow-up analyses incorporating such information could provide additional information on the different motif preferences at binding sites of GR and AR.

Lastly, I identified GC-content as an important factor in establishing binding specificity between GR and AR. Specifically, I observed that GR preferentially binds genomic sites with a higher GC-content compared to AR. AR-specific sites, on the other hand, exhibited particularly low GC-content in the direct flanking region of the core binding sites, which is in accordance with a previous study describing AR's preference for sites flanked by poly(A) sequences [34]. Strikingly, GR's preference for GC-rich regions extended beyond the actual binding sites and was also observed in a 10 kb window around the binding site. This observation appears to be a more general phenomenon of GR binding, since similar results were found in two other cell types. The importance of the GC-content of the larger genomic area surrounding binding sites has previously also been described to affect binding specificities of transcription factors from different families [163]. Hence, these results suggest that the larger genomic environment, not just the binding sites and its immediate flanks, direct transcription factors binding. Mechanistically, it remains unclear how the extended sequence environment of a binding site influences binding. One could speculate that transcription factors are able to scan the DNA sequence composition of the surrounding genomic area which ultimately guides them to their binding sites. Yet,

future research is needed to investigate a potential mechanism.

In summary, the analysis of GR and AR binding specificities has underlined the importance of chromatin accessibility and DNA sequence composition in driving receptor binding (Fig. 4.3). Elucidating the genomic factors important in shaping binding specificities does not only provide deeper insights the binding preferences of GR and AR, but also addresses the question of how binding specificity can be achieved between paralogous transcription factors. Thus, the findings of this study might also apply, to some extent, to other related transcription factors and could therefore guide future studies aiming to investigate divergent genomic occupancy of other related transcription factors.

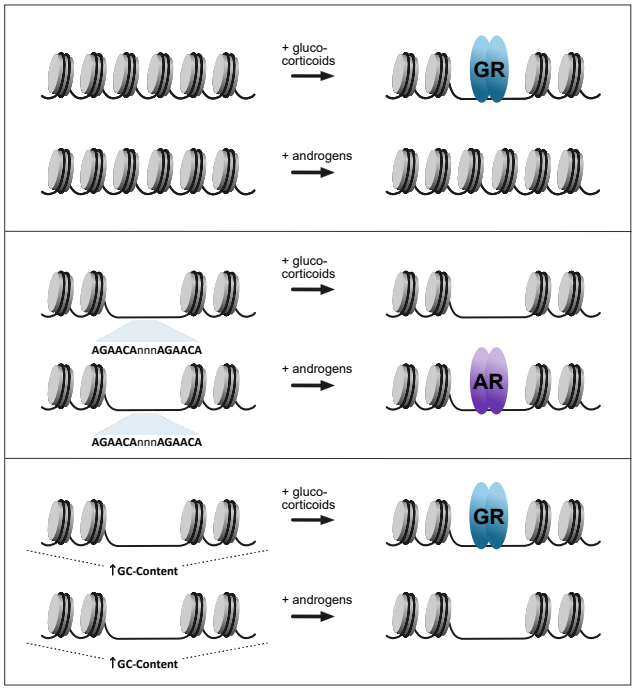

Fig. 4.3: Model summarizing role of chromatin and DNA sequence in shaping GR- and AR-specific occupancy. GR and AR binding is affected by (1) the level of chromatin accessibility, (2) the exact sequence of their recogition motif and (3) the GC-content directly at the binding sites and the surrounding genomic region.

4.6 Additional Projects I Have Worked on During my Doctoral Studies

Throughout my doctoral studies, I made contributions to multiple research projects investigating transcriptional processes and the interplay between transcriptional regulation and the chromatin environment. The two projects that I have presented in this thesis, in which I studied GR's potential to induce transcriptional memory as well as the genomic binding preferences of the related receptors GR and AR, represent my most extensive projects. Below, I listed my contributions to multiple other projects which have now been published.

One of the publications I was involved in, by Tolkachov et al. (2018), studied the different genomic actions of the transcription factor GATA2 (GATA Binding Protein 2) in mesenchymal and hematopoietic cells. My contribution to this collaborative project with the group of Prof. Dr. Michael Schupp involved the analysis of available GATA2 ChIP-seq binding sites to investigate the differences in GATA2 binding between the two types of cells. Further, I analyzed available histone modification ChIP-seq as well as DNase-seq data to explore the influence of the chromatin environment on shaping cell type-specific binding of GATA2.

Tolkachov, A. et al. Loss of the Hematopoietic Stem Cell Factor GATA2 in the Osteogenic Lineage Impairs Trabecularization and Mechanical Strength of Bone. Molecular and Cellular Biology 38. issn: 0270-7306 (*Mar. 2018*).

The study by Schöne et al. (2018) used a STARR-seq approach to assess GR's ability to drive transcription when bound to different variants of its recognition sequence. The study provided evidence that the exact sequence composition of a binding site influences GR's transcriptional activity. My contribution to this study was of experimental and of computational nature. Specifically, I experimentally validated the STARR activity of individual sequence variants using STARR-seq reporters. Further, I made use of available ChIP-exo data, which is a high-resolution version of ChIP that includes an exonuclease digestion step to identify the exact DNA sequence bound to a transcription factor [161], to computationally generate GR footprints at sequence variants using the ExoProfiler tool [153].

Schöne, S. et al. Synthetic STARR-seq reveals how DNA shape and sequence modulate transcriptional output and noise. PLoS Genetics 14. issn: 15537404 (*Nov. 2018*).

Moreover, I also contributed to the publication by Thormann et al. (2019). In this study, GR binding sequences were integrated just upstream of genes that were not regulated by GR. Following integration, some genes were successfully converted to GR-responsive

genes and showed upregulation upon glucocorticoid treatment. I contributed experimentally and computationally by performing ATAC-seq experiments and subsequent data analysis to explore to what extent the accessible chromatin landscape determined whether a gene could be converted into a GR-target gene or not.

Thormann, V. et al. Expanding the repertoire of glucocorticoid receptor target genes by engineering genomic response elements. Life Science Alliance 2. issn: 25751077 (2019).

4.7 Conclusion

In the present thesis, I have presented my work in which I investigated the genomic effects of activation of GR, focusing, in particular, on the receptor's binding preferences as well as its short- and long-term effects on chromatin and transcription. Gaining a deeper understanding of GR action and the ways by which GR affects the transcriptional output of cells is critical, due to GR's central role in major biological processes and its clinical relevance. This work explores to what extent a cell can 'remember' activation of genomic binding of GR and provides evidence of glucocorticoid-induced transcriptional memory. Additionally, this thesis further underlines the important role of the chromatin context and DNA sequence composition in limiting and/or enabling transcription factor binding.

Given the importance of GR as a therapeutic target and the broad range of biological processes its actions affect, studying the actions of this transcription factor are of great interest. This work provides valuable insights into the genomic effects of GR activation and its results might contribute to shaping the direction of future experiments.

5 Supplement

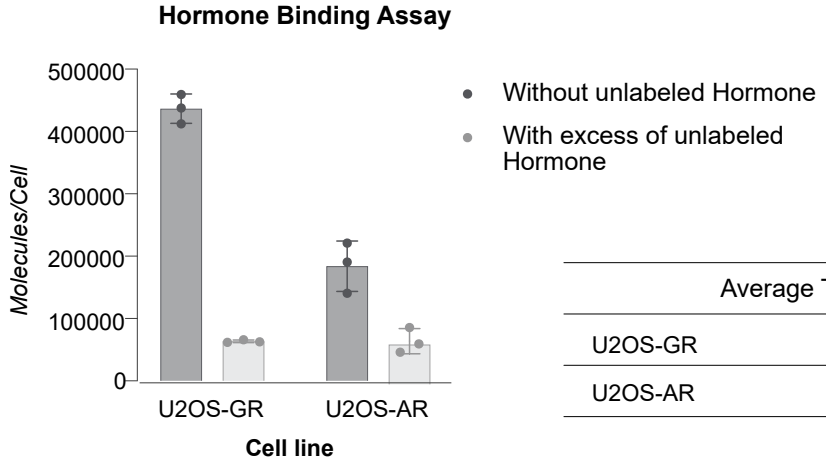

	Average Total Molecules/Cell
U2OS-GR	**373.090**
U2OS-AR	**120.151**

Specific Binding

Total [Molecules/Cell] = [Molecules/Cell (without unlabeled Hormone)] -

[Molecules/Cell (with excess of unlabeled Hormone)]

Fig. 5.1: Quantification of receptor molecules in U2OS-GR and U2OS-AR cells. Receptor levels were determined by liquid scintillattion counting. U2OS-GR cells were exposed to 100 nM [^{3}H]-dexamethasone, either in the presence or absence of 10 μM excess of unlabeled dexamethasone. U2OS-AR cells were treated in the same way, though using R1881 instead of dexamethasone. The total number of moleucles was caluclated as indicated. Three biological replicates were performed. Error bars represent $\pm$ S.D. Marina Kulik performed the experiment, data analysis and figure illustration, as described in [129]. The figure is taken and adpated from our publication [129].

Table 5.1: qPCR primers for the quantification of gene expression

Name	Sequence 5′ to 3′
ZBTB16	fwd: AGAGGGAGCTGTTCAGCAAG
	rev: TCGTTATCAGGAAGCTCGAC
FKBP5	fwd: TGAAGGGTTAGCGGAGCAC
	rev: CTTGGCACCTTCATCAGTAGTC
RPL19	fwd: ATGTATCACAGCCTGTACCTG
	rev: TTCTTGGTCTCTTCCTCCTTG
GILZ	fwd: CCATGGACATCTTCAACAGC
	rev: TTGGCTCAATCTCTCCCATC

Table 5.2: PCR primers for ATAC library amplification (adapted from [177])

Name	Sequence 5′ to 3′
Universal Primer	AATGATACGGCGACCACCGAGATCTACACTCGTCGGCAGCGTC
Barcode Primer 1	CAAGCAGAAGACGGCATACGAGATGGATGTTCTGTCTCGTGGGCTCGG
Barcode Primer 2	CAAGCAGAAGACGGCATACGAGATCTTATCCAGGTCTCGTGGGCTCGG
Barcode Primer 3	CAAGCAGAAGACGGCATACGAGATGTAAGTCACGTCTCGTGGGCTCGG
Barcode Primer 4	CAAGCAGAAGACGGCATACGAGATTTCAGTGAGGTCTCGTGGGCTCGG

Table 5.3: qPCR primers for the quantification of ChIP and ATAC samples

Name	Sequence 5′ to 3′
ZBTB16 (2)	fwd: AACTTTGTGTGATCCCTATC
	rev: GGCAGTATCTAGATGGTAGC
DUSP1	fwd: TACAAACAGATCTCCATGC
	rev: CAAATGAGGAGGTTAGACAG
FKBP5	fwd: CATCACTTAAACTGGAGCTC
	rev: GGGTGTTCTGTGCTCTTC
SLC9A8	fwd: TTCAGGAAGAATACTCAAGC
	rev: ACTCCCTATTGTTTCACATG
PTK2B	fwd: TGGGACCTAATGATTAACTG
	rev: AACCTAATACCCACACAGTC
OR2A1	fwd: TGCATGACGCAGACCTTTCT
	rev: ATGAGAACCACATGGGCCAG
ZBTB16 (1)	fwd: ATATCCTGGACCTATCAATG
	rev: ACAGATTCAGGGAAGAGG
FGF5	fwd: GTAGATAGCATGTACAGAGCGC
	rev: AATCCCATGCCTTCCTGCTC
CYP24A1	fwd: TGAACCCAATTGCTCCCGTC
	rev: TGCCTACCCTGACAGTCATG
NTSR1	fwd: AGCTCCACTTCTGATCTGTCAC
	rev: GTTCGATCCGGTTTGCTGAG
GILZ	fwd: GAGAGATTAATGCCTTTCTG
	rev: CCATATACTTCCGATCATTC
FKBP5 (2)	fwd: CTGGCCTACTTGTACACAC
	rev: TGCAGTAACACAATGTACAG
SRPK2	fwd: GACATCACACCTCGTCTC
	rev: GGATGTGCTCTTCATGTC
ZBTB16 (3)	fwd: GCCTGTGTTTGTTATTGTAG
	rev: TGTGTATGATGACAAACTTGG
ZBTB16 (4)	fwd: CTCTCCCTACTCTGAATTTG
	rev: ATAAACTCTCTGGAATGCTG
ZBTB16 promoter	fwd: GTGGGTGCTCTTATGTATG
	rev: ATCTACTCGTCAGCTCCTC
FKBP5 promoter	fwd: TACTGAACGGCGGCCAAACG
	rev: ATCGGGTTCTGCAGTGGTGG
GILZ promoter	fwd: CTCTAATCAGACTCCACCTC
	rev: TAGACAACAAGATCGAACAG
ZNF536 promoter	fwd: ATAGGATCTGGACTCAAGTG
	rev: AGCTGAATTACCTTGAGAAC

Table 5.4: 4C primer sequences for inverse PCR (1st PCR)

Viewpoint	Sequence 5′ to 3′
Promoter	fwd: TACACGACGCTCTTCCGATCTAGCAGAGAGGAGTTGAGG
	rev: ACTGGAGTTCAGACGTGTGCTCTTCCGATCTTAGTGAACCAGGTGCCAG
Intronic	fwd: TACACGACGCTCTTCCGATCTATGTGTGCGTTCATGTATGT
	rev: ACTGGAGTTCAGACGTGTGCTCTTCCGATCTGAGGAAAGGTTAGGAAGTGG

Table 5.5: 4C primer sequences for inverse PCR (2nd PCR, primers from [132])

Name	Sequence 5′ to 3′
Universial Primer	AATGATACGGCGACCACCGAGATCTACACTCTTTCCCTACACGACGCTCTTCCGATCT
Barcode Primer 1	CAAGCAGAAGACGGCATACGAGATCGTGATGTGACTGGAGTTCAGACGTGTGCT
Barcode Primer 2	CAAGCAGAAGACGGCATACGAGATACATCGGTGACTGGAGTTCAGACGTGTGCT
Barcode Primer 3	CAAGCAGAAGACGGCATACGAGATGCCTAAGTGACTGGAGTTCAGACGTGTGCT
Barcode Primer 4	CAAGCAGAAGACGGCATACGAGATTGGTCAGTGACTGGAGTTCAGACGTGTGCT

6 Abbreviations

3C	Chromosome conformation capture
3D	Three-dimensional
4C	Circularized chromosome conformation capture
ACTH	Adrenocorticotrophic hormone
ATAC	Assay for Transposase-Accessible Chromatin
AP1	Activator protein 1
AR	Androgen receptor
bp	Base pair
ChIP	Chromatin immunoprecipitation
COF	Cofactor
CRH	Corticotrophin-releasing hormone r
Dex	Dexamethasone
EtOH	Ethanol
FISH	Fluorescence *in situ* hybridization
FKBP5	FK506-binding protein 51
GC	Glucocorticoids
GILZ	Glucocorticoid induced leucine zipper
GR	Glucocorticoid receptor
GTF	General transcription factor
H3K27ac	Acetylation at lysine 27 on histone 3),
H3K27me3	Trimethylation at lysine 27 on histone 3),
H3K4me3	Monomethylation at lysine 4 on histone 3),
H3K4me3	Trimethylation at lysine 4 on histone 3),
H3K9me3	Trimethylation at lysine 9 on histone 3),
HPA	Hypothalamic-pituitary-adrenal
kp	kilobase
MMTV	Mouse mammary tumor virus
MR	Mineralocorticoid receptor
nGRE	Negative glucocorticoid response element
PBS	Phosphate buffered saline
PCR	Polymerase chain reaction
PR	Progesterone receptor
PIC	Pre-initiation complex
Pol2	RNA polymerase II
TF	Transcription factor
TSS	Transcription start site
ZBTB16	Zinc Finger And BTB Domain Containing 16

List of Figures

List of Tables

7 References

1. Lee, T. I. & Young, R. A. Transcriptional regulation and its misregulation in disease. *Cell* **152,** 1237–1251. ISSN: 00928674 (Mar. 2013).
2. ROEDER, R. The role of general initiation factors in transcription by RNA polymerase II. *Trends in Biochemical Sciences* **21,** 327–335. ISSN: 09680004 (Sept. 1996).
3. Spitz, F. & Furlong, E. E. Transcription factors: From enhancer binding to developmental control. *Nature Reviews Genetics* **13,** 613–626. ISSN: 14710056 (Sept. 2012).
4. Shlyueva, D., Stampfel, G. & Stark, A. Transcriptional enhancers: From properties to genome-wide predictions. *Nature Reviews Genetics* **15,** 272–286. ISSN: 14710064 (2014).
5. Hampsey, M. Molecular Genetics of the RNA Polymerase II General Transcriptional Machinery. *Microbiology and Molecular Biology Reviews* **62,** 465–503. ISSN: 1092-2172 (June 1998).
6. Yankulov, K., Blau, J., Purton, T., Roberts, S. & Bentley, D. L. Transcriptional elongation by RNA polymerase II is stimulated by transactivators. *Cell* **77,** 749–759. ISSN: 00928674 (June 1994).
7. Lambert, S. A. *et al.* The Human Transcription Factors. *Cell* **172,** 650–665. ISSN: 10974172 (Feb. 2018).
8. Pujols, L. *et al.* Expression of glucocorticoid receptor α- and β-isoforms in human cells and tissues. *American Journal of Physiology - Cell Physiology* **283.** ISSN: 03636143 (2002).
9. Sapolsky, R. M., Romero, L. M. & Munck, A. U. How Do Glucocorticoids Influence Stress Responses? Integrating Permissive, Suppressive, Stimulatory, and Preparative Actions*. *Endocrine Reviews* **21,** 55–89. ISSN: 0163-769X (Feb. 2000).
10. Sacta, M. A., Chinenov, Y. & Rogatsky, I. Glucocorticoid Signaling: An Update from a Genomic Perspective. *Annual Review of Physiology* **78,** 155–180. ISSN: 15451585 (Feb. 2016).
11. Coutinho, A. E. & Chapman, K. E. The anti-inflammatory and immunosuppressive effects of glucocorticoids, recent developments and mechanistic insights. *Molecular and Cellular Endocrinology* **335,** 2–13. ISSN: 03037207 (Mar. 2011).

12. Cain, D. W. & Cidlowski, J. A. Immune regulation by glucocorticoids. *Nature Reviews Immunology* **17,** 233–247. ISSN: 14741741 (Apr. 2017).

13. Kadmiel, M. & Cidlowski, J. A. Glucocorticoid receptor signaling in health and disease. *Trends in Pharmacological Sciences* **34,** 518–530. ISSN: 01656147 (Sept. 2013).

14. Kuo, T., McQueen, A., Chen, T. C. & Wang, J. C. Regulation of glucose homeostasis by glucocorticoids. *Advances in Experimental Medicine and Biology* **872,** 99–126. ISSN: 22148019 (2015).

15. Miller, W. L. & Auchus, R. J. The molecular biology, biochemistry, and physiology of human steroidogenesis and its disorders. *Endocrine Reviews* **32,** 81–151. ISSN: 0163769X (Feb. 2011).

16. Lightman, S. Rhythms within rhythms: The importance of oscillations for glucocorticoid hormones. *Research and Perspectives in Endocrine Interactions* **0,** 87–99. ISSN: 18630685 (2016).

17. Walker, J. J. *et al.* The origin of glucocorticoid hormone oscillations. *PLoS Biology* **10.** ISSN: 15449173 (June 2012).

18. Chung, S., Son, G. H. & Kim, K. Circadian rhythm of adrenal glucocorticoid: Its regulation and clinical implications. *Biochimica et Biophysica Acta - Molecular Basis of Disease* **1812,** 581–591. ISSN: 09254439 (May 2011).

19. Droste, S. K. *et al.* Corticosterone levels in the brain show a distinct ultradian rhythm but a delayed response to forced swim stress. *Endocrinology* **149,** 3244–3253. ISSN: 00137227 (July 2008).

20. Schäcke, H., Döcke, W. D. & Asadullah, K. Mechanisms involved in the side effects of glucocorticoids. *Pharmacology and Therapeutics* **96,** 23–43. ISSN: 01637258 (Oct. 2002).

21. Rodriguez, J. M., Monsalves-Alvarez, M., Henriquez, S., Llanos, M. N. & Troncoso, R. Glucocorticoid resistance in chronic diseases. *Steroids* **115,** 182–192. ISSN: 18785867 (2016).

22. Kumar, R. & Thompson, E. B. The structure of the nuclear hormone receptors. *Steroids* **64,** 310–319. ISSN: 0039128X (May 1999).

23. Mangelsdorf, D. J. *et al.* The nuclear receptor superfamily: The second decade. *Cell* **83,** 835–839. ISSN: 00928674 (Dec. 1995).

24. Luisi, B. F. *et al.* Crystallographic analysis of the interaction of the glucocorticoid receptor with DNA. *Nature* **352,** 497–505. ISSN: 00280836 (1991).

25. Khan, A. *et al.* JASPAR 2018: Update of the open-access database of transcription factor binding profiles and its web framework. *Nucleic Acids Research* **46,** D260–D266. ISSN: 13624962 (Jan. 2018).

26. Davey, R. A. & Grossmann, M. Androgen Receptor Structure, Function and Biology: From Bench to Bedside. *The Clinical biochemist. Reviews* **37,** 3–15. ISSN: 0159-8090 (Feb. 2016).

27. Tarjus, A., Amador, C., Michea, L. & Jaisser, F. Vascular mineralocorticoid receptor and blood pressure regulation. *Current Opinion in Pharmacology* **21,** 138–144. ISSN: 14714973 (2015).

28. Conneely, O. M., Jericevic, B. M. & Lydon, J. P. Progesterone Receptors in Mammary Gland Development and Tumorigenesis. *Journal of Mammary Gland Biology and Neoplasia* **8,** 205–214. ISSN: 10833021 (Apr. 2003).

29. Kuo, T., Harris, C. A. & Wang, J. C. Metabolic functions of glucocorticoid receptor in skeletal muscle. *Molecular and Cellular Endocrinology* **380,** 79–88. ISSN: 03037207 (Nov. 2013).

30. Bhasin, S. *et al.* The Mechanisms of Androgen Effects on Body Composition: Mesenchymal Pluripotent Cell as the Target of Androgen Action. *Journals of Gerontology - Series A Biological Sciences and Medical Sciences* **58,** 1103–1110. ISSN: 10795006 (2003).

31. Arora, V. K. *et al.* Glucocorticoid receptor confers resistance to antiandrogens by bypassing androgen receptor blockade. *Cell* **155,** 1309–1322. ISSN: 00928674 (Dec. 2013).

32. Sahu, B. *et al.* Androgen receptor uses relaxed response element stringency for selective chromatin binding and transcriptional regulation in vivo. *Nucleic Acids Research* **42,** 4230–4240. ISSN: 13624962 (2014).

33. Sahu, B. *et al.* FoxA1 specifies unique androgen and glucocorticoid receptor binding events in prostate cancer cells. *Cancer Research* **73,** 1570–1580. ISSN: 00085472 (Mar. 2013).

34. Zhang, L. *et al.* SelexGLM differentiates androgen and glucocorticoid receptor DNA-binding preference over an extended binding site. *Genome Research* **28,** 111–121. ISSN: 15495469 (Jan. 2018).

35. Belikov, S., Berg, O. G. & Wrange, Ö. Quantification of transcription factor-DNA binding affinity in a living cell. *Nucleic Acids Research* **44,** 3045–3058. ISSN: 13624962 (Dec. 2015).

36. Claessens, F., Joniau, S. & Helsen, C. Comparing the rules of engagement of androgen and glucocorticoid receptors. *Cellular and Molecular Life Sciences* **74,** 2217–2228. ISSN: 14209071 (June 2017).

37. Schoenmakers, E. *et al.* Differences in DNA binding characteristics of the androgen and glucocorticoid receptors can determine hormone-specific responses. *Journal of Biological Chemistry* **275,** 12290–12297. ISSN: 00219258 (Apr. 2000).

38. Shaffer, P. L., Jivan, A., Dollins, D. E., Claessens, F. & Gewirth, D. T. Structural basis of androgen receptor binding to selective androgen response elements. *Proceedings of the National Academy of Sciences of the United States of America* **101,** 4758–4763. ISSN: 00278424 (Apr. 2004).

39. Radman-Livaja, M. & Rando, O. J. Nucleosome positioning: How is it established, and why does it matter? *Developmental Biology* **339,** 258–266. ISSN: 1095564X (Mar. 2010).

40. Bonifer, C. & Cockerill, P. N. Chromatin mechanisms regulating gene expression in health and disease. *Advances in Experimental Medicine and Biology* **711,** 12–25. ISSN: 00652598 (2011).

41. Li, B., Carey, M. & Workman, J. L. The Role of Chromatin during Transcription. *Cell* **128,** 707–719. ISSN: 00928674 (Feb. 2007).

42. Picard, D. *et al.* Reduced levels of hsp90 compromise steroid receptor action in vivo. *Nature* **348,** 166–168. ISSN: 00280836 (1990).

43. Vandevyver, S., Dejager, L. & Libert, C. On the Trail of the Glucocorticoid Receptor: Into the Nucleus and Back. *Traffic* **13,** 364–374. ISSN: 13989219 (Mar. 2012).

44. McDowell, I. C. *et al.* Glucocorticoid receptor recruits to enhancers and drives activation by motif-directed binding. *Genome Research* **28,** 1272–1284. ISSN: 15495469 (Sept. 2018).

45. Strahle, U., Klock, G. & Schutz, G. A DNA sequence of 15 base pairs is sufficient to mediate both glucocorticoid and progesterone induction of gene expression. *Proceedings of the National Academy of Sciences of the United States of America* **84,** 7871–7875. ISSN: 00278424 (1987).

46. Surjit, M. *et al.* Widespread negative response elements mediate direct repression by agonist-liganded glucocorticoid receptor. *Cell* **145,** 224–241. ISSN: 00928674 (Apr. 2011).

47. Hudson, W. H., Youn, C. & Ortlund, E. A. The structural basis of direct glucocorticoid-mediated transrepression. *Nature Structural and Molecular Biology* **20,** 53–58. ISSN: 15459993 (Jan. 2013).

48. Uhlenhaut, N. H. *et al.* Insights into Negative Regulation by the Glucocorticoid Receptor from Genome-wide Profiling of Inflammatory Cistromes. *Molecular Cell* **49,** 158–171. ISSN: 10972765 (Jan. 2013).

49. De Bosscher, K., Vanden Berghe, W. & Haegeman, G. The interplay between the glucocorticoid receptor and nuclear factor-κB or activator protein-1: Molecular mechanisms for gene repression. *Endocrine Reviews* **24,** 488–522. ISSN: 0163769X (Aug. 2003).

50. Ray, A. & Prefontaine, K. E. Physical association and functional antagonism between the p65 subunit of transcription factor NF-κB and the glucocorticoid receptor. *Proceedings of the National Academy of Sciences of the United States of America* **91,** 752–756. ISSN: 00278424 (Jan. 1994).

51. Jonat, C. *et al.* Antitumor promotion and antiinflammation: Down-modulation of AP-1 (Fos/Jun) activity by glucocorticoid hormone. *Cell* **62,** 1189–1204. ISSN: 00928674 (Sept. 1990).

52. Schüle, R. *et al.* Functional antagonism between oncoprotein c-Jun and the glucocorticoid receptor. *Cell* **62,** 1217–1226. ISSN: 00928674 (Sept. 1990).

53. Yang-Yen, H. F. *et al.* Transcriptional interference between c-Jun and the glucocorticoid receptor: Mutual inhibition of DNA binding due to direct protein-protein interaction. *Cell* **62,** 1205–1215. ISSN: 00928674 (Sept. 1990).

54. Weikum, E. R. *et al.* Tethering not required: The glucocorticoid receptor binds directly to activator protein-1 recognition motifs to repress inflammatory genes. *Nucleic Acids Research* **45,** 8596–8608. ISSN: 13624962 (Aug. 2017).

55. Hudson, W. H. *et al.* Cryptic glucocorticoid receptor-binding sites pervade genomic NF-κB response elements. *Nature Communications* **9.** ISSN: 20411723 (Dec. 2018).

56. Escoter-Torres, L., Greulich, F., Quagliarini, F., Wierer, M. & Uhlenhaut, N. H. Anti-inflammatory functions of the glucocorticoid receptor require DNA binding. *Nucleic Acids Research* **48,** 8393–8407. ISSN: 13624962 (Sept. 2020).

57. Ratman, D. *et al.* How glucocorticoid receptors modulate the activity of other transcription factors: A scope beyond tethering. *Molecular and Cellular Endocrinology* **380,** 41–54. ISSN: 03037207 (Nov. 2013).

58. Sasse, S. K. *et al.* Nascent transcript analysis of glucocorticoid crosstalk with TNF defines primary and cooperative inflammatory repression. *Genome Research* **29,** 1753–1765. ISSN: 15495469 (2019).

59. Oh, K. S. *et al.* Anti-Inflammatory Chromatinscape Suggests Alternative Mechanisms of Glucocorticoid Receptor Action. *Immunity* **47,** 298–309.e5. ISSN: 10974180 (Aug. 2017).

60. Reddy, T. E. *et al.* Genomic determination of the glucocorticoid response reveals unexpected mechanisms of gene regulation. *Genome Research* **19,** 2163–2171. ISSN: 10889051 (Dec. 2009).

61. Portuguez, A. S. *et al.* Gene activation and repression by the glucocorticoid receptor are mediated by sequestering Ep300 and two modes of chromatin binding. *bioRxiv,* 764480 (Sept. 2019).

62. Schmidt, S. F., Larsen, B. D., Loft, A. & Mandrup, S. Cofactor squelching: Artifact or fact? *BioEssays* **38,** 618–626. ISSN: 15211878 (July 2016).

63. Mortazavi, A., Williams, B. A., McCue, K., Schaeffer, L. & Wold, B. Mapping and quantifying mammalian transcriptomes by RNA-Seq. *Nature Methods* **5,** 621–628. ISSN: 15487091 (July 2008).

64. Ameur, A. *et al.* Total RNA sequencing reveals nascent transcription and widespread co-transcriptional splicing in the human brain. *Nature Structural and Molecular Biology* **18,** 1435–1440. ISSN: 15459993 (Dec. 2011).

65. Gray, J. M. *et al.* SnapShot-Seq: A method for extracting genome-wide, in Vivo mRNA dynamics from a single total RNA sample. *PLoS ONE* **9.** ISSN: 19326203 (Feb. 2014).

66. Madsen, J. G. S. *et al.* iRNA-seq: Computational method for genome-wide assessment of acute transcriptional regulation from total RNA-seq data. *Nucleic Acids Research* **43,** e40. ISSN: 13624962 (Mar. 2015).

67. Herzel, L., Ottoz, D. S., Alpert, T. & Neugebauer, K. M. Splicing and transcription touch base: Co-transcriptional spliceosome assembly and function. *Nature Reviews Molecular Cell Biology* **18,** 637–650. ISSN: 14710080 (Oct. 2017).

68. Tang, F. *et al.* mRNA-Seq whole-transcriptome analysis of a single cell. *Nature Methods* **6,** 377–382. ISSN: 15487091 (Apr. 2009).

69. Femino, A. M., Fay, F. S., Fogarty, K. & Singer, R. H. Visualization of single RNA transcripts in situ. *Science* **280,** 585–590. ISSN: 00368075 (Apr. 1998).

70. Luger, K., Mäder, A. W., Richmond, R. K., Sargent, D. F. & Richmond, T. J. Crystal structure of the nucleosome core particle at 2.8 Å resolution. *Nature* **389,** 251–260. ISSN: 00280836 (1997).

71. Woodcock, C. L., Safer, J. P. & Stanchfield, J. E. Structural repeating units in chromatin. I. Evidence for their general occurrence. *Experimental Cell Research* **97,** 101–110. ISSN: 00144827 (1976).

72. Rowley, M. J. & Corces, V. G. Organizational principles of 3D genome architecture. *Nature Reviews Genetics* **19,** 789–800. ISSN: 14710064 (Dec. 2018).

73. Lee, C. K., Shibata, Y., Rao, B., Strahl, B. D. & Lieb, J. D. Evidence for nucleosome depletion at active regulatory regions genome-wide. *Nature Genetics* **36,** 900–905. ISSN: 10614036 (Aug. 2004).

74. Thurman, R. E. *et al.* The accessible chromatin landscape of the human genome. *Nature* **489,** 75–82. ISSN: 00280836 (Sept. 2012).

75. Sheffield, N. C. & Furey, T. S. Identifying and characterizing regulatory sequences in the human genome with chromatin accessibility assays. *Genes* **3,** 651–670. ISSN: 20734425 (Dec. 2012).

76. Boyle, A. P. *et al.* High-Resolution Mapping and Characterization of Open Chromatin across the Genome. *Cell* **132,** 311–322. ISSN: 00928674 (Jan. 2008).

77. John, S. *et al.* Chromatin accessibility pre-determines glucocorticoid receptor binding patterns. *Nature Genetics* **43,** 264–268. ISSN: 10614036 (Mar. 2011).

78. Minnoye, L. *et al.* Chromatin accessibility profiling methods. *Nature Reviews Methods Primers* **1,** 1–24 (Dec. 2021).

79. Buenrostro, J. D., Giresi, P. G., Zaba, L. C., Chang, H. Y. & Greenleaf, W. J. Transposition of native chromatin for fast and sensitive epigenomic profiling of open chromatin, DNA-binding proteins and nucleosome position. *Nature Methods* **10,** 1213–1218. ISSN: 15487091 (Dec. 2013).

80. Biddie, S. C. *et al.* Transcription Factor AP1 Potentiates Chromatin Accessibility and Glucocorticoid Receptor Binding. *Molecular Cell* **43,** 145–155. ISSN: 10972765 (July 2011).

81. Love, M. I. *et al.* Role of the chromatin landscape and sequence in determining cell type-specific genomic glucocorticoid receptor binding and gene regulation. *Nucleic Acids Research* **45,** 1805–1819. ISSN: 13624962 (Feb. 2017).

82. Fryer, C. J. & Archer, T. K. Chromatin remodelling by the glucocorticoid receptor requires the BRG1 complex. *Nature* **393,** 88–91. ISSN: 00280836 (May 1998).

83. John, S. *et al.* Interaction of the Glucocorticoid Receptor with the Chromatin Landscape. *Molecular Cell* **29,** 611–624. ISSN: 10972765 (Mar. 2008).

84. Burd, C. J. & Archer, T. K. Chromatin architecture defines the glucocorticoid response. *Molecular and Cellular Endocrinology* **380,** 25–31. ISSN: 03037207 (Nov. 2013).

85. Stavreva, D. A. *et al.* Dynamics of chromatin accessibility and long-range interactions in response to glucocorticoid pulsing. *Genome Research* **25,** 845–857. ISSN: 15495469 (June 2015).

86. Voss, T. C. *et al.* Dynamic exchange at regulatory elements during chromatin remodeling underlies assisted loading mechanism. *Cell* **146,** 544–554. ISSN: 10974172 (Aug. 2011).

87. Perlmann, T. & Wrange, O. Specific glucocorticoid receptor binding to DNA reconstituted in a nucleosome. *The EMBO journal* **7,** 3073–3079. ISSN: 02614189 (Oct. 1988).

88. Li, Q. & Wrange, O. Translational positioning of a nucleosomal glucocorticoid response element modulates glucocorticoid receptor affinity. *Genes and Development* **7,** 2471–2482. ISSN: 08909369 (1993).

89. Li, Q. & Wrange, O. Accessibility of a glucocorticoid response element in a nucleosome depends on its rotational positioning. *Molecular and Cellular Biology* **15,** 4375–4384. ISSN: 0270-7306 (Aug. 1995).

90. Johnson, G. D. *et al.* Human genome-wide measurement of drug-responsive regulatory activity. *Nature Communications* **9.** ISSN: 20411723 (Dec. 2018).

91. Hoffman, J. A., Trotter, K. W., Ward, J. M. & Archer, T. K. BRG1 governs glucocorticoid receptor interactions with chromatin and pioneer factors across the genome. *eLife* **7.** ISSN: 2050084X (May 2018).

92. Mayran, A. & Drouin, J. Pioneer transcription factors shape the epigenetic landscape. *Journal of Biological Chemistry* **293,** 13795–13804. ISSN: 1083351X (Sept. 2018).

93. Marmorstein, R. & Trievel, R. C. Histone modifying enzymes: Structures, mechanisms, and specificities. *Biochimica et Biophysica Acta - Gene Regulatory Mechanisms* **1789,** 58–68. ISSN: 18749399 (Jan. 2009).

94. Lawrence, M., Daujat, S. & Schneider, R. Lateral Thinking: How Histone Modifications Regulate Gene Expression. *Trends in Genetics* **32,** 42–56. ISSN: 13624555 (Jan. 2016).

95. Creyghton, M. P. *et al.* Histone H3K27ac separates active from poised enhancers and predicts developmental state. *Proceedings of the National Academy of Sciences of the United States of America* **107,** 21931–21936. ISSN: 00278424 (Dec. 2010).

96. Heintzman, N. D. *et al.* Distinct and predictive chromatin signatures of transcriptional promoters and enhancers in the human genome. *Nature Genetics* **39,** 311–318. ISSN: 10614036 (Mar. 2007).

97. Wiles, E. T. & Selker, E. U. H3K27 methylation: a promiscuous repressive chromatin mark. *Current Opinion in Genetics and Development* **43,** 31–37. ISSN: 18790380 (Apr. 2017).

98. Nicetto, D. & Zaret, K. S. Role of H3K9me3 heterochromatin in cell identity establishment and maintenance. *Current Opinion in Genetics and Development* **55,** 1–10. ISSN: 18790380 (Apr. 2019).

99. Grbesa, I. & Hakim, O. Genomic effects of glucocorticoids. *Protoplasma* **254,** 1175–1185. ISSN: 0033183X (May 2017).

100. Glass, C. K., Rose, D. W. & Rosenfeld, M. G. Nuclear receptor coactivators. *Current Opinion in Cell Biology* **9,** 222–232. ISSN: 09550674 (1997).

101. Vockley, C. M. *et al.* Direct GR Binding Sites Potentiate Clusters of TF Binding across the Human Genome. *Cell* **166,** 1269–1281.e19. ISSN: 10974172 (Aug. 2016).

102. Liu, X. *et al.* The structural basis of protein acetylation by the p300/CBP transcriptional coactivator. *Nature* **451,** 846–850. ISSN: 14764687 (Feb. 2008).

103. Kuznetsova, T. *et al.* Glucocorticoid receptor and nuclear factor kappa-b affect three-dimensional chromatin organization. *Genome Biology* **16,** 264. ISSN: 1474760X (Dec. 2015).

104. Oudelaar, A. M. & Higgs, D. R. The relationship between genome structure and function. *Nature Reviews Genetics* **22.** ISSN: 14710064 (Mar. 2020).

105. Bonev, B. & Cavalli, G. Organization and function of the 3D genome. *Nature Reviews Genetics* **17,** 661–678. ISSN: 14710064 (Oct. 2016).

106. Schoenfelder, S. & Fraser, P. Long-range enhancer–promoter contacts in gene expression control. *Nature Reviews Genetics* **20,** 437–455. ISSN: 14710064 (Aug. 2019).

107. Lupiáñez, D. G. *et al.* Disruptions of topological chromatin domains cause pathogenic rewiring of gene-enhancer interactions. *Cell* **161,** 1012–1025. ISSN: 10974172 (May 2015).

108. Dekker, J., Rippe, K., Dekker, M. & Kleckner, N. Capturing chromosome conformation. *Science* **295,** 1306–1311. ISSN: 00368075 (Feb. 2002).

109. Van De Werken, H. J. *et al.* 4C technology: Protocols and data analysis. *Methods in Enzymology* **513,** 89–112. ISSN: 15577988 (2012).

110. Hakim, O. *et al.* Diverse gene reprogramming events occur in the same spatial clusters of distal regulatory elements. *Genome Research* **21,** 697–706. ISSN: 10889051 (May 2011).

111. Thormann, V. *et al.* Expanding the repertoire of glucocorticoid receptor target genes by engineering genomic response elements. *Life Science Alliance* **2.** ISSN: 25751077 (2019).

112. Thormann, V. *et al.* Genomic dissection of enhancers uncovers principles of combinatorial regulation and cell type-specific wiring of enhancer-promoter contacts. *Nucleic Acids Research* **46,** 2868–2882. ISSN: 13624962 (Apr. 2018).

113. D'Ippolito, A. M. *et al.* Pre-established Chromatin Interactions Mediate the Genomic Response to Glucocorticoids. *Cell Systems* **7,** 146–160.e7. ISSN: 24054720 (Aug. 2018).

114. Jubb, A. W., Boyle, S., Hume, D. A. & Bickmore, W. A. Glucocorticoid Receptor Binding Induces Rapid and Prolonged Large-Scale Chromatin Decompaction at Multiple Target Loci. *Cell Reports* **21,** 3022–3031. ISSN: 22111247 (Dec. 2017).

115. Richter, K., Haslbeck, M. & Buchner, J. The Heat Shock Response: Life on the Verge of Death. *Molecular Cell* **40,** 253–266. ISSN: 10972765 (Oct. 2010).

116. Vihervaara, A., Duarte, F. M. & Lis, J. T. Molecular mechanisms driving transcriptional stress responses. *Nature Reviews Genetics* **19,** 385–397. ISSN: 14710064 (June 2018).

117. D'Urso, A. & Brickner, J. H. Epigenetic transcriptional memory. *Current Genetics* **63,** 435–439. ISSN: 14320983 (June 2017).

118. D'Urso, A. & Brickner, J. H. Mechanisms of epigenetic memory. *Trends in Genetics* **30,** 230–236. ISSN: 13624555 (2014).

119. Lämke, J. & Bäurle, I. Epigenetic and chromatin-based mechanisms in environmental stress adaptation and stress memory in plants. *Genome Biology* **18.** ISSN: 1474760X (June 2017).

120. Bäurle, I. & Trindade, I. Chromatin regulation of somatic abiotic stress memory. *Journal of Experimental Botany* **71,** 5269–5279. ISSN: 14602431 (Aug. 2020).

121. Vihervaara, A. *et al.* Stress-Induced Transcriptional Memory Accelerates Promoter-Proximal Pause-Release and Decelerates Termination Over Mitotic Divisions. *SSRN Electronic Journal* (June 2019).

122. Light, W. H. *et al.* A Conserved Role for Human Nup98 in Altering Chromatin Structure and Promoting Epigenetic Transcriptional Memory. *PLoS Biology* **11.** ISSN: 15449173 (Mar. 2013).

123. Gialitakis, M., Arampatzi, P., Makatounakis, T. & Papamatheakis, J. Gamma Interferon-Dependent Transcriptional Memory via Relocalization of a Gene Locus to PML Nuclear Bodies. *Molecular and Cellular Biology* **30,** 2046–2056. ISSN: 0270-7306 (Apr. 2010).

124. Bevington, S. L. *et al.* Inducible chromatin priming is associated with the establishment of immunological memory in T cells. *The EMBO Journal* **35,** 515–535. ISSN: 0261-4189 (Mar. 2016).

125. Siwek, W., Tehrani, S. S., Mata, J. F. & Jansen, L. E. Activation of Clustered IFNγ Target Genes Drives Cohesin-Controlled Transcriptional Memory. *Molecular Cell* **80,** 396–409.e6. ISSN: 10974164 (Nov. 2020).

126. D'Urso, A. *et al.* Set1/COMPASS and mediator are repurposed to promote epigenetic transcriptional memory. *eLife* **5.** ISSN: 2050084X (June 2016).

127. Zaret, K. S. & Yamamoto, K. R. Reversible and persistent changes in chromatin structure accompany activation of a glucocorticoid-dependent enhancer element. *Cell* **38,** 29–38. ISSN: 00928674 (1984).

128. Rogatsky, I., Trowbridge, J. M. & Garabedian, M. J. Glucocorticoid receptor-mediated cell cycle arrest is achieved through distinct cell-specific transcriptional regulatory mechanisms. *Molecular and Cellular Biology* **17,** 3181–3193. ISSN: 0270-7306 (June 1997).

129. Kulik, M. *et al.* Androgen and glucocorticoid receptor direct distinct transcriptional programs by receptor-specific and shared DNA binding sites — Nucleic Acids Research — Oxford Academic. *Nucleic Acids Research* (2021).

130. Corces, M. R. *et al.* An improved ATAC-seq protocol reduces background and enables interrogation of frozen tissues. *Nature Methods* **14,** 959–962. ISSN: 15487105 (Oct. 2017).

131. Van De Werken, H. J. *et al.* 4C technology: Protocols and data analysis. *Methods in Enzymology* **513,** 89–112. ISSN: 15577988 (2012).

132. Krijger, P. H., Geeven, G., Bianchi, V., Hilvering, C. R. & de Laat, W. 4C-seq from beginning to end: A detailed protocol for sample preparation and data analysis. *Methods* **170,** 17–32. ISSN: 10959130 (Jan. 2020).

133. Schöne, S. *et al.* Synthetic STARR-seq reveals how DNA shape and sequence modulate transcriptional output and noise. *PLoS Genetics* **14.** ISSN: 15537404 (Nov. 2018).

134. Dobin, A. *et al.* STAR: Ultrafast universal RNA-seq aligner. *Bioinformatics* **29,** 15–21. ISSN: 13674803 (Jan. 2013).

135. Li, H. *et al.* The Sequence Alignment/Map format and SAMtools. *Bioinformatics* **25,** 2078–2079. ISSN: 13674803 (Aug. 2009).

136. Ramírez, F., Dündar, F., Diehl, S., Grüning, B. A. & Manke, T. DeepTools: A flexible platform for exploring deep-sequencing data. *Nucleic Acids Research* **42.** ISSN: 13624962 (July 2014).

137. Robinson, J. T. *et al.* Integrative genomics viewer. *Nature Biotechnology* **29,** 24–26. ISSN: 10870156 (Jan. 2011).

138. Navarro Gonzalez, J. *et al.* The UCSC genome browser database: 2021 update. *Nucleic Acids Research* **49,** D1046–D1057. ISSN: 13624962 (Jan. 2021).

139. Lawrence, M. *et al.* Software for Computing and Annotating Genomic Ranges. *PLoS Computational Biology* **9.** ISSN: 1553734X (Aug. 2013).

140. Liao, Y., Smyth, G. K. & Shi, W. FeatureCounts: An efficient general purpose program for assigning sequence reads to genomic features. *Bioinformatics* **30,** 923–930. ISSN: 14602059. arXiv: 1305.3347 (Apr. 2014).

141. Liao, Y., Smyth, G. K. & Shi, W. The R package Rsubread is easier, faster, cheaper and better for alignment and quantification of RNA sequencing reads. *Nucleic Acids Research* **47.** ISSN: 13624962 (May 2019).

142. Love, M. I., Huber, W. & Anders, S. Moderated estimation of fold change and dispersion for RNA-seq data with DESeq2. *Genome Biology* **15.** ISSN: 1474760X (Dec. 2014).

143. Langmead, B. & Salzberg, S. L. Fast gapped-read alignment with Bowtie 2. *Nature Methods* **9,** 357–359. ISSN: 15487091 (Apr. 2012).

144. Zhang, Y. *et al.* Model-based analysis of ChIP-Seq (MACS). *Genome Biology* **9.** ISSN: 14747596 (Sept. 2008).

145. Quinlan, A. R. & Hall, I. M. BEDTools: A flexible suite of utilities for comparing genomic features. *Bioinformatics* **26,** 841–842. ISSN: 13674803 (Jan. 2010).

146. Amemiya, H. M., Kundaje, A. & Boyle, A. P. The ENCODE Blacklist: Identification of Problematic Regions of the Genome. *Scientific Reports* **9.** ISSN: 20452322 (Dec. 2019).

147. Dunham, I. *et al.* An integrated encyclopedia of DNA elements in the human genome. *Nature* **489,** 57–74. ISSN: 14764687 (Sept. 2012).

148. Schiller, B. J., Chodankar, R., Watson, L. C., Stallcup, M. R. & Yamamoto, K. R. Glucocorticoid receptor binds half sites as a monomer and regulates specific target genes. *Genome Biology* **15.** ISSN: 1474760X (July 2014).

149. McLeay, R. C. & Bailey, T. L. Motif Enrichment Analysis: A unified framework and an evaluation on ChIP data. *BMC Bioinformatics* **11.** ISSN: 14712105 (Apr. 2010).

150. Bailey, T. L. *et al.* MEME Suite: Tools for motif discovery and searching. *Nucleic Acids Research* **37.** ISSN: 03051048 (2009).

151. Crooks, G. E., Hon, G., Chandonia, J. M. & Brenner, S. E. WebLogo: A sequence logo generator. *Genome Research* **14,** 1188–1190. ISSN: 10889051 (June 2004).

152. Chen, Z. *et al.* Agonist and antagonist switch DNA motifs recognized by human androgen receptor in prostate cancer. *The EMBO Journal* **34,** 502–516. ISSN: 0261-4189 (Feb. 2015).

153. Starick, S. R. *et al.* ChIP-exo signal associated with DNA-binding motifs provides insight into the genomic binding of the glucocorticoid receptor and cooperating transcription factors. *Genome Research* **25,** 825–835. ISSN: 15495469 (June 2015).

154. Kent, W. J., Zweig, A. S., Barber, G., Hinrichs, A. S. & Karolchik, D. BigWig and BigBed: Enabling browsing of large distributed datasets. *Bioinformatics* **26,** 2204–2207. ISSN: 13674803 (July 2010).

155. Bothe, M., Buschow, R. & Meijsing, S. H. Glucocorticoid receptor activation induces gene-specific transcriptional memory and universally reversible changes in chromatin accessibility. *bioRxiv,* 2021.01.05.425406 (Jan. 2021).

156. Munck, A. & Foley, R. Kinetics of glucocorticoid-receptor complexes in rat thymus cells. *Journal of Steroid Biochemistry* **7,** 1117–1122. ISSN: 00224731 (1976).

157. Eick, D. & Geyer, M. The RNA polymerase II carboxy-terminal domain (CTD) code. *Chemical Reviews* **113,** 8456–8490. ISSN: 00092665 (Nov. 2013).

158. Fenouil, R. *et al.* CpG islands and GC content dictate nucleosome depletion in a transcription-independent manner at mammalian promoters. *Genome Research* **22,** 2399–2408. ISSN: 10889051 (Dec. 2012).

159. Wang, J. *et al.* Sequence features and chromatin structure around the genomic regions bound by 119 human transcription factors. *Genome Research* **22,** 1798–1812. ISSN: 10889051 (Sept. 2012).

160. Schwartz, U. *et al.* Characterizing the nuclease accessibility of DNA in human cells to map higher order structures of chromatin. *Nucleic Acids Research* **47,** 1239–1254. ISSN: 13624962 (Feb. 2019).

161. Rhee, H. S. & Pugh, B. F. ChiP-exo method for identifying genomic location of DNA-binding proteins with near-single-nucleotide accuracy. *Current Protocols in Molecular Biology* **Chapter 21.** ISSN: 19343639 (2012).

162. Heinlein, C. A. & Chang, C. Androgen receptor in prostate cancer. *Endocrine Reviews* **25,** 276–308. ISSN: 0163769X (Apr. 2004).

163. Dror, I., Golan, T., Levy, C., Rohs, R. & Mandel-Gutfreund, Y. A widespread role of the motif environment in transcription factor binding across diverse protein families. *Genome Research* **25,** 1268–1280. ISSN: 15495469 (Sept. 2015).

164. Arnold, C. D. *et al.* Genome-wide quantitative enhancer activity maps identified by STARR-seq. *Science* **339,** 1074–1077. ISSN: 10959203 (Mar. 2013).

165. Reddy, T. E., Gertz, J., Crawford, G. E., Garabedian, M. J. & Myers, R. M. The Hypersensitive Glucocorticoid Response Specifically Regulates Period 1 and Expression of Circadian Genes. *Molecular and Cellular Biology* **32,** 3756–3767. ISSN: 0270-7306 (Sept. 2012).

166. Stavreva, D. A. *et al.* Ultradian hormone stimulation induces glucocorticoid receptor-mediated pulses of gene transcription. *Nature Cell Biology* **11,** 1093–1102. ISSN: 14657392 (2009).

167. De Souza-Talarico, J. N., Marin, M. F., Sindi, S. & Lupien, S. J. Effects of stress hormones on the brain and cognition evidence from normal to pathological aging. *Dementia e Neuropsychologia* **5,** 8–16. ISSN: 19805764 (2011).

168. Barna, M., Hawe, N., Lee, N. & Pandolfi, P. P. Plzf regulates limb and axial skeletal patterning. *Nature Genetics* **25,** 166–172. ISSN: 10614036 (June 2000).

169. Costoya, J. A. *et al.* Essential role of Plzf in maintenance of spermatogonial stem cells. *Nature Genetics* **36,** 653–659. ISSN: 10614036 (June 2004).

170. Plaisier, C. L. *et al.* Zbtb16 has a role in brown adipocyte bioenergetics. *Nutrition and Diabetes* **2.** ISSN: 20444052 (Sept. 2012).

171. Chen, S. *et al.* Control of hepatic gluconeogenesis by the promyelocytic leukemia zinc finger protein. *Molecular Endocrinology* **28,** 1987–1998. ISSN: 19449917 (2014).

172. Suliman, B. A., Xu, D. & Williams, B. R. G. The promyelocytic leukemia zinc finger protein: Two decades of molecular oncology. *Frontiers in Oncology* **2 JUL.** ISSN: 2234943X (2012).

173. Šeda, O. *et al.* ZBTB16 and metabolic syndrome: A network perspective. *Physiological Research* **66,** S357–S365. ISSN: 18029973 (2017).

174. Krupková, M. *et al.* Single-gene congenic strain reveals the effect of Zbtb16 on Dexamethasone-induced insulin resistance. *Frontiers in Endocrinology* **9.** ISSN: 16642392 (Apr. 2018).

175. Martin, P. J., Delmotte, M. H., Formstecher, P. & Lefebvre, P. PLZF is a negative regulator of retinoic acid receptor transcriptional activity. *Nuclear Receptor* **1.** ISSN: 14781336 (Sept. 2003).

176. Cusanovich, D. A. *et al.* Multiplex single-cell profiling of chromatin accessibility by combinatorial cellular indexing. *Science* **348,** 910–914. ISSN: 10959203 (May 2015).

177. Buenrostro, J. D. *et al.* Single-cell chromatin accessibility reveals principles of regulatory variation. *Nature* **523,** 486–490. ISSN: 14764687 (July 2015).

178. Greenberg, M. V. & Bourc'his, D. The diverse roles of DNA methylation in mammalian development and disease. *Nature Reviews Molecular Cell Biology* **20,** 590–607. ISSN: 14710080 (Oct. 2019).

179. Deleris, A., Halter, T. & Navarro, L. DNA Methylation and Demethylation in Plant Immunity. *Annual Review of Phytopathology* **54,** 579–603. ISSN: 15452107 (Aug. 2016).

180. Wang, X. *et al.* Hypermethylation reduces expression of tumor-suppressor PLZF and regulates proliferation and apoptosis in non-small-cell lung cancers. *FASEB Journal* **27,** 4194–4203. ISSN: 15306860 (Oct. 2013).

181. Matsuda, A. *et al.* DNA methylation analysis of human trabecular meshwork cells during dexamethasone stimulation. *Investigative Ophthalmology and Visual Science* **56,** 3801–3809. ISSN: 15525783 (2015).

182. Thomassin, H., Flavin, M., Espinás, M. L. & Grange, T. Glucocorticoid-induced DNA demethylation and gene memory during development. *EMBO Journal* **20,** 1974–1983. ISSN: 02614189 (Apr. 2001).

183. Weirauch, M. T. *et al.* Determination and inference of eukaryotic transcription factor sequence specificity. *Cell* **158,** 1431–1443. ISSN: 10974172 (2014).

184. Thornton, J. W. Evolution of vertebrate steroid receptors from an ancestral estrogen receptor by ligand exploitation and serial genome expansions. *Proceedings of the National Academy of Sciences of the United States of America* **98,** 5671–5676. ISSN: 00278424 (May 2001).

185. Shen, N. *et al.* Divergence in DNA Specificity among Paralogous Transcription Factors Contributes to Their Differential In Vivo Binding. *Cell Systems* **6,** 470–483.e8. ISSN: 24054720 (Apr. 2018).

186. Koubovec, D., Ronacher, K., Stubsrud, E., Louw, A. & Hapgood, J. P. Synthetic progestins used in HRT have different glucocorticoid agonist properties. *Molecular and Cellular Endocrinology* **242,** 23–32. ISSN: 03037207 (Oct. 2005).

187. Vedder, H., Weiß, I., Holsboer, F. & Reul, J. M. Glucocorticoid and mineralocorticoid receptors in rat neocortical and hippocampal brain cells in culture: characterization and regulatory studies. *Brain Research* **605,** 18–24. ISSN: 00068993 (Mar. 1993).

188. Helsen, C. *et al.* Structural basis for nuclear hormone receptor DNA binding. *Molecular and Cellular Endocrinology* **348,** 411–417. ISSN: 03037207 (Jan. 2012).